(1)

STABILITY SOLUTION TO LINEARIZED EQUATIONS OF MOTION FOR A SYMMETRIC SPINNING SATELLITE IN AN ELLIPTICAL ORBIT APPLIED TO THE NON-LINEAR EQUATIONS

THESIS

Dale E. Shell
Captain, USAF

AFIT/GA/AA/88D-09

DEPARTMENT OF THE AIR FORCE
AIR UNIVERSITY
AIR FORCE INSTITUTE OF TECHNOLOGY
Wright-Patterson Air Force Base, Ohio

(1)

AFIT/GA/AA/88D-09

STABILITY SOLUTION TO LINEARIZED EQUATIONS OF MOTION FOR A SYMMETRIC SPINNING SATELLITE IN AN ELLIPTICAL ORBIT APPLIED TO THE NON-LINEAR EQUATIONS

THESIS

Dale E. Shell
Captain, USAF

AFIT/GA/AA/88D-09

Approved for public release; Distribution unlimited

AFIT/GA/AA/88D-09

STABILITY SOLUTION TO LINEARIZED EQUATIONS OF MOTION FOR A SYMMETRIC SPINNING SATELLITE IN AN ELLIPTICAL ORBIT APPLIED TO THE NON-LINEAR EQUATIONS

THESIS

Presented to the Faulty of the School of Engineering
of the Air Force Institute of Technology
Air University
In Partial Fulfillment of the
Requirements for the Degree of
Master of Science in Astronautical Engineering

Dale E. Shell, B.S., A.S.

Captain, USAF

December 1988

Preface

This thesis expands on the work of Myers in the control of linear periodic systems. It applies the control developed for the linear system using modal variables to the non-linear equations of motion. While only one example is investigated in this thesis, the technique can be applied to periodic systems in general. This thesis used uncontrolled modal variables with scalar control and work needs to be expanded involving the controlled modal variables and other control schemes to fully understand the effect of large perturbations on the non-linear equations.

I would like to thank Dr. Wiesel for his help with the computer programs used in this thesis. I would also like to thank Capt. Bain for his technical assistance , at any hour, and the large amount of moral support he provided. I would especially like to thank Dr. Calico for his time and assistance in teaching me the concepts used in this thesis. I would also like to thank him for his great patience. Finally, I would like to thank my wife, [redacted] for all the things she had to handle while I was busy studying. Without her this thesis would not have been possible.

Table of Contents

List of Figures

List of Tables

List of Symbols

A	Orbital Reference Frame; System Periodic Matrix; Moment of Inertia
a	Semi-major Axis
B	Control Matrix
C	Moment of Inertia
c	Constant Matrix
e	Eccentricity
F	Periodic Solution Matrix
f	Element of F matrix
G	Gain Matrix
g	Mode Controlability Matrix
H	Angular Momentum
I	Inertial Frame; Moment of Inertia Matrix; Identity Matrix
J	Jordan Matrix
K	Inertia Parameter
k	Gain Vector
L	Periodic Adjoint Solution Matrix
l	Element of L Matrix
M	External Moments
n	Orbital Parameter
r	Orbital Radius
T	Orbit Period
t	Time
u	Control Vector
x	State Variable
y	Adjoint State Variable

α	Spin Rate Parameter
ζ	Nondimensional Distance
η	Modal Variable
θ	Angle of Rotation
λ	Characteristic Eigenvalues
ν	True Anomaly
τ	Nondimensional Time
Φ	Principal Fundamental Matrix
ϕ	Angle between spin axis and orbit normal; Element of Φ;
ψ	Fundamental Matrix
ω	Angular Velocity; Characteristic (Poincaré) Exponents

Abstract

The attitude of a spinning symmetrical satellite in an elliptical orbit is analyzed. The perturbed motion of the satellite is described by linear equations with periodic coefficients. Stability is determined by Floquet theory. Active control is added to the system and results lead to a linear periodic control law. Scalar control from the linearized system is implemented to evaluate the performance of the control law on the non-linear equations of motion. For small disturbances, it is illustrated the controlled non-linear response duplicates the linear case. For larger disturbances, phase portraits show the resulting behavior of the coupled modes. As the perturbed motion increases in magnitude stability regions appear. Initial motion results either a return to the initial equilibrium, an oscillation around the equilibrium point or divergence from the initial equilibrium.

Chapter 1

Introduction

Since satellites were first put into orbit, designers have been concerned with maintaining the attitude with respect to some fixed reference. As satellites have grown more complex and expensive, this concern has increased. With this increased complexity has come an increase in the need for precision pointing. Attitude control of a satellite is now of extreme concern. Through the years various methods have been used to achieve this attitude control (ref 1). Satellites in near circular orbits can be designed to take advantage of the gravity gradient to produce attitude control. However, this method has one main restriction. Low natural frequencies result in long decay times for any disturbance. While this may be sufficient for some systems, it certainly would not be sufficient for any precision surveillance. Active control must be used for many satellites. While there are many possible control systems, each with its advantages and disadvantages, the one of interest here is the gyroscope.

The gyroscope, with its large angular momentum and torque free motion has long been utilized as an ideal attitude reference device. The next natural step was to make the satellite a gyroscope by spinning it about one of its axes. The stability of a spinning unsymmetrical satellite in a circular orbit was investigated by Kane and Shippy (ref 5) in 1963. Kane and Barba

(ref 4) also studied a spinning symmetrical satellite in an elliptical orbit in 1966. Both these investigations yielded equations which were non-linear and non-autonomous. In both cases the satellites were modeled as a time periodic linear system, with the stability determined by Floquet theory. In Kane and Barba's study of a satellite in an elliptical orbit, it was demonstrated that the stability was dependent on the inertial properties, orbit eccentricity, and satellite spin rate.

The need for more precise attitude control has eliminated gravity gradient stabilization on these satellites. For spinning satellites in an elliptical orbit, many configurations are unstable. Linearized systems with periodic coefficients have recently been given their deserved attention. Myers (ref 7) investigated this type of system for a satellite with two unstable modes. The scheme employed transforming the state variables to modal variables. Calico and Yeakel (ref 2) used a similar technique with one unstable mode.

This thesis extends on the above work by taking the solutions of the linearized equations and applying these solutions to the non-linear equations. Theory states that for 'small' disturbances the non-linear system should be consistent with the linearized system. The unresolved question which remains; How small is 'small'? The modal variables plotted on phase portraits provide information that aid in determining the answer.

Chapter 2

THEORY

In this chapter the equations of motion of an spinning symmetric satellite in an elliptical orbit around the earth are developed. The equations describing both the attitude motion and the trajectory motion of the satellite will be presented. The trajectory equations are uncoupled from the attitude equations but the attitude motion is affected by the periodic orbital motion. The attitude equations are linearized into a system of time periodic linear equations and Floquet theory is used to determine the stability of the system. In Reference 1, it has been shown the unstable system may be stabilized by using feedback control. This control may be supplied by either scalar or a vector control. Scalar control is developed in this thesis. Once the control for the linear system has been developed for 'small' disturbances the control will be applied to stabilized the non-linear system.

2.1 Equations of Motion

The development of the equations of motion presented below is described by Kane and Barba (ref 4). This thesis develops two basic equations for the trajectory of a satellite around a spherical symmetrical attracting body. As described, these equations are developed in any introductory astrodynamics text.

$$\ddot{r} - r\dot{\nu}^2 + \frac{n^2 a^3}{r^2} = 0 \qquad (2.2.1)$$

$$r^2\dot{\nu} = a^2 n \sqrt{1-e^2} \qquad (2.2.2)$$

where;

$$n \equiv \frac{2\pi}{T} \tag{2.2.3}$$

T is defined as the period of the satellite. The orbital elements r, ν, a, and e are defined in Figure 1,

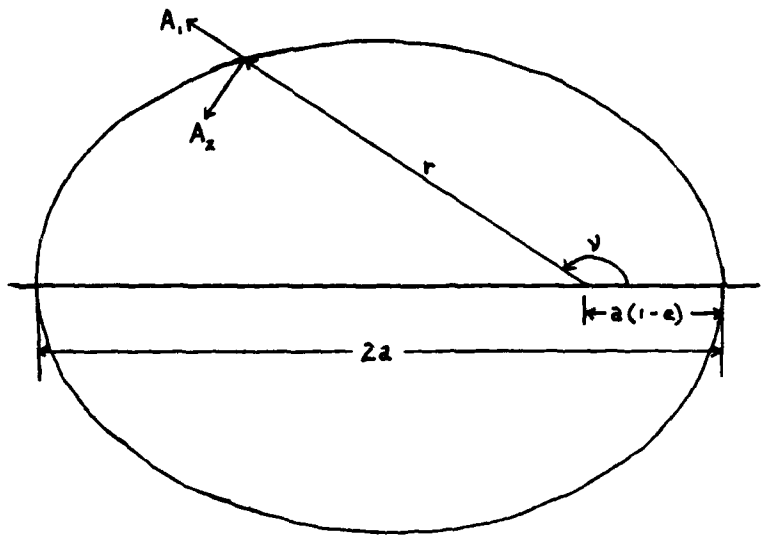

Figure 2.1 Elliptical Orbit Elements

Equations (2.1.1) and (2.1.2) is non-dimensionalized by defining the two non-dimensional variables for time and distance as;

$$\tau = nt \qquad t=\frac{\tau}{n}$$

$$\zeta = \frac{r}{a} \qquad r=\zeta a \tag{2.1.4}$$

Solving equation (2.1.2) for $\dot{\nu}$ yields;

$$\dot{\nu} = \frac{a^2 n\sqrt{1-e^2}}{r^2} \tag{2.1.5}$$

Inserting this value in equation (2.1.1) yields;

$$\ddot{r} - \frac{a^4 n^2 (1-e^2)}{r^3} + \frac{n^2 a^3}{r^2} = 0 \qquad (2.1.6)$$

Before this equation can be non-dimensionalized, differentiation with respect to τ must be defined, (represented by primes)

$$\dot{r} = \frac{dr}{dt} = \frac{d}{d\tau}\left(\frac{d\tau}{dt} r\right) = \frac{d}{d\tau}\left(n\zeta a\right) = \zeta' na$$

$$\ddot{r} = \frac{d}{dt}\left(\frac{dr}{dt}\right) = \frac{d}{d\tau}\left(\frac{d\tau}{dt}\left(\frac{dr}{dt}\right)\right) = \zeta'' n^2 a \qquad (2.1.7)$$

Rearranging equation (2.1.6) yields

$$\frac{\ddot{r}}{n^2 a} + \frac{(e^2-1)a^4 n^2}{r^3 \; a\, n^2} + \frac{n^2 a^3}{n^2 a\, r^2} = 0 \qquad (2.1.8)$$

and using equations (2.1.7) reduces this to

$$\zeta'' + \frac{e^2-1}{\zeta^3} + \frac{1}{\zeta^2} = 0 \qquad (2.1.9)$$

The value of t_o or τ_o can be arbitrarily selected. Therefore, for convenience, it is assumed the satellite is at perigee for $t=\tau=0$. Hence,

$$r_p = a(1-e) \qquad \dot{r}_p = 0$$

$$\zeta(0) = \frac{r}{a} = 1-e \qquad \zeta'(0) = 0 \qquad (2.1.10)$$

Non-dimensionalizing the true anomaly in equation (2.1.5), and noting primes represent differentiation with respect to τ produces

$$\frac{d\nu}{d\tau} = \frac{d\nu}{dt}\frac{dt}{d\tau} = \frac{a^2 n\sqrt{1-e^2}}{r^2}\frac{1}{n} \qquad (2.1.11)$$

$$\nu' = \frac{\sqrt{1-e^2}}{\zeta^2}$$

$$\frac{d}{d\tau}\left(\frac{d\nu}{d\tau}\right) = \frac{d}{d\tau}\left[\frac{\sqrt{1-e^2}}{\zeta^2}\right] \qquad (2.1.12)$$

$$\nu'' = \frac{-2\sqrt{1-e^2}}{\zeta^3}\,\zeta'$$

Note that ζ is a periodic function of τ with period 2π.

To develop the equations of motion for a spinning satellite in an elliptical orbit, it is assumed the satellite's orbit is not effected by the orientation of the satellite (i.e., the satellite is considered to be a point mass).

The satellite's orientation with respect to the orbital axes is determined by defining an orbital reference frame A. Frame A is defined such that A_1 points outward along the radius vector. A_2 will be perpendicular to A_1 in the orbital plane and defined such that at perigee and apogee the satellite will be moving in the positive A_2 direction only. A_3 will be perpendicular to both A_2 and A_3 in such a way to form a right handed coordinate system (illustrated in Figure 2.1).

The body axes is defined in frame X and is obtained from frame A by a 1-2-3 rotation through angle θ_1,θ_2, and θ_3 (illustrated in Figure 2.2). The satellite is symmetrical, having two equal moments of inertia, therefore, a nodal axes will be used which is one rotation away from the body axes. Thus it can be

obtained through a 1-2 rotation.

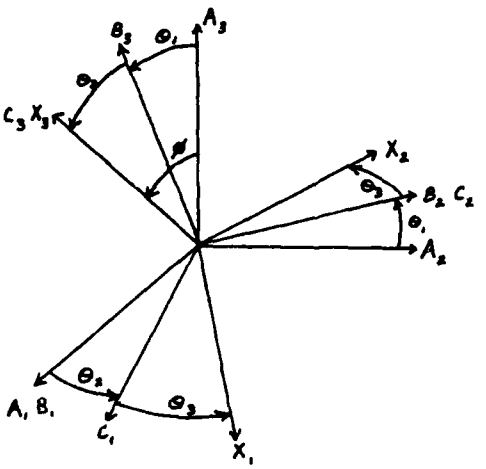

Figure 2.2 1-2-3 Rotation

The angular velocity of the orbital reference frame A, with respect to an inertial frame, $\bar{\omega}^{A/I}$ and the angular velocity of the satellite, $\bar{\omega}^{X/I}$, expressed in the nodal axes are respectively,

$$\bar{\omega}^{A/I} = \dot{\nu}\hat{e}_{A_3} \qquad \bar{\omega}^{X/I} = \begin{Bmatrix} \omega_1 \\ \omega_2 \\ \omega_3 \end{Bmatrix}_N \tag{2.1.13}$$

Stepping through the rotations will develop the orbital rates of the different frames, .

Rotations -

i) about A_1 through Θ_1 to F_B (Frame B)

$$\bar{\omega}^{B/A} = \dot{\Theta}_1\hat{e}_{B_1} = \dot{\Theta}_1\hat{e}_{A_1} \tag{2.1.14}$$

ii) about B_2 through Θ_2 to F_C (nodal)

$$\bar{\omega}^{C/B} = \dot{\Theta}_2\hat{e}_{B_2} = \dot{\Theta}_2\hat{e}_{C_2} \tag{2.1.15}$$

The angular velocities may be added when in the same reference frame.

$$\left\{\omega^{C/I}\right\}_C = \left\{\omega^{C/B}\right\}_C + L_{CB}\left\{\omega^{B/A}\right\}_B + L_{CA}\left\{\omega^{A/I}\right\}_A \qquad (2.1.16)$$

The transformation matrices used in equation (2.1.16) are defined as follows;

$$L_{CB} = \begin{bmatrix} \cos\theta_2 & 0 & -\sin\theta_2 \\ 0 & 1 & 0 \\ \sin\theta_2 & 0 & \cos\theta_2 \end{bmatrix} \qquad (2.1.17)$$

$$L_{BA} = \begin{bmatrix} 1 & 0 & 0 \\ 0 & \cos\theta_1 & \sin\theta_1 \\ 0 & -\sin\theta_1 & \cos\theta_1 \end{bmatrix} \qquad (2.1.18)$$

$$L_{CA} = \begin{bmatrix} \cos\theta_2 & \sin\theta_1\sin\theta_2 & -\cos\theta_1\sin\theta_2 \\ 0 & \cos\theta_1 & \sin\theta_1 \\ \sin\theta_2 & -\sin\theta_1\cos\theta_2 & \cos\theta_1\cos\theta_2 \end{bmatrix} \qquad (2.1.19)$$

Expanding equation (2.1.16) and using equations (2.1.17) and (2.1.19), yields the expression for angular velocity expressed in frame C, the nodal frame.

$$\left\{\omega^{C/I}\right\}_C = \dot{\theta}_2\hat{e}_{C_2} + \begin{bmatrix} \cos\theta_2 & 0 & -\sin\theta_2 \\ 0 & 1 & 0 \\ \sin\theta_2 & 0 & \cos\theta_2 \end{bmatrix} \begin{Bmatrix} \theta_1 \\ 0 \\ 0 \end{Bmatrix}$$

$$+ \begin{bmatrix} \cos\theta_2 & \sin\theta_1\sin\theta_2 & -\cos\theta_1\sin\theta_2 \\ 0 & \cos\theta_1 & \sin\theta_1 \\ \sin\theta_2 & -\sin\theta_1\cos\theta_2 & \cos\theta_1\cos\theta_2 \end{bmatrix} \begin{Bmatrix} 0 \\ 0 \\ \dot{\nu} \end{Bmatrix} \qquad (2.1.20)$$

Performing the linear algebra yields;

$$\left\{\omega^{C/I}\right\}_C = \dot{\theta}_2\hat{e}_{C_2} + \dot{\theta}_1\cos\theta_2\hat{e}_{C_1} + \dot{\theta}_1\sin\theta_2\hat{e}_{C_3}$$
$$+ -\dot{\nu}\cos\theta_1\sin\theta_2\hat{e}_{C_1} + \dot{\nu}\sin\theta_1\hat{e}_{C_2} + \dot{\nu}\cos\theta_1\cos\theta_2\hat{e}_{C_3} \qquad (2.1.21)$$

Or written in matrix form;

$$\left\{\omega^{C/I}\right\}_C = \begin{Bmatrix} \dot{\theta}_1 \cos\theta_2 - \dot{\nu}\cos\theta_1\sin\theta_2 \\ \dot{\theta}_2^e + \dot{\nu}\sin\theta_1 \\ \dot{\theta}\sin\theta_2 + \dot{\nu}\cos\theta_1\cos\theta_2 \end{Bmatrix} \qquad (2.1.22)$$

This is the angular velocity with respect to the inertial frame written in the nodal frame.

iii) The last rotation θ_3, is about C_3 to obtain to the body frame X. It is expressed in the nodal frame in order to achieve the final form as

$$\left\{\omega^{X/C}\right\}_C = \begin{Bmatrix} 0 \\ 0 \\ \dot{\theta}_3 \end{Bmatrix} \qquad (2.1.23)$$

$$\left\{\omega^{X/I}\right\}_C = \left\{\omega^{C/I}\right\}_C + \left\{\omega^{X/C}\right\}_C \qquad (2.1.24)$$

$$\left\{\omega^{X/I}\right\}_C = \begin{Bmatrix} \omega_1 \\ \omega_2 \\ \omega_3 \end{Bmatrix} = \begin{Bmatrix} \dot{\theta}_1\cos\theta_2 - \dot{\nu}\cos\theta_1\sin\theta_2 \\ \dot{\theta}_2 + \dot{\nu}\sin\theta_1 \\ \dot{\theta}_1\sin\theta_2 + \dot{\nu}\cos\theta_1\cos\theta_2 + \dot{\theta}_3 \end{Bmatrix} \qquad (2.1.25)$$

Defining $\omega_3' \equiv \omega_3 - \dot{\theta}_3$ or,

$$\omega_3' = \dot{\theta}_1\sin\theta_2 + \dot{\nu}\cos\theta_1\cos\theta_2 \qquad (2.1.26)$$

produces,

$$\left\{\omega^{X/I}\right\}_C = \begin{Bmatrix} \omega_1 \\ \omega_2 \\ \omega_3' + \dot{\theta}_3 \end{Bmatrix} \qquad (2.1.27)$$

Angular momentum vector about the center of mass is defined as;

$$\left\{H_C\right\}_C = \left[I_C\right]_C \left\{\omega^{X/I}\right\}_C \qquad (2.2.28)$$

Assuming a symmetric satellite, the moment of inertia matrix has

the form;

$$\left[I_C\right]_C = \begin{bmatrix} A & 0 & 0 \\ 0 & A & 0 \\ 0 & 0 & C \end{bmatrix} \tag{2.1.29}$$

therefore;

$$\left\{H_C\right\}_C = \begin{bmatrix} A & 0 & 0 \\ 0 & A & 0 \\ 0 & 0 & C \end{bmatrix} \begin{Bmatrix} \omega_1 \\ \omega_2 \\ \omega_3 \end{Bmatrix} \tag{2.1.30}$$

From Euler's moment equation;

$$\frac{d^I}{dt}\left\{H_C\right\}_C = \left\{M_C\right\}_C \tag{2.1.31}$$

$$\frac{d^C}{dt}\left\{H_C\right\}_C + \tilde{\omega}^{C/I}\left\{H_C\right\}_C = \left\{M_C\right\}_C \tag{2.1.32}$$

where

$$\tilde{\omega}^{C/I} = \begin{bmatrix} 0 & -\omega_3' & \omega_2 \\ \omega_3' & 0 & -\omega_1 \\ -\omega_2 & \omega_1 & 0 \end{bmatrix} \tag{2.1.33}$$

Noting $\left[I_C\right]_C$ in equation (2.1.28) is constant, equation (2.1.32) becomes;

$$\begin{bmatrix} A & 0 & 0 \\ 0 & A & 0 \\ 0 & 0 & C \end{bmatrix} \begin{Bmatrix} \dot{\omega}_1 \\ \dot{\omega}_2 \\ \dot{\omega}_3 \end{Bmatrix} + \begin{bmatrix} 0 & -\omega_3' & \omega_2 \\ \omega_3' & 0 & -\omega_1 \\ -\omega_2 & \omega_1 & 0 \end{bmatrix} \begin{bmatrix} A & 0 & 0 \\ 0 & A & 0 \\ 0 & 0 & C \end{bmatrix} \begin{Bmatrix} \omega_1 \\ \omega_2 \\ \omega_3 \end{Bmatrix} = \begin{Bmatrix} M_1 \\ M_2 \\ M_3 \end{Bmatrix} \tag{2.1.34}$$

Again, linear algebra operations yield;

$$\begin{Bmatrix} A\dot{\omega}_1 \\ A\dot{\omega}_2 \\ C\dot{\omega}_3 \end{Bmatrix} + \begin{bmatrix} 0 & -\omega_3' & \omega_2 \\ \omega_3' & 0 & -\omega_1 \\ -\omega_2 & \omega_1 & 0 \end{bmatrix} \begin{Bmatrix} A\omega_1 \\ A\omega_2 \\ C\omega_3 \end{Bmatrix} = \begin{Bmatrix} M_1 \\ M_2 \\ M_3 \end{Bmatrix} \tag{2.1.35}$$

Further linear algebra gives three equations;

$$A\dot{\omega}_1 + \left[-A\omega_2\omega_3' + C\omega_2\omega_3\right] = M_1 \qquad (2.1.36a)$$

$$A\dot{\omega}_2 + A\omega_1\omega_3' - C\omega_1\omega_3 = M_2 \qquad (2.1.36b)$$

$$C\dot{\omega}_3 - A\omega_1\omega_2 + A\omega_1\omega_2 = M_3 \qquad (2.1.36c)$$

Expanding equations (2.1.36) with the definition of ω_3' gives

$$A\dot{\omega}_1 - A\omega_2\omega_3 + A\omega_2\dot{\theta}_3 + C\omega_2\omega_3 = M_1 \qquad (2.1.37a)$$

$$A\dot{\omega}_2 - A\omega_1\omega_3 - A\omega_1\dot{\theta}_3 - C\omega_1\omega_3 = M_2 \qquad (2.1.37b)$$

$$C\dot{\omega}_3 = M_3 \qquad (2.1.37c)$$

Dividing by the moment of inertia A, and combining terms produces

$$\dot{\omega}_1 + \frac{C-A}{A}\omega_2\omega_3 + \omega_2\dot{\theta}_3 = \frac{M_1}{A} \qquad (2.1.38a)$$

$$\dot{\omega}_2 + \frac{A-C}{A}\omega_1\omega_3 - \omega_1\dot{\theta}_3 = \frac{M_2}{A} \qquad (2.1.38b)$$

$$\dot{\omega}_3 = \frac{M_3}{C} \qquad (2.1.38c)$$

With the applied moments being (4;403)

$$M_1 = 0 \qquad (2.1.39a)$$

$$M_2 = 3\frac{n^2}{\zeta^3}(A-C)\sin\theta_2\cos\theta_2 \qquad (2.1.39b)$$

$$M_3 = 0 \qquad (2.1.39c)$$

To simplify notation, define;

$$K \equiv \frac{C-A}{A} \qquad (2.1.40)$$

and rewrite equations (2.1.38) as;

$$\dot{\omega}_1 + K\omega_2\omega_3 + \omega_2\dot{\theta}_3 = 0 \qquad (2.1.41a)$$

$$\dot{\omega}_2 - K\omega_1\omega_3 - \omega_1\dot{\theta}_3 = \frac{-3n^2K\sin\theta_2\cos\theta_2}{\zeta^3} \qquad (2.1.41b)$$

$$\dot{\omega}_3 = 0 \qquad (2.1.41c)$$

Taking the derivative with respect to time of equation (2.1.25) also results in expressions for the rate of change for the angular velocity,

$$\dot{\omega}_1 = \ddot{\theta}_1\cos\theta_2 - \dot{\theta}_1\dot{\theta}_2\sin\theta_2 - \ddot{\nu}\cos\theta_1\sin\theta_2 + \dot{\nu}\dot{\theta}_1\sin\theta_1\sin\theta_2 - \dot{\nu}\dot{\theta}_2\cos\theta_1\cos\theta_2$$

$$\dot{\omega}_2 = \ddot{\theta}_2 + \ddot{\nu}\sin\theta_1 + \dot{\nu}\dot{\theta}_1\cos\theta_1 \qquad (2.1.42)$$

$$\dot{\omega}_3 = \ddot{\theta}_1\sin\theta_2 + \dot{\theta}_1\dot{\theta}_2\sin\theta_2 + \ddot{\nu}\cos\theta_1\cos\theta_2 - \dot{\nu}\dot{\theta}_1\sin\theta_1\cos\theta_2 - \dot{\nu}\dot{\theta}_2\cos\theta_1\sin\theta_2 + \ddot{\theta}_3$$

The next step in solving the equations of motion is to linearize the equations about an equilibrium point. Later, this solution will be inserted into the non-linear equations. The equilibrium point is chosen such that $\theta_1 = \theta_2 = 0$. θ_3 is chosen after small angle approximations are made on equation (2.1.22);

$$\omega_1 = \dot{\theta}_1 - \dot{\nu}\theta_2 \qquad (2.1.43a)$$

$$\omega_2 = \dot{\theta}_2 + \dot{\nu}\theta_1 \qquad (2.1.43b)$$

$$\omega_3 = \dot{\theta}_3 + \dot{\nu} \qquad (2.1.43c)$$

Integrating equation (2.1.43c) yields,

$$\omega_3 t = \theta_3 + \theta_{3_o} + \nu + \nu_o \qquad (2.1.44)$$

dropping the subscript on ω and with $\nu_o = \theta_{3_o} = 0$, solving for θ_3;

$$\theta_3 = \omega t - \nu \qquad (2.1.45)$$

where $\omega = n(1+\alpha)$ with n defined in equation (2.1.3) and α is the constant spin rate about the C_3 axis. With these values substituted in equations (2.1.42) and (2.1.39), the accelerations $\dot{\omega}_i = 0$ and the external moments $M_i = 0$. With this equilibrium point, the C_3 axis remains perpendicular to the orbital plane. If this is a stable equilibrium point the satellite will return to

this orientation if disturbed by a 'small' amount. To determine if this is a stable point, state variables are defined;

$$\bar{x}^T = \left[\theta_1 \; \theta_2 \; \theta_1' \; \theta_2' \right] \tag{2.1.46}$$

and the perturbation of the state vector in the linearized system,

$$\bar{x}' = A\bar{x} \tag{2.1.47}$$

The first two rows of the A matrix are trivial, the remaining two rows are found by taking derivatives of equations (2.1.43);

$$\dot{\omega}_1 = \ddot{\theta}_1 - \ddot{\nu}\theta_2 - \dot{\nu}\dot{\theta}_2 \tag{2.1.48a}$$

$$\dot{\omega}_2 = \ddot{\theta}_2 + \dot{\nu}\dot{\theta}_1 + \ddot{\nu}\theta \tag{2.1.48b}$$

$$\dot{\omega}_3 = \ddot{\theta}_3 + \ddot{\nu} \tag{2.1.48c}$$

Substituting the values of ω from equations (2.1.43) and $\dot{\omega}$ from equations (2.1.48) in equation (2.1.41a) yields;

$$\ddot{\theta}_1 - \ddot{\nu}\theta_2 - \dot{\nu}\dot{\theta}_2 + K\left[\dot{\theta}_2 + \dot{\nu}\theta_1\right]\left[\dot{\theta}_3 + \dot{\nu}\right] + \left[\dot{\theta}_2 + \dot{\nu}\theta_1\right]\dot{\theta}_3 = 0 \tag{2.1.49}$$

$$\ddot{\theta}_1 = -\dot{\nu}\left[\dot{\theta}_3 + K\dot{\nu} + K\dot{\theta}_3\right]\theta_1 + \ddot{\nu}\theta_2 + \left[\dot{\nu} - \dot{\theta}_3 - K\left[\dot{\nu} + \dot{\theta}_3\right]\right]\dot{\theta}_2 \tag{2.1.50}$$

and using the chain rule, the derivative w.r.t. τ is produced,

$$n^2\theta_1'' = -n\nu'\left[n\theta_3' + Kn\nu' + Kn\theta_3'\right]\theta_1 + n^2\nu''\theta_2 + \left[n\nu' - n\theta_3' - Kn\left[\nu' + \theta_3'\right]\right]n\theta_2'$$

This reduces to the identical equation as (2.1.50) but, w.r.t. τ;

$$\theta_1'' = -\nu'\left[\theta_3' + K\nu' + K\theta_3'\right]\theta_1 + \nu''\theta_2 + \left[\nu' - \theta_3' - K\left[\nu' + \theta_3'\right]\right]\theta_2' \tag{2.1.51}$$

Equation (2.1.51) produces the third row of the A matrix. Utilizing equation (2.1.41b) and again using small angle approximations on the right side produces an equation for $\ddot{\theta}_2$;

$$\ddot{\theta}_2+\dot{\nu}\dot{\theta}_1+\ddot{\nu}\theta_1-K\left[\dot{\theta}_1-\dot{\nu}\theta_2\right]\left[\dot{\theta}_3+\dot{\nu}\right]-\left[\dot{\theta}_1-\dot{\nu}\theta_2\right]\dot{\theta}_3=\frac{-3n^2K\theta_2}{\zeta} \qquad (2.1.52)$$

Changing the derivatives to primes, solving for θ_2'' and factoring terms yield the fourth row;

$$\theta_2''=-\nu''\theta_1+\left[-\nu'\left(\theta_3'+K\nu'+K\theta_3'\right)-\frac{3K}{\zeta^3}\right]\theta_2-\left[\nu'-\theta_3'-K\left[\nu'+\theta_3'\right]\right]\theta_1' \qquad (2.1.53)$$

Equation (2.1.47) may now be written as,

$$\begin{Bmatrix}\theta_1'\\ \theta_2'\\ \theta_1''\\ \theta_2''\end{Bmatrix}=\begin{bmatrix}0 & 0 & 1 & 0\\ 0 & 0 & 0 & 1\\ A_{31} & \nu'' & 0 & A_{34}\\ -\nu'' & A_{42} & -A_{34} & 0\end{bmatrix}\begin{Bmatrix}\theta_1\\ \theta_2\\ \theta_1'\\ \theta_2'\end{Bmatrix} \qquad (2.1.54)$$

where elements of A are defined as shown and;

$$A_{31}=-\nu'\left(\theta_3'+K\nu'+K\theta_3'\right)$$
$$A_{34}=\nu'-\theta_3'-K\left(\nu'+\theta_3'\right)$$
$$A_{42}=A_{31}-\frac{3K}{\zeta^3}$$

A is now expressed in terms of ν', ν'', θ_3' and ζ. It is desirable to have A expressed in terms of one variable ζ and its derivative ζ'. This can be easily done by replacing ν' and ν'' using equations (2.1.11) and (2.1.12). θ_3' may be eliminated by noting $\dot{\omega}_3=0$, hence ω_3 is a constant, or from equation (2.1.43c),

$$\nu'+\theta_3'=\text{constant} \qquad (2.1.55)$$

Let the constant be $(\alpha+1)$, then

$$\theta_3'=(\alpha+1)-\frac{\sqrt{1-e^2}}{\zeta^2} \qquad (2.1.56)$$

A is now expressed in a more convenient form with the non-zero

elements of equation (2.1.54) as

$$A_{13} = A_{24} = 1$$

$$A_{31} = \frac{(1-e^2)}{\zeta^4} - (\alpha+1)(1+K)\frac{\sqrt{1-e^2}}{\zeta^2}$$

$$A_{32} = \frac{-2\sqrt{1-e^2}}{\zeta^3}\zeta'$$

$$A_{34} = 2\frac{\sqrt{1-e^2}}{\zeta^2} - (\alpha+1)(1+K)$$

$$A_{42} = A_{31} - \frac{3K}{\zeta^3}$$

2.2 FLOQUET THEORY

The system here is time periodic with period T,

$$A(\tau) = A(\tau+T) \tag{2.2.1}$$

therefore the stability can be found using Floquet Theory. Floquet discovered this technique in the latter half of the 1800's. Our time periodic system is represented by;

$$\bar{x}' = A(\tau)\bar{x} \tag{2.2.2}$$

where $\bar{x}$ is the state vector and $\bar{x}'$ is the derivative with respect to τ. The variable τ is used, instead of time, as a non-dimensional variable. $A(\tau)$ is known and is a periodic matrix with period T. Any solution $\bar{x}(\tau)$ may be written in the form

$$\bar{x}(\tau) = \psi(\tau,\tau_o)\bar{c} \tag{2.2.3}$$

where $\psi(\tau,\tau_o)$ is a fundamental matrix and $\bar{c}$ a constant vector.

Solving for $\bar{c}$ yields,

$$\bar{c}=\psi^{-1}(\tau_o,\tau_o)\bar{x}(\tau_o) \qquad (2.2.4)$$

When $\psi(\tau_o,\tau_o)$ = I, the identity matrix, $\psi(\tau,\tau_o)$ is termed the Principal Fundamental Matrix and (2.2.3) becomes

$$\bar{x}(\tau)=\Phi(\tau,\tau_o)\bar{x}(\tau_o) \qquad (2.2.5)$$

where the Principal Fundamental Matrix is denoted by Φ and has the property

$$\Phi(\tau_o,\tau_o)= I \qquad (2.2.6)$$

By letting $\tau_o=0$,

$$\Phi(0,0)= I \qquad (2.2.7)$$

The $\Phi(\tau,0)$ matrix has columns ϕ_i, of which the first, $\bar{\phi}_1$ is obtained by solving

$$\dot{\bar{\phi}}_1=A(\tau)\bar{\phi}_1 \qquad (2.2.8)$$

In general,

$$\dot{\bar{\phi}}_i=A(\tau)\bar{\phi}_i \ , \quad \bar{\phi}_i(0)=\left\{\begin{matrix}0\\ \vdots\\ 1\ \text{ith}\\ \vdots\\ 0\end{matrix}\right\} \qquad (2.2.9)$$

or,

$$\dot{\Phi}(\tau,0)=A(\tau)\Phi(\tau,0) \qquad (2.2.10)$$

Equation 2.2.10 can be solved numerically using the initial conditions from equation 2.2.7. Numerical integration would also be used to simultaneously solve for the variables ζ and ζ' contained in the matrix A.

All of the above equations are true for all time dependent matrices. Floquet Theory states $\Phi(\tau,0)$ can be factored into two

matrices, F and J, in the manner,

$$\Phi(\tau,\theta)=F(\tau)e^{J\tau}F^{-1}(\theta) \qquad (2.2.11)$$

The J matrix is a constant matrix and, for convenience, is expressed in Jordan normal form. The diagonals of the J matrix are the analog of the eigenvalues for a constant coefficient system and are called the Poincaré exponents, ω_i.

The matrix $F(\tau)$ is a time periodic matrix with the same period, T, as the original system (equation (2.2.2)). If the system had constant coefficients, F would be the constant matrix of eigenvalues. Thus, solving the Floquet problem reduces to determining the constant matrix J and the periodic matrix F over one period.

Evaluating $\Phi(T,\theta)$ (recall T is the system period), yields

$$\Phi(T,\theta)=F(T)e^{JT}F^{-1}(\theta) \qquad (2.2.12)$$

However, $F(T)=F(\theta)$ since $F(\tau)$ is periodic. Therefore equation (2.2.12) becomes

$$\Phi(T,\theta)=F(\theta)e^{JT}F^{-1}(\theta) \qquad (2.2.13)$$

The matrix $\Phi(T,\theta)$ is called the monodromy matrix and $F(\theta)$ is the matrix of eigenvectors of $\Phi(T,\theta)$. The technique of constructing the monodromy matrix is to numerically integrate equation 2.2.10.

From equation (2.2.13) it is seen $\Phi(T,\theta)$ and e^{JT} are similar and therefore have the same eigenvalues, λ_i. If the λ_i were real, J would be a diagonal matrix with the Poincaré exponents, ω_i, on the diagonal. The eigenvalues of J, the Poincaré exponents ω_i, are related to the eigenvalues of e^{JT} (or $\Phi(T,\theta)$) by

$$\lambda_i=\exp(\omega_i T) \qquad (2.2.14)$$

or

$$\omega_i = \frac{1}{T} \ln \lambda_i \tag{2.2.15}$$

If the λ_i are complex then taking the log requires,

$$\omega_i = \frac{1}{T} \left[\ln |\lambda_i| + i \arg(\lambda_i) \right] \tag{2.2.16}$$

The stability of the system is now available. Since $F(\tau)$ is periodic, the stability of the system is governed by ω_i (or λ_i). If all of the Poincaré exponents, ω_i, have negative real parts, or, if working with λ_i, $|\lambda_i|<1$, then the system is stable.

Usually Floquet analysis is used only to determine stability, and therefore stops at this point. For this study, however, the complete solution is required, so $F(\tau)$ over one period must be determined. Substituting equation (2.2.11) into equation (2.2.10) produces

$$\frac{d}{d\tau} F(\tau) = A(\tau)F(\tau) - F(\tau)J \tag{2.2.17}$$

Once $F(\tau)$ is determined numerically, since it is periodic, it can be expressed in terms of its Fourier coefficients.

Since both matrices F and J may be complex, the above results may be inconvenient. However, they can be arranged so that both are real. F should be arranged in column vectors, f_i, if the eigenvalues are real. If they are complex, the column will be f_{ireal}, f_{iimag}. The matrix J will no longer be in Jordon normal form, instead it will consist of diagonal real entries ω_i if the eigenvalues are real or for a pair of complex ω_i, J will have diagonal blocks of the form;

$$\begin{bmatrix} Re(\omega_i) & Im(\omega_i) \\ -Im(\omega_i) & Re(\omega_i) \end{bmatrix} \tag{2.2.18}$$

The matrix $\exp(J\tau)$ will contain diagonal entries $\exp(\omega_i\tau)$ for real entries, or diagonal blocks;

$$\exp\left(\mathrm{Re}(\omega_i)\tau\right)\begin{bmatrix} \cos\mathrm{Im}(\omega_i)\tau & \sin\mathrm{Im}(\omega_i)\tau \\ -\sin\mathrm{Im}(\omega_i)\tau & \cos\mathrm{Im}(\omega_i)\tau \end{bmatrix} \qquad (2.2.19a)$$

for blocks of J of the form of Eq. (2.2.18). With these changes, the previous formulae stay unaltered. Since this is a periodic system, after one period $\exp(\omega_i T)$ is simply λ_i, therefore the matrix $\exp(JT)$ is easily constructed as

$$\exp(JT)=\begin{bmatrix} \mathrm{Re}(\lambda_i) & \mathrm{Im}(\lambda_i) \\ -\mathrm{Im}(\lambda_i) & \mathrm{Re}(\lambda_i) \end{bmatrix} \qquad (2.2.19b)$$

It is often necessary, or at least more convenient, to use the inverse matrix $F^{-1}(\tau)$. The state transition matrix is never singular (ref 1), therefore $F(\tau)$ is always invertable. One method of obtaining $F^{-1}(\tau)$ is to invert $F(\tau)$ at a given value of τ. However, this method can be expensive in both time and round off errors. Another method is to differentiate the identity $FF^{-1}=I$,

$$\frac{d}{d\tau}\left(F\right)F^{-1}+F\,\frac{d}{d\tau}\left(F^{-1}\right)=0$$

$$\frac{d}{d\tau}\left(F^{-1}\right)=-F^{-1}\,\frac{d}{d\tau}\left(F\right)\,F^{-1} \qquad (2.2.20)$$

and the value for F' substituted from Eq. (2.2.17),

$$\frac{d}{d\tau}\left(F^{-1}\right)=-F^{-1}[A(\tau)F(\tau)-F(\tau)J]\,F^{-1}$$

$$\frac{d}{d\tau}\left(F^{-1}\right)=-F^{-1}A(\tau)+JF^{-1} \qquad (2.2.21)$$

Therefore $F^{-1}(\tau)$ can be constructed by numerical integration and transformed into its Fourier series coefficients without having to find $F(\tau)$. To develop the system with $F^{-1}(\tau)$ the initial

conditions, or $F^{-1}(\theta)$ must be known. Since it has been shown from equation (2.2.13), $F(\theta)$ is the matrix of eigenvectors of $\Phi(T)$ (which may be complex), a real matrix $F(\theta)$ can be constructed in the same manner as was developed with the F and J matrices. Taking the inverse of this constant real matrix.

$$F^{-1}(\theta)=\left[\begin{matrix}\overline{f}_{1_{real}} & \overline{f}_{1_{imag}} & \overline{f}_{3_{real}} & \overline{f}_{3_{imag}}\end{matrix}\right]^{-1} \tag{2.2.22}$$

and constructing J from the Poincaré exponents,

$$J = \begin{bmatrix} \mathrm{Re}\left(\omega_1\right) & \mathrm{Im}\left(\omega_1\right) & 0 & 0 \\ -\mathrm{Im}\left(\omega_1\right) & \mathrm{Re}\left(\omega_1\right) & 0 & 0 \\ 0 & 0 & \mathrm{Re}\left(\omega_3\right) & \mathrm{Im}\left(\omega_3\right) \\ 0 & 0 & -\mathrm{Im}\left(\omega_3\right) & \mathrm{Re}\left(\omega_3\right) \end{bmatrix} \tag{2.2.23}$$

$F^{-1}(\tau)$ may also be related to the modal matrix associated with equation (2.2.2), i.e., the adjoint problem;

$$\frac{d}{d\tau}y(\tau) = -A^{T}y(\tau) \tag{2.2.24}$$

Letting the modal matrix associated with $-A^{T}$ be $L(\tau)$, it can be found that

$$\begin{aligned}\frac{d}{d\tau}L(\tau) &= -A^{T}(\tau)L(\tau)+L(\tau)J^{T} \\ &= L(\tau)J^{T}- A^{T}(\tau)L(\tau)\end{aligned} \tag{2.2.25}$$

or taking the transpose,

$$\frac{d}{d\tau}L^{T}(\tau) = -L^{T}(\tau)A(\tau)+JL(\tau)^{T} \tag{2.2.26}$$

By comparing this equation with (2.2.21) it can be seen that

$$F^{-1}(\tau)=L^{T}(\tau) \tag{2.2.27a}$$

or

$$L(\tau)=\left[F^{-1}(\tau)\right]^{T} \tag{2.2.27b}$$

with

$$L(\theta)=\left[F^{-1}(\theta)\right]^{T} \tag{2.2.27c}$$

This illustrates the orthogonality between the eigenvalues of the adjoint problem to the eigenvalues of the original system. Solving equation (2.2.25) is the preferred technique for constructing $F^{-1}(\tau)$.

Introducing a new modal variable η such that

$$x(\tau)=F(\tau)\eta(\tau) \tag{2.2.28}$$

and substituting into equation (2.2.2), an equation for η' is developed.

$$x'=F'\eta+F\eta'$$

$$x'=Ax \longrightarrow F'\eta+F\eta'=AF\eta$$

$$\eta'=F^{-1}AF\eta-F^{-1}F'\eta$$

$$\eta'=\left[F^{-1}AF-F^{-1}F'\right]\eta$$

$$\eta'=\left[F^{-1}AF-F^{-1}(AF-FJ)\right]\eta$$

$$\eta'=\left[F^{-1}AF-F^{-1}AF-F^{-1}FJ\right]\eta$$

which reduces to

$$\eta'=J\eta \tag{2.2.30}$$

Therefore, the eigenvector matrix $F(\tau)$ is a periodic transformation which changes the time periodic system of equation (2.2.2) to a constant coefficient system, (2.2.30), since J is a constant matrix. If the Poincaré exponents are real and distinct, J is diagonal and the system described by equation (2.2.30)

reduces to n uncoupled ordinary differential equations. If the Poincaré exponents are complex, J is put in a block diagonal form with the real parts on the diagonal and the imaginary parts on the off-diagonal. Each complex pair results in a pair of coupled equations.

2.3 Modal Control Theory

The open-loop characteristics of equation (2.2.2) are determined by the Poincaré exponents. These exponents, and therefore the system stability, can be changed by adding feedback control. The system has the form of a standard control problem

$$x'(\tau)=A(\tau)x(\tau)+B(\tau)u(\tau) \qquad (2.3.1)$$

where the control matrix $B(\tau)$ is either constant of periodic with the same period T as the fundamental system and $u(\tau)$ is the control vector. Assuming full state feedback;

$$u(\tau)=G(\tau)x(\tau) \qquad (2.3.2)$$

where $G(\tau)$ is the gain matrix. Denoting the closed-loop state as x_c, equation (2.3.1) becomes

$$x_c'=(A+BG)x_c \qquad (2.3.3)$$

Using modal variables,

$$x_c=F\eta_c$$

$$x_c'=F'\eta_c+F\eta_c$$

equation (2.3.3) becomes

$$F'\eta_c+F\eta_c=(A+BG)F\eta_c$$

$$F'\eta_c+F\eta_c=AF\eta_c+BGF\eta_c$$

$$\eta_c' = F^{-1}AF\eta_c - F^{-1}F'\eta_c + F^{-1}BGF\eta_c$$

$$\eta_c' = \left[F^{-1}AF - F^{-1}F' + F^{-1}BGF\right]\eta_c$$

$$\eta_c' = \left[J + F^{-1}BGF\right]\eta_c \qquad (2.3.4)$$

which is a Floquet problem if it is assumed that, at worst, $G(\tau)$ is periodic with period T. $G(\tau)$ must be determined such that the closed-loop system has acceptable properties. For this analysis a modal control technique was used for a periodic system in which the control will be a scalar control. This scalar control was implemented on the Poincaré exponents which are complex conjugates.

For scalar control equation (2.3.4) is

$$\eta' = J\eta + g(\tau)u(\tau) \qquad (2.3.5)$$

where $g(\tau)$ is the n x 1 periodic mode controlability matrix,

$$g(\tau) = L^{T}(\tau)\, B(\tau) \qquad (2.3.6)$$

Modes η_{ci} are controllable if the corresponding element g_i is non-zero. In the case considered here two modes will be controlled at once; the two having complex conjugates of the Poincaré exponents with positive real parts. Therefore the control is given by

$$u = k(\tau)\,\eta \qquad (2.3.7)$$

where $k = [0, 0, \ldots, k_i, \ldots, k_j, \ldots]$. The elements i and j may be made to occur consecutively by simply reordering the equations. The resulting closed-loop equations can be expressed in matrix form with j replaced by $i+1$ as

$$\eta_c' = \begin{bmatrix} \omega_1 & k_i g_1 & k_{i+1} g_1 & 0 \\ \cdots & \cdots & \cdots & \cdots \\ 0 & \omega_i + k_i g_i & k_{i+1} g_i & 0 \\ 0 & k_i g_{i+1} & \omega_{i+1} + k_{i+1} g_{i+1} & 0 \\ \cdots & \cdots & \cdots & \cdots \\ 0 & k_i g_N & k_{i+1} g_N & \omega_N \end{bmatrix} \eta_c \qquad (2.3.8)$$

From equation (2.3.8), it can be seen, except for the ith and i+1 term, this closed-loop system has the same Poincaré exponents as the open-loop system. These two components are determined from the coupled equations for the two modes η_i and η_{i+1}. Since these two equations are decoupled from the remainder of equation (2.3.8), they can be separated into the two dimensional system

$$\eta_c' = \begin{bmatrix} \omega_1 + k_1 g_1 & k_2 g_1 \\ k_1 g_2 & \omega_2 + k_2 g_2 \end{bmatrix} \eta_c \qquad (2.3.9)$$

It was shown by Calico and Wiesel (ref 1) that when g_1 and g_2 have constant terms in their Fourier series, and constant gains k_1 and k_2 are used, the new Poincaré exponents will be related to the old exponents by

$$\omega_1' + \omega_2' = \omega_1 + \omega_2 + k_1 g_{1c} + k_2 g_{2c} \qquad (2.3.10)$$

This allows the sum of the new Poincaré exponents to be set to any desired value. While this does not provide the ability to set the new exponents individually, it does allow the movement of the coupled pair of exponents. For stability, the sum of these two exponents must be negative. This is a necessary and not a sufficient condition since it does not guarantee the real parts of both exponents are negative (just their sum). Numerical

integration of the new monodromy matrix will determine the actual values of the new Poincaré exponents. In the case where the original Poincaré exponents were complex conjugates, equation (2.3.18) only determines the sum of the real parts. The actual values may be either real or have imaginary parts.

2.4 Development of Non-Linear Equations

The development of the non-linear equations follows from inserting the values for ω_1, ω_2, $\dot{\omega}_1$ and $\dot{\omega}_2$ given in equations (2.1.25), and (2.1.42) into equations (2.1.41a) and (2.1.41b). As in the linear case, since the satellite is spinning about its axis of symmetry, ω_3 is a constant and is $\alpha+1$. Therefore ω_3 can be eliminated from the equations. Setting ω_3 in equation (2.1.25) equal to $\alpha+1$ and solving for θ_3 will also allow the elimination of $\dot{\theta}_3$ from the equations.

$$\dot{\theta}_3 = \alpha+1 - \dot{\theta}_1\sin\theta_2 - \dot{\nu}\cos\theta_1\cos\theta_2 \tag{2.4.1}$$

Working with equation (2.1.41a) first,and noting that derivatives with respect to time and τ only differ by a factor of n for each order derivative yields,

$$\ddot{\theta}_1\cos\theta_2 - \dot{\theta}_1\dot{\theta}_2\sin\theta_2 - \ddot{\nu}\cos\theta_1\sin\theta_2 + \dot{\nu}\dot{\theta}_1\sin\theta_1\sin\theta_2 - \dot{\nu}\dot{\theta}_2\cos\theta_1\cos\theta_2 \tag{2.4.2}$$
$$+ K\left[\dot{\theta}_2 + \dot{\nu}\sin\theta_1\right]\left[\alpha+1\right] + \left[\dot{\theta}_2 + \nu\sin\dot{\theta}_1\right]\dot{\theta}_3 = 0$$

Rearranging and further simplifying yields

$$\ddot{\theta}_1\cos\theta_2 - \dot{\theta}_1\dot{\theta}_2\sin\theta_2 - \ddot{\nu}\cos\theta_1\sin\theta_2 + \dot{\nu}\dot{\theta}_1\sin\theta_1\sin\theta_2 - \dot{\nu}\dot{\theta}_2\cos\theta_1\cos\theta_2$$

$$+ K\left[\dot{\theta}_2 + \dot{\nu}\sin\theta_1\right]\left[\alpha+1\right] + \left[\dot{\theta}_2 + \nu\sin\dot{\theta}_1\right]\left[\alpha+1 - \dot{\theta}_1\sin\theta_2 - \dot{\nu}\cos\theta_1\cos\theta_2\right] = 0$$

$$\ddot{\theta}_1 - \dot{\theta}_1\dot{\theta}_2\tan\theta_2 - \ddot{\nu}\cos\theta_1\tan\theta_2 + \dot{\nu}\dot{\theta}_1\sin\theta_1\tan\theta_2 - \dot{\nu}\dot{\theta}_2\cos\theta_1$$

$$+ \left[\dot{\theta}_2 + \dot{\nu}\sin\theta_1\right]\left[(K+1)(\alpha+1)\sec\theta_2 - \dot{\theta}_1\tan\theta_2 - \dot{\nu}\cos\theta_1\right] = 0$$

$$\ddot{\theta}_1 - \dot{\theta}_1\dot{\theta}_2\tan\theta_2 - \ddot{\nu}\cos\theta_1\tan\theta_2 + \dot{\nu}\dot{\theta}_1\sin\theta_1\tan\theta_2 - \dot{\nu}\dot{\theta}_2\cos\theta_1$$

$$+ \dot{\theta}_2(K+1)(\alpha+1)\sec\theta_2 - \dot{\theta}_1\dot{\theta}_2\tan\theta_2 - \dot{\nu}\dot{\theta}_2\cos\theta_1 \qquad (2.4.3)$$

$$+ \dot{\nu}(K+1)(\alpha+1)\sin\theta_1\sec\theta_2 - \dot{\nu}\dot{\theta}_1\sin\theta_1\tan\theta_2 - \dot{\nu}^2\sin\theta_1\cos\theta_1 = 0$$

This equation may be simplified and solved for $\ddot{\theta}_1$.

$$\ddot{\theta}_1 = 2\dot{\theta}_1\dot{\theta}_2\tan\theta_2 + 2\dot{\nu}\,\dot{\theta}_2\cos\theta_1 - \left[\dot{\theta}_2 + \dot{\nu}\sin\theta_1\right]\left[K+1\right]\left[\alpha+1\right]\sec\theta_2 \qquad (2.4.4)$$
$$+\ddot{\nu}\cos\theta_1\tan\theta_2 + \dot{\nu}^2\sin\theta_1\cos\theta_1$$

This is the same form of the equation if the derivative was with respect to τ. Similar substitutions into equation (2.1.41b) yields,

$$\ddot{\theta}_2 + \ddot{\nu}\sin\theta_1 + \dot{\nu}\dot{\theta}_1\cos\theta_1 - K\left[\dot{\theta}_1\cos\theta_2 - \dot{\nu}\cos\theta_1\sin\theta_2\right]\left[\alpha+1\right]$$

$$- \left[\dot{\theta}_1\cos\theta_2 - \dot{\nu}\cos\theta_1\sin\theta_2\right]\left[\alpha+1 - \dot{\theta}_1\sin\theta_2 - \dot{\nu}\cos\theta_1\cos\theta_2\right] \qquad (2.4.5)$$

$$= \frac{3K\sin\theta_2\cos\theta_2}{\zeta^3}$$

(notice the n^2 term is missing from the right hand side when compared to equation (2.1.41b) since the derivative is now with respect to τ.

Similar steps as those between equations (2.4.2) and (2.4.4) will yield from equation (2.4.5) an expression for $\ddot{\theta}_2$. Derivatives with respect to τ and will be represented by dotted terms.

$$\ddot{\theta}_2 = \left[K+1\right]\left[\alpha+1\right]\left[\dot{\theta}_1\cos\theta_2 - \dot{\nu}\cos\theta_1\sin\theta_2\right] - \ddot{\nu}\sin\theta_1 - 2\dot{\nu}\dot{\theta}_1\cos\theta_1\cos^2\theta_2 \qquad (2.4.6)$$

$$- \left[\dot{\theta}_1^2 - \dot{\nu}^2\cos\theta_1 + \frac{3K}{\zeta^3}\right]\sin\theta_2\cos\theta_2$$

The expressions for $\dot{\nu}$ and $\ddot{\nu}$ can be found from equations (2.1.11) and (2.1.12) respectively. The non-linear terms are now expressed in a manner that may be programmed and numerically integrated. These two equations will replace the last two in equation (2.1.54) and the feedback can be added in a similar manner. Again, for 'small' initial conditions this non-linear system should behave similarly to the linear system.

CHAPTER 3

RESULTS

In this chapter the sequence of procedures and the results of the example tested will be discussed. The example was accomplished employing various computer programs to solve the equations developed in the last chapter. The programs utilized were run on a Personal Computer and were written in Fortran 77 Microsoft version 4.01. This allowed IMSL subroutines to be used. Numerical integration was accomplished by the HAMING subroutine. It was decided that scalar control on a system with two unstable modes would be implemented and the computer programs were used to determine what parameters would be used in the feedback.

3.1 Parameter Space

The basic system was expressed in the linear form

$$\bar{x}' = A(\tau)\bar{x} \qquad (2.2.2)$$

where the elements of $A(\tau)$ are expressed in equations (2.1.54) and (2.1.57). These elements are functions of K, α and e. Therefore the stability of the system is determined by these three parameters. In Kane and Barba (4;405) stability is shown in the K, α parameter plane for various values of the eccentricity. The values of the Poincaré exponents for various values of K and α with eccentricity, e=0.5, is shown in Table 3.1. This example is the same as used by Myers (ref;5). Myers used values of 0.7, 1.0

α=	K= 1.0	
3.0	0.0000 +/- j0.1395	0.0000 +/- j0.3525
2.0	0.0000 +/- j0.1174	0.0000 +/- j0.4937
1.0	0.0000 +/- j0.1549	0.0000 +/- j0.3766
0.0	+/- 0.1878 + j0.5000	0.0000 +/- j0.3556 †,††
-1.0	0.6718 - 0.6718	0.0000 +/- j0.3728
-2.0	0.3876 - 0.3876	0.0000 +/- j0.2952 ††
-3.0	+/- 0.0953 + 0.5000	0.0000 +/- j0.4673 †

	K= 0.8	
3.0	0.0000 +/- j0.1489	0.0000 +/- j0.4907
2.0	0.0000 +/- j0.2241	0.0000 +/- j0.2820
1.0	0.0000 +/- j0.1701	0.0000 +/- j0.4595
0.0	+/- 0.0525 + j0.5000	0.0000 +/- j0.2638 †,††
-1.0	0.6072 - 0.6072	0.0000 +/- j0.2866
-2.0	0.0000 +/- j0.1272	0.0000 +/- j0.4209
-3.0	+/- 0.0854 + j0.5000	0.0000 +/- j0.0129 †

	K= 0.6	
3.0	0.0000 +/- j0.1519	0.0000 +/- j0.3791
2.0	0.0000 +/- j0.0486	0.0000 +/- j0.3082
1.0	+/- 0.0885 + j0.5000	0.0000 +/- j0.2811 †,††
0.0	+/- 0.0555 + j0.5000	0.1476 - 0.1476 †
-1.0	0.5067 - 0.5067	0.0000 +/- j0.0175 ††
-2.0	0.0000 +/- j0.1206	0.0000 +/- j0.4005
-3.0	0.0000 +/- j0.4149	0.0000 +/- j0.4414

	K= 0.4	
3.0	0.0000 +/- j0.2559	0.0000 +/- j0.1447
2.0	0.0000 +/- j0.1368	0.0000 +/- j0.4276
1.0	0.0000 +/- j0.2980	0.0000 +/- j0.0349
0.0	0.1249 +/- j0.2959	-0.1249 +/- j0.2959
-1.0	0.2943 - 0.2943	0.0000 +/- j0.2163
-2.0	0.0000 +/- j0.4390	0.0000 +/- j0.2173
-3.0	0.0000 +/- j0.2863	0.0000 +/- j0.0651

	K= 0.2	
3.0	0.0000 +/- j0.1215	0.0000 +/- j0.1099
2.0	0.0000 +/- j0.3073	0.0000 +/- j0.1282
1.0	+/- 0.0742 + j0.5000	0.0000 +/- j0.1762 †
0.0	+/- 0.0710 + j0.5000	0.0000 +/- j0.2547 †
-1.0	0.1860 +/- j0.4857	-0.1860 +/- j0.4857
-2.0	0.0000 +/- j0.2793	0.0000 +/- j0.4692
-3.0	0.0000 +/- j0.1724	0.0000 +/- j0.4328

Table 3.1 (ref 6) Poincaré Exponents for K vs. α, with e=0.5

† Apparent error from calculating complex logs corrected
†† Math error corrected

	α=	K= 0.0		
	3.0	0.0000 +/- j0.0000	0.0000 +/- j0.0000	
	2.0	0.0000 +/- j0.0000	0.0000 +/- j0.0000	
	1.0	0.0000 +/- j0.0000	0.0000 +/- j0.0000	
	0.0	0.0000 0.0000	0.0000 0.0000	
	-1.0	0.0000 +/- j0.0003	0.0000 +/- j0.0003	††
	-2.0	0.0000 +/- j0.0000	0.0000 +/- j0.0000	††
	-3.0	0.0000 +/- j0.0000	0.0000 +/- j0.0000	
K=-0.2	3.0	0.0384 +/- j0.0932	-0.0384 +/- j0.0932	
	2.0	0.0983 +/- j0.1756	-0.0983 +/- j0.1756	
	1.0	0.1829 +/- j0.3833	-0.1829 +/- j0.3833	
	0.0	+/- 0.5257 + j0.5000	+/-0.2162 + j0.5000	†
	-1.0	0.6017 +/- j0.0094	-0.6017 +/- j0.0094	
	-2.0	0.4319 +/- j0.3953	-0.4319 +/- j0.3953	
	-3.0	0.2297 +/- j0.2971	-0.2297 +/- j0.2971	
K=-0.4	3.0	0.4215 - 0.4215	0.0000 +/- j0.3602	
	2.0	+/- 0.4385 + j0.5000	+/-0.3361 +/- j0.5000	†
	1.0	+/- 0.6614 + j0.5000	+/-0.3876 +/- j0.5000	†
	0.0	+/- 0.7834 + j0.5000	+/-0.6559 +/- j0.5000	†
	-1.0	0.8141 +/-j0.0339	-0.8141 +/- j0.0339	
	-2.0	0.7568 +/-j0.2810	-0.7568 +/- j0.2810	
	-3.0	0.4537 + j0.4128	-0.4537 +/- j0.4128	
K=-0.6	3.0	+/- 0.3735 + j0.5000	0.5384 - 0.5384	†
	2.0	+/- 0.8482 + j0.5000	0.5259 - 0.5259	†
	1.0	+/- 1.0741 + j0.5000	+/-0.5117 + j0.5000	†
	0.0	0.9275 +/- j0.3540	-0.9275 +/- j0.3540	
	-1.0	0.9702 +/- j0.0681	-0.9702 +/- j0.0681	
	-2.0	0.9559 +/- j0.1550	-0.9559 +/- j0.1550	
	-3.0	0.8834 +/- j0.3668	-0.8834 +/- j0.3668	
K=-0.8	3.0	+/- 1.2424 + j0.5000	+/-0.6066 + j0.5000	†
	2.0	+/- 1.2570 + j0.5000	+/-0.7543 + j0.5000	†
	1.0	+/- 1.1584 + j0.5000	+/-0.9504 + j0.5000	†
	0.0	1.0840 +/- j0.2540	-1.0840 +/- j0.2540	
	-1.0	1.0985 +/- j0.1107	-1.0985 +/- j0.1107	
	-2.0	1.1002 +/- j0.0117	-1.1002 +/- j0.0117	
	-3.0	1.0896 +/- j0.1272	-1.0896 +/- j0.1272	
K=-1.0	3.0	1.2095 +/- j0.1618	-1.2095 +/- j0.1618	
	2.0	1.2095 +/- j0.1618	-1.2095 +/- j0.1618	
	1.0	1.2095 +/- j0.1618	-1.2095 +/- j0.1618	
	0.0	1.2095 +/- j0.1618	-1.2095 +/- j0.1618	
	-1.0	1.2095 +/- j0.1618	-1.2095 +/- j0.1618	
	-2.0	1.2095 +/- j0.1618	-1.2095 +/- j0.1618	
	-3.0	1.2095 +/- j0.1618	-1.2095 +/- j0.1618	

Table 3.1 (continued)

and 0.5 for K, α and e respectively. These values resulted in two complex conjugate pairs with two stable and two unstable roots.

Modal variables are used to decouple the four equations into two coupled pairs. Phase plots can then be used to view the stability and the effect of control on the system. Since the modal variables are four in number, graphical presentation is difficult. Therefore phase portraits will plot η_1 versus η_2 and η_3 versus η_4. In the non-linear system, since modes 3 and 4 are stable, emphasis will be place on modes 1 and 2 with initial conditions of η_3 and η_4 set to zero. Modes 3 and 4 are monitored to insure they do not become unstable, but the motion resulting from the control to stabilize modes 1 and 2 are the primary concern. Once the feedback is implemented, the original modal variables will no longer decouple the two sets of modes. However, useful information can be obtained from this set of original modal variables. In order for the new equations to be decoupled, a new J matrix needs to be developed and found numerically for the new controlled system. This will be left to later investigations.

3.2 Uncontrolled Linearized System

The parameters used in this thesis are K=0.7, α=1.0 and e=0.5. This represents the most common type of instability, but the methods used to control this case are applicable to other cases. With no control added, the characteristic exponents are;

$$\omega_{1,2} = 0.0177 \pm j0.3667 \quad \text{unstable}$$

$$\omega_{3,4} = -0.0177 \pm j0.3667 \quad \text{stable}$$

While all the motions of the satellite are important, a variable ϕ which is the angle between the satellite spin axis and the orbit normal, shows the combined movement of θ_1 and θ_2 and is defined by

$$\phi = \arccos(\cos\theta_1 * \cos\theta_2) \tag{3.2.1}$$

(See Figure (2.2)) The motion of the uncontrolled system is shown in Figures (3.1) through (3.11). Figures (3.1) through (3.4) show the motion of the state variables. This motion is started by an initial displacement, i.e., the state variable's initial values, in radians are

$$x(0)=\begin{Bmatrix}0.02\\0.02\\0.00\\0.00\end{Bmatrix} \tag{3.2.2}$$

Figure (3.5) reveals the combined motion of θ_1 and θ_2. Figures (3.6) through (3.9) display the modal response. The initial values for the modal variables are defined by the use of inverting equation (2.2.28) hence;

$$\eta(0)=F(0)^{-1}x(0)$$
$$\text{or} \tag{3.2.3}$$
$$\eta(0)=L(0)^{T}x(0)$$

Figures (3.10) and (3.11) are the phase portraits of the linearized uncontrolled responses. It can be seen from these modal plots that the first mode pair spiral outward and therefore is unstable while the second pair spirals inward indicating a stable mode pair.

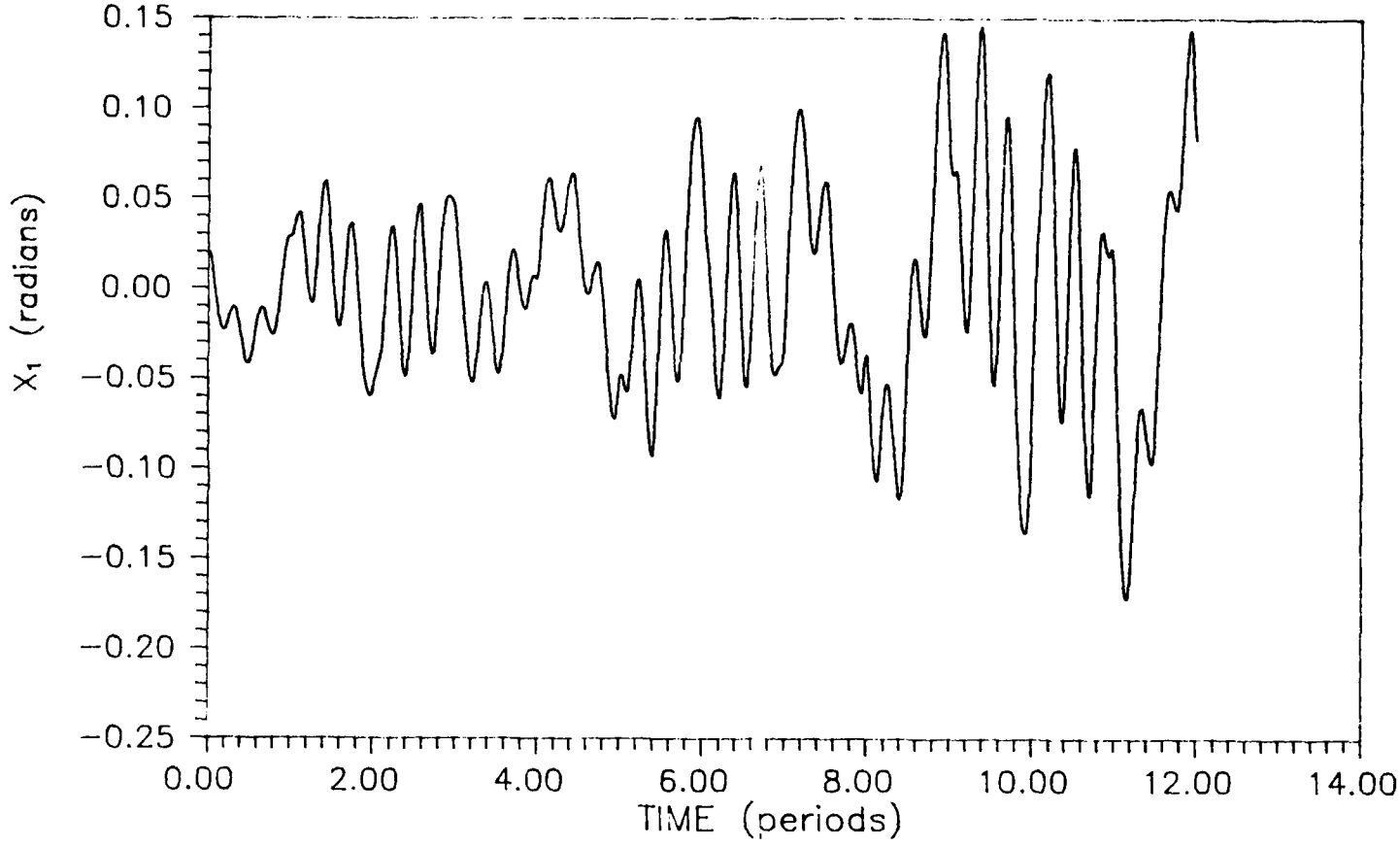

Figure 3.1 – Uncontrolled Linearized X_1 response

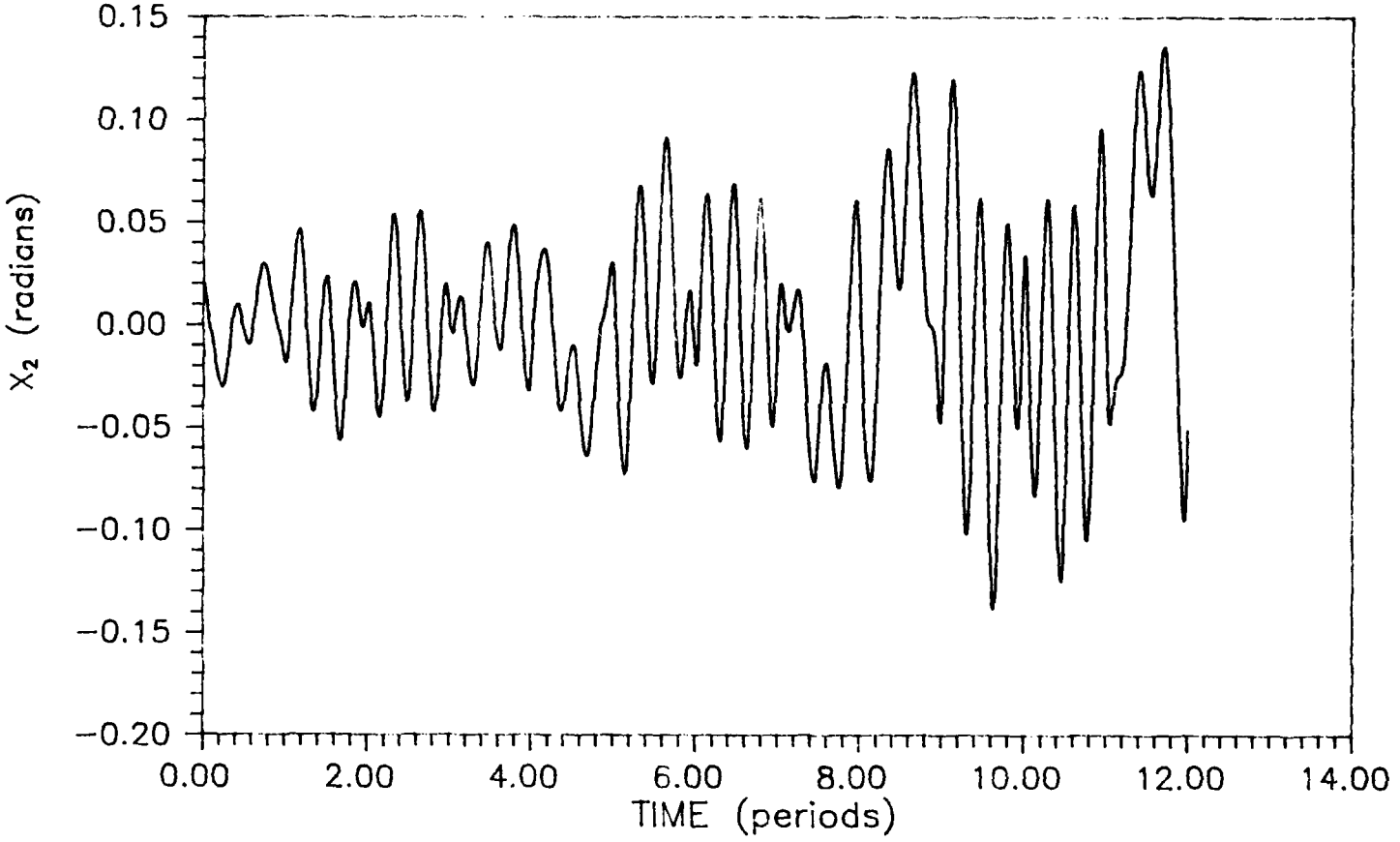

Figure 3.2 – Uncontrolled Linearized X_2 response

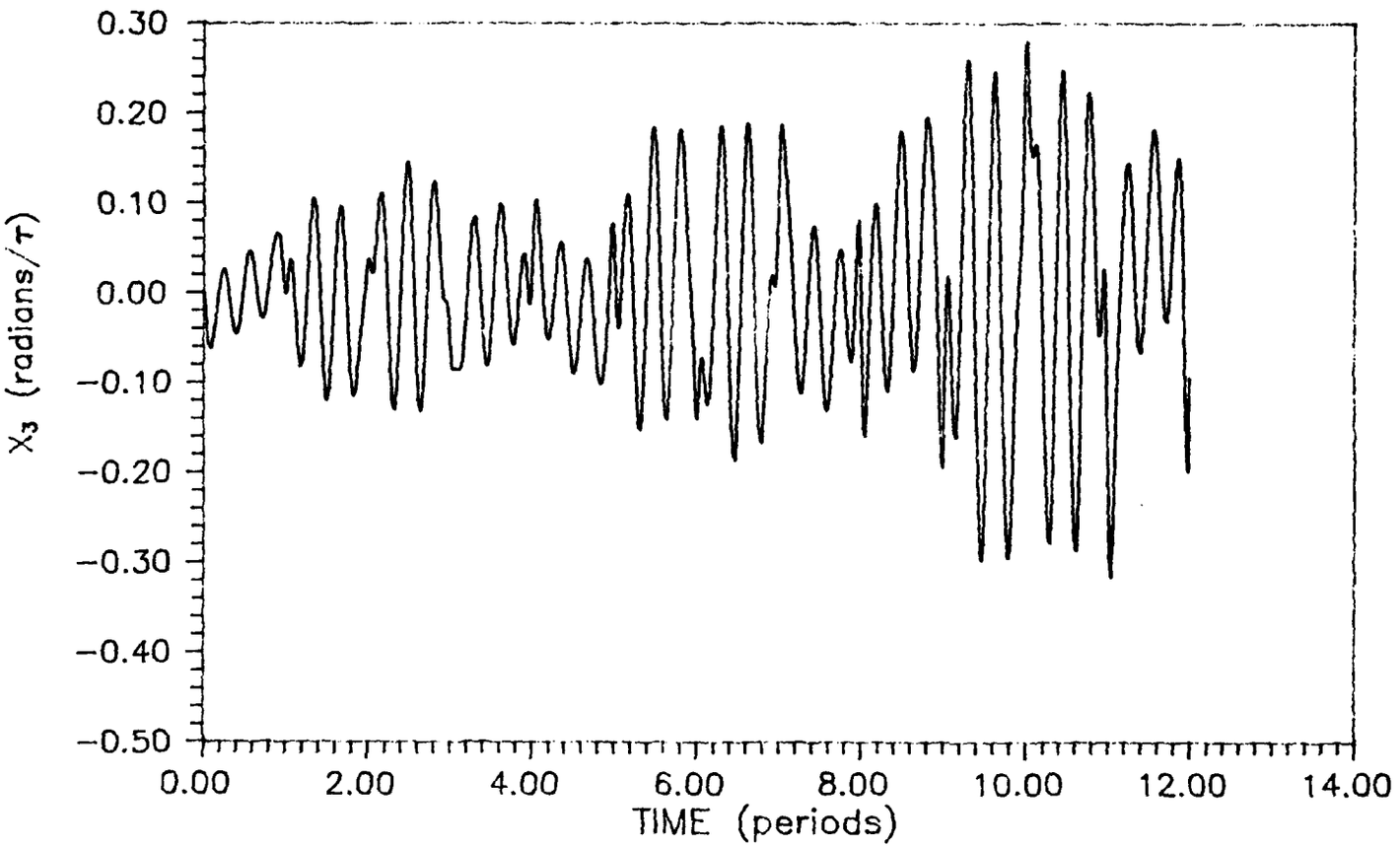

Figure 3.3 -- Uncontrolled Linearized X_3 response

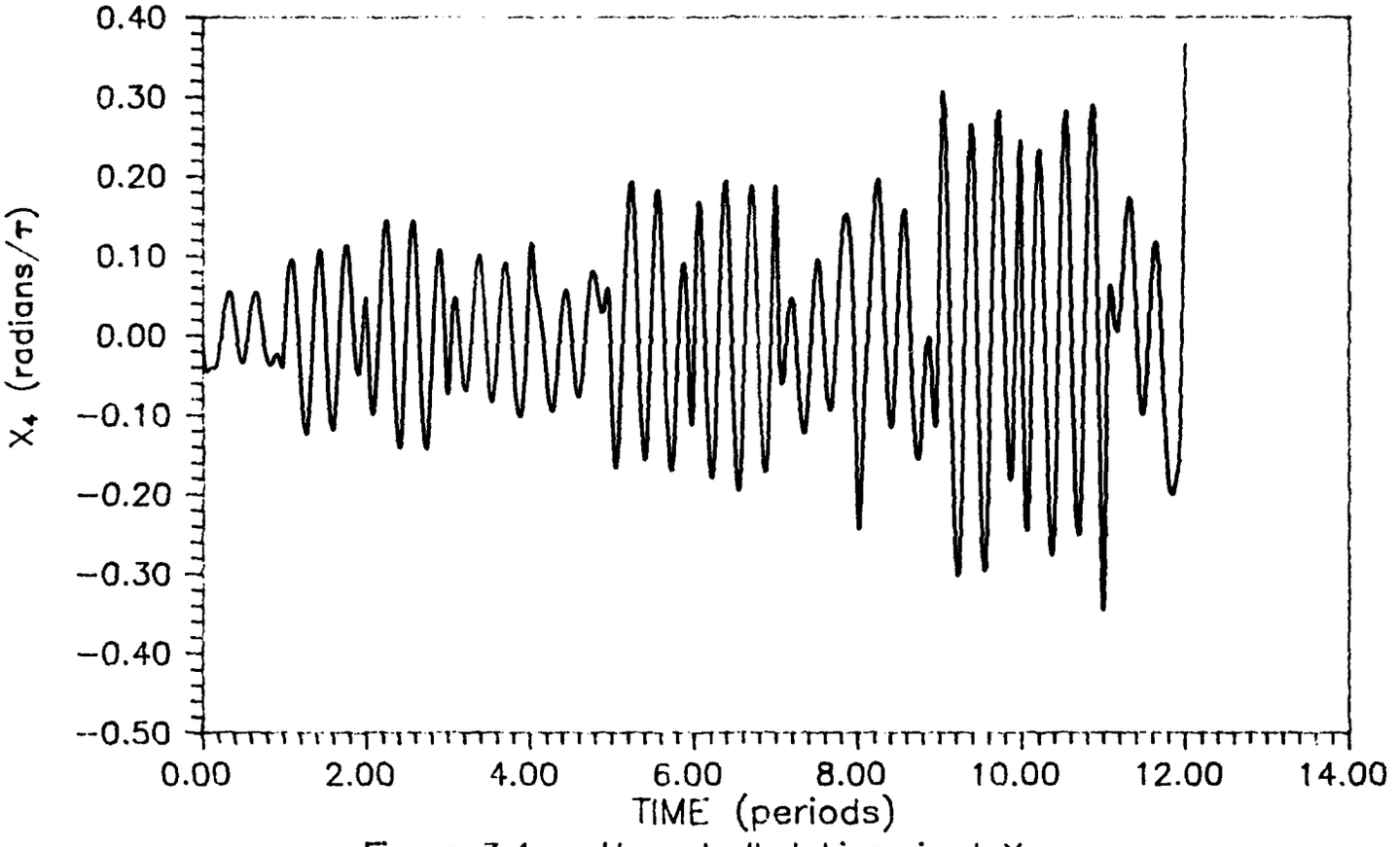

Figure 3.4 – Uncontrolled Linearized X_4 response

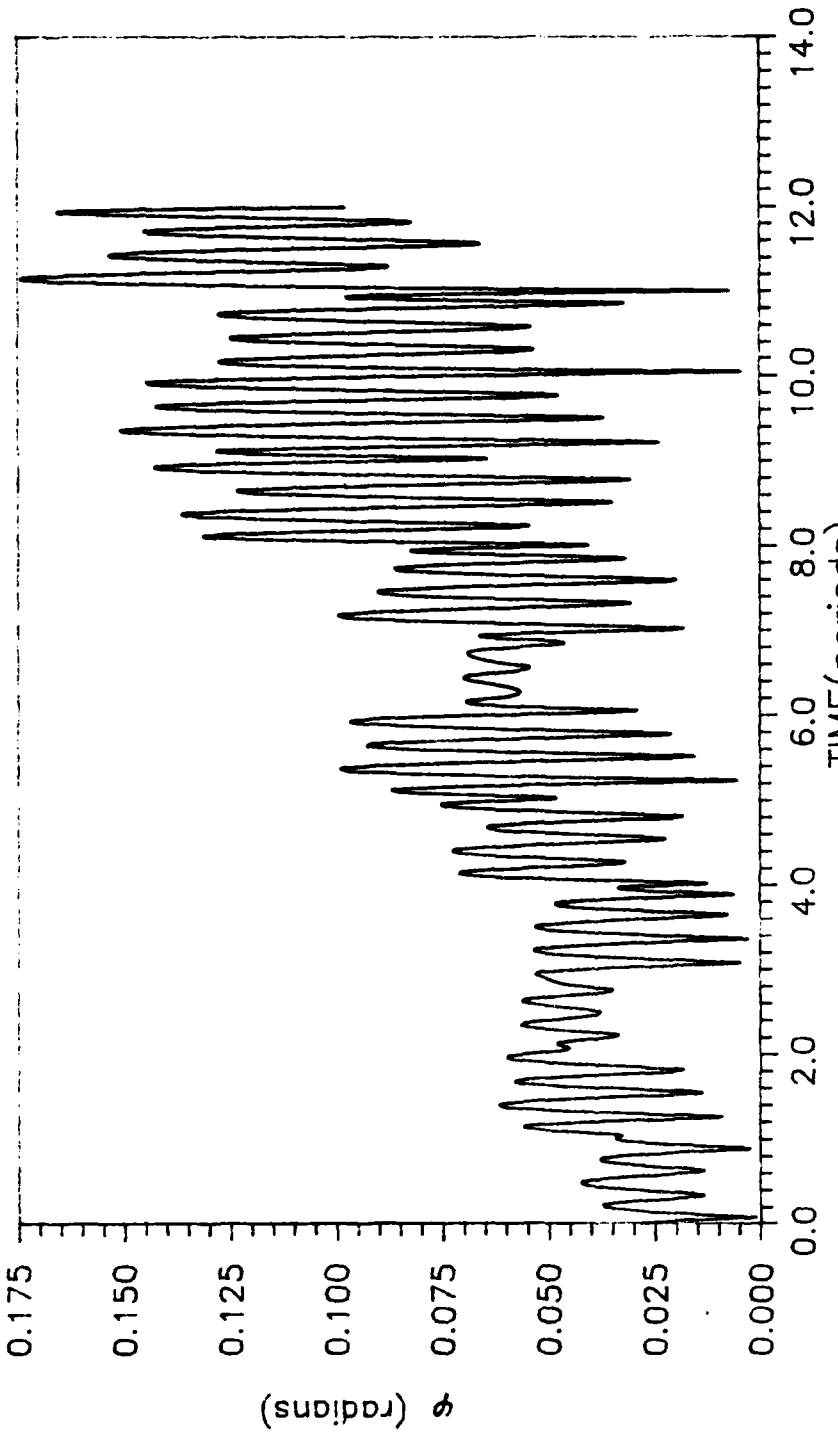

Figure 3.5 – Uncontrolled Linearized φ response

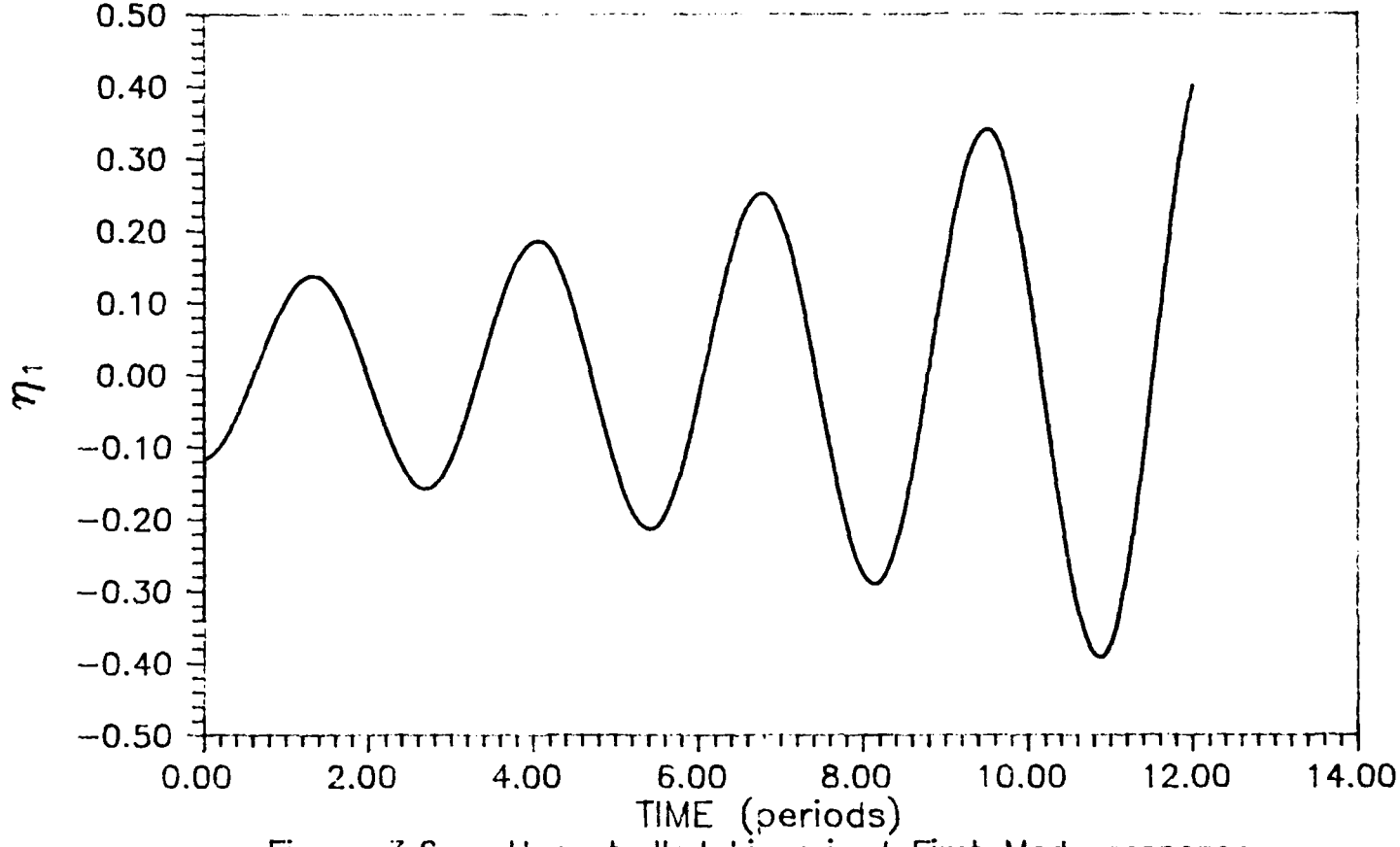

Figure 3.6 – Uncontrolled Linearized First Mode response

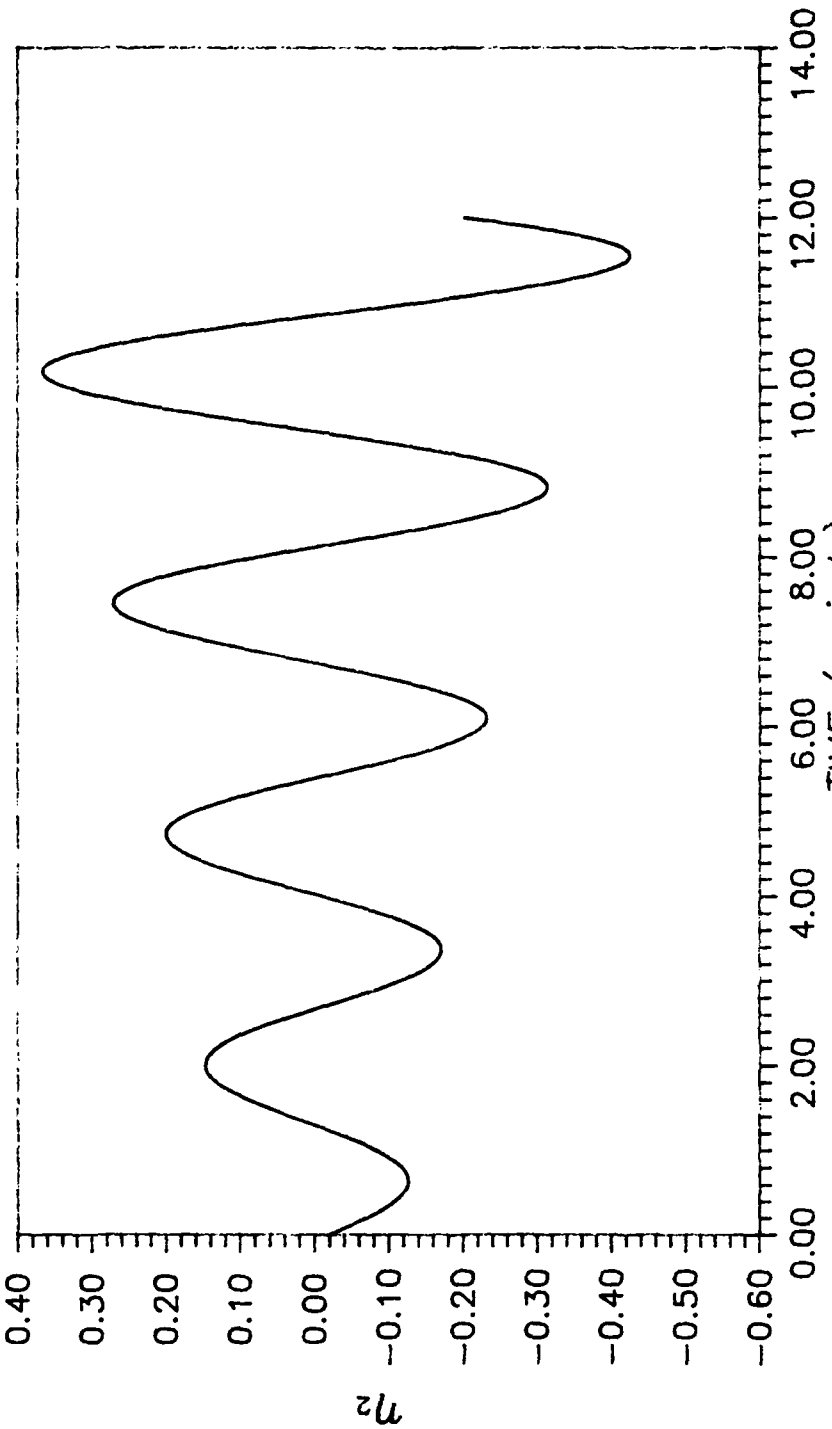

Figure 3.7 – Uncontrolled Linearized Second Mode response

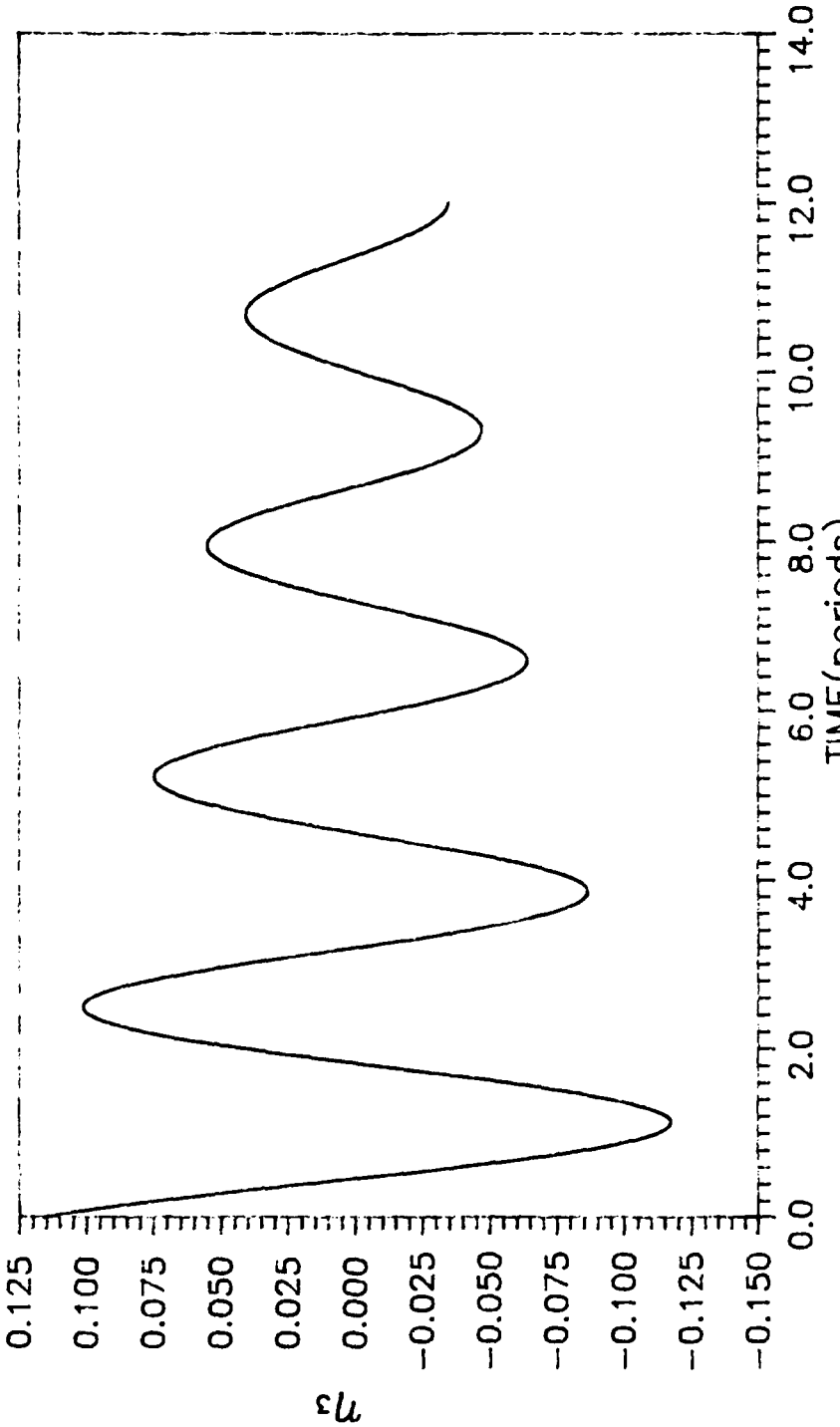

Figure 3.8 – Uncontrolled Linearized Third Mode response

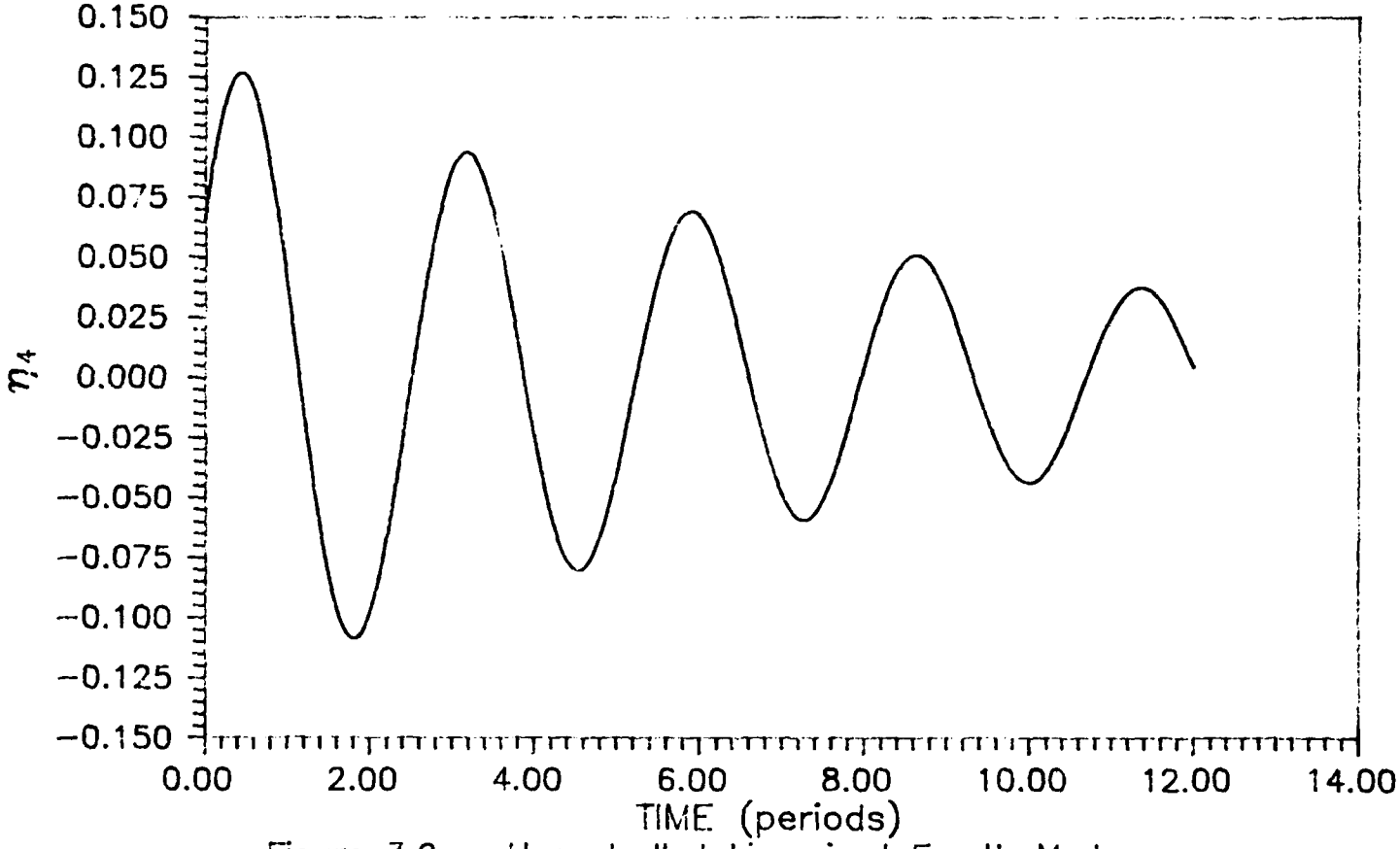

Figure 3.9 – Uncontrolled Linearized Fourth Mode response

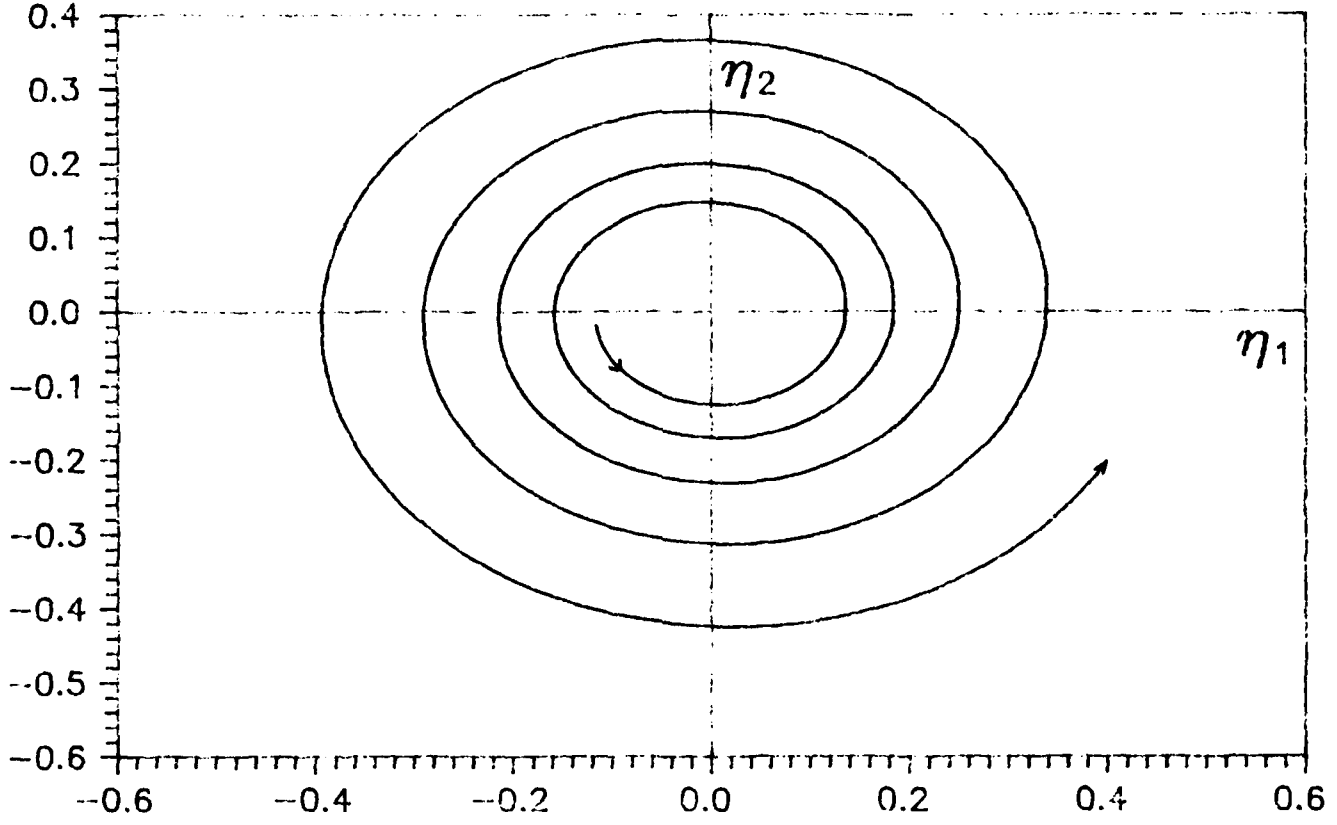

Figure 3.10 – Phase Portrait for First Pair of Uncontrolled Linearized Modes

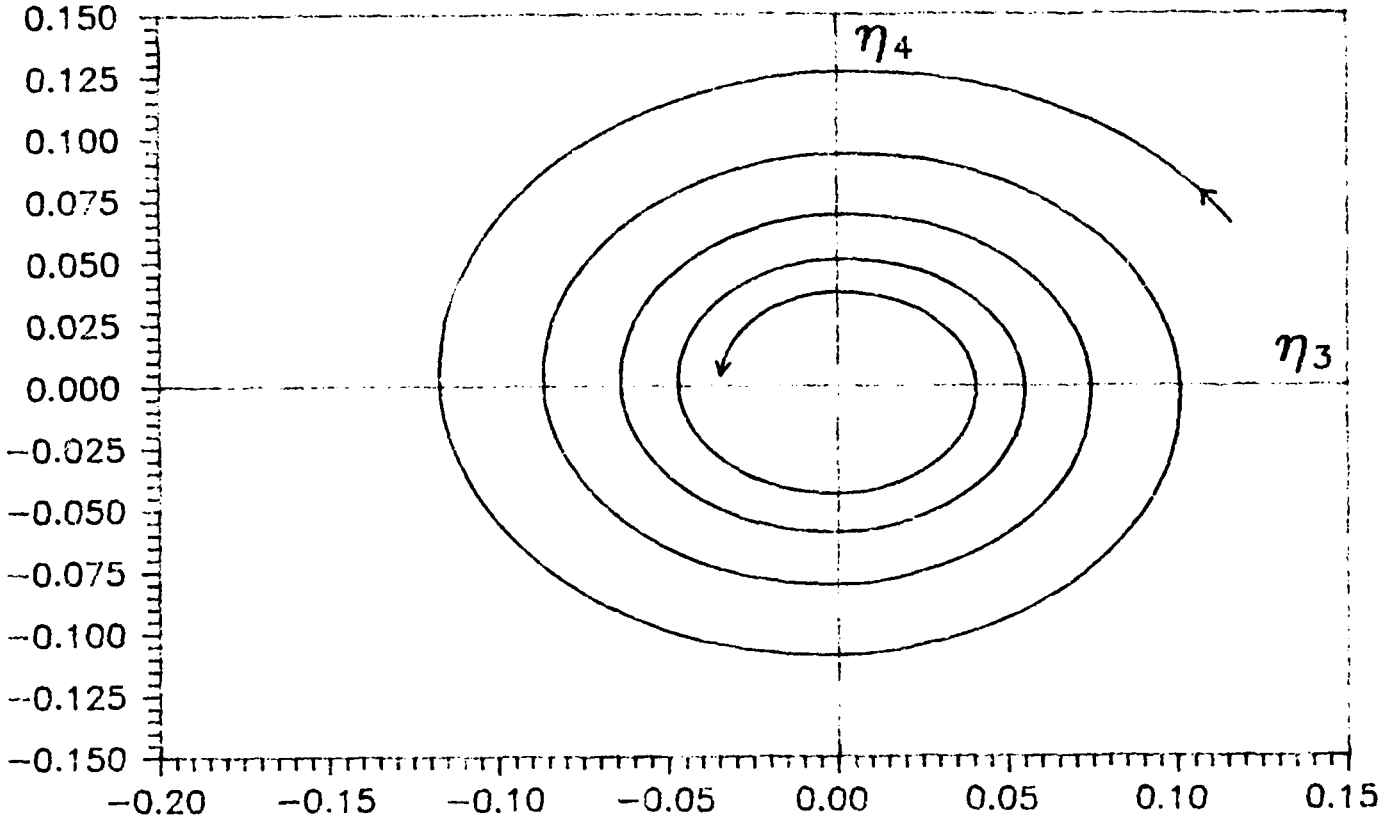

Figure 3.11 – Phase Portrait for Second Pair of Uncontrolled Linearized Modes

3.3 Scalar Control of Linearized System

From Floquet theory in chapter 2, a solution to the linear system of equation (2.2.2) is given by equation (2.2.11);

$$\Phi(\tau)=F(\tau)e^{J\tau}F^{-1}(0) \qquad (2.2.11)$$

with J constructed as

$$J = \begin{bmatrix} 0.0177 & -0.3667 & 0.0000 & 0.0000 \\ 0.3667 & -0.0177 & 0.0000 & 0.0000 \\ 0.0000 & 0.0000 & -0.0177 & -0.3667 \\ 0.0000 & 0.0000 & 0.3667 & -0.0177 \end{bmatrix} \qquad (3.3.1)$$

The values for the elements of the periodic F matrix could have been found by numerical integration and a computer program used to express these elements in terms of their Fourier coefficients. Instead, the adjoint problem was solved, hence the values of $\left[F^{-1}\right]^T$ were needed. This matrix was expressed as the $L(\tau)$ matrix and the Fourier coefficients of the L matrix were found. A typical element of L is

$$\begin{aligned} l_{11} = {} & 0.9242 - 0.6855\cos(\tau) - 0.4349\cos(2\tau) - 0.0124\cos(3\tau) \\ & + 0.0011\cos(4\tau) + 0.0271\cos(5\tau) + 0.0354\cos(6\tau) \\ & + 0.0340\cos(7\tau) + \ldots \\ & + 0.6927\sin(\tau) - 0.1637\sin(2\tau) + 0.1957\sin(3\tau) \\ & - 0.1269\sin(4\tau) - 0.0503\sin(5\tau) - 0.0160\sin(6\tau) \\ & - 0.0005\sin(7\tau) + \ldots \end{aligned}$$

where the values of the higher frequency coefficients become increasingly smaller in magnitude. A list of the Fourier coefficients of selected elements of the L matrix is included in Appendix A. The linearized system has two unstable modes and the control implemented is angular rate feedback. In this case the

form of equation (2.3.8) will be used with the vectors $\bar{k}$ and $\bar{B}$ as

$$k = \begin{bmatrix} k_1 k_2 0 & 0 \end{bmatrix} \tag{3.3.2}$$

and

$$B = \begin{bmatrix} 0 \\ 0 \\ 1 \\ 1 \end{bmatrix} \tag{3.3.3}$$

From equation (2.3.6) this produces a q vector of the form

$$g_c = \begin{bmatrix} l_{31} + l_{41} \\ l_{32} + l_{42} \\ l_{33} + l_{43} \\ l_{34} + l_{44} \end{bmatrix} \tag{3.3.4}$$

Using the trace method described by Calico and Wiesel (1;674) gives equation (2.3.11) in the form

$$\omega_1' + \omega_2' = \omega_1 + \omega_2 + k_1\left[l_{31} + l_{41}\right] + k_2\left[l_{32} + l_{42}\right] \tag{3.3.5}$$

where the values of l will be the constant terms of the Fourier coefficients. Therefore the first two elements of g_c are chosen to be

$$g_{1c} = 0.1967 \tag{3.3.6}$$

$$g_{2c} = -0.8486 \tag{3.3.7}$$

The list of Fourier coefficients for the first two elements of the g_c vector is also included in Appendix A. As stated in chapter 2, while the values of the new characteristic exponents can not be individually chosen, their sum can.

$$\omega_1' + \omega_2' = 2(0.0177) + k_1(0.1967) + k_2(-0.8486) \tag{3.3.8}$$

The values k_1 and k_2 are picked to be -0.4 and 0.4 respectively. This makes the new sum

$$\omega_1' + \omega_2' = 0.0354 - 0.4(1.0453) = -0.3827 \qquad (3.3.9)$$

Integrating the new Φ matrix over a period of 2π and using Floquet theory yields the new characteristic exponents,

$$\omega_1' = -0.0454 + j0.5000 \quad \text{and} \quad \omega_2' = -0.3373 + j0.5000$$

The imaginary parts of the new exponents exist because with control the period is now twice the old period. When the new Φ is integrated over 4π, the values of the characteristic exponents are the real values with no imaginary part. The resulting controlled motion is shown in Figures (3-12) through (3-14). Figure (3-12) shows the combined θ_1 and θ_2 response and Figures (3-13) and (3-14) are phase portraits of the controlled linearized modes using the uncontrolled modal variables. Figure (3-13) shows how fast the first mode pair now converges to a stable condition while it can be seen in Figure (3-14) the second pair is effected only slightly and remains stable. For these plots to be as smooth as Figures (3-10) and (3-11) new modal variables would have to be defined for the control system.

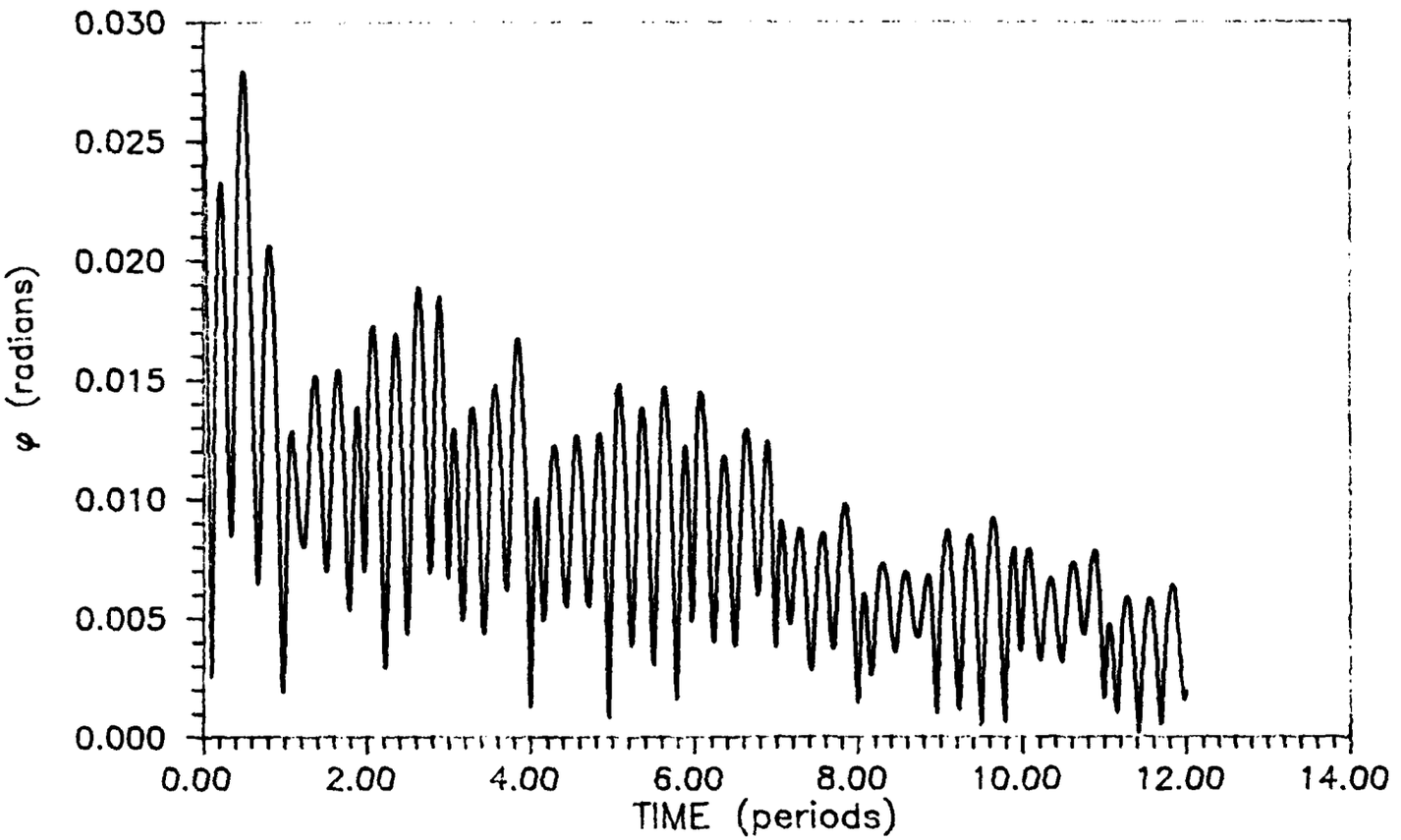

Figure 3.12 – Controlled Linearized φ response

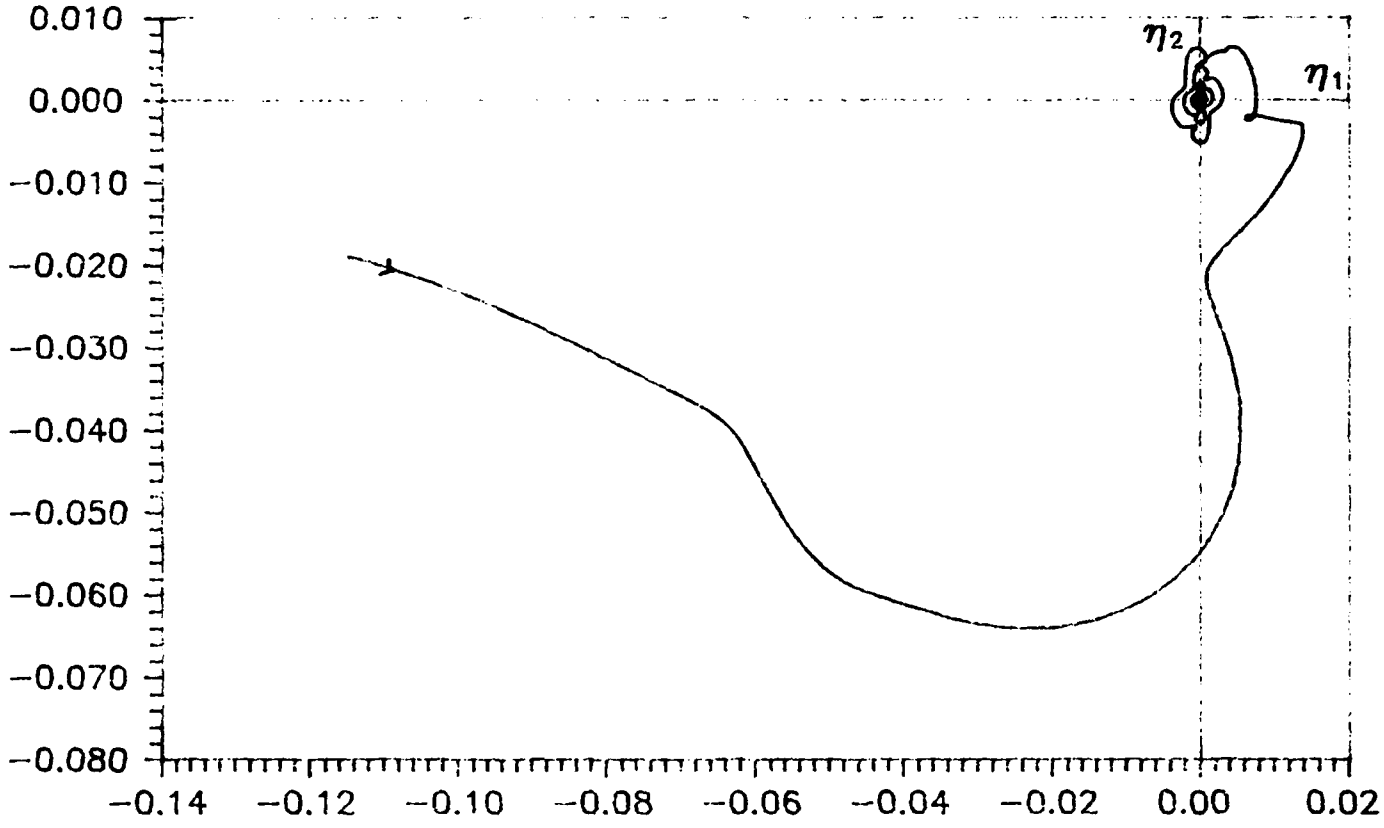

Figure 3.13 – Phase Portrait for First Pair of Controlled Linearized Modes

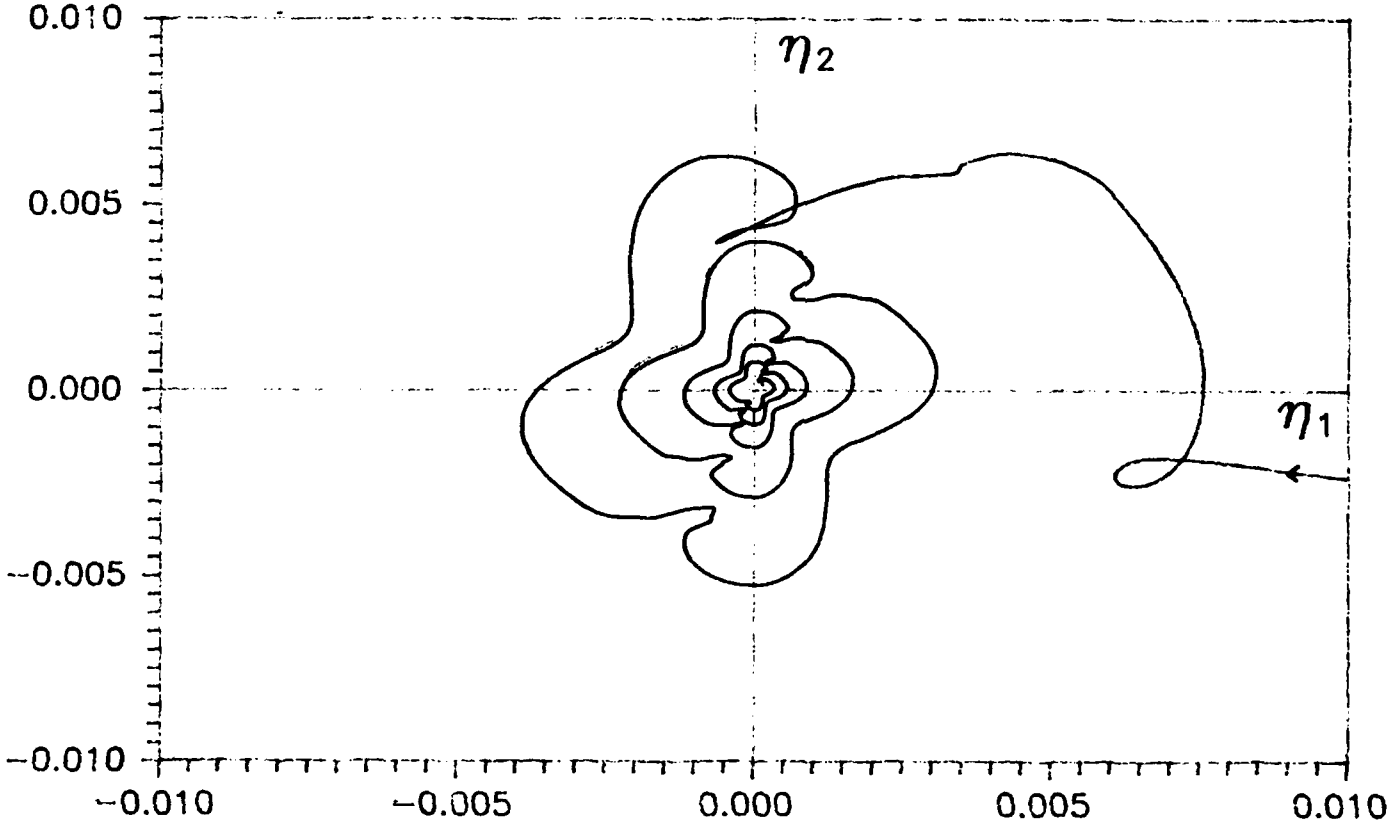

Figure 3.13e -- Figure 3.13 Expanded

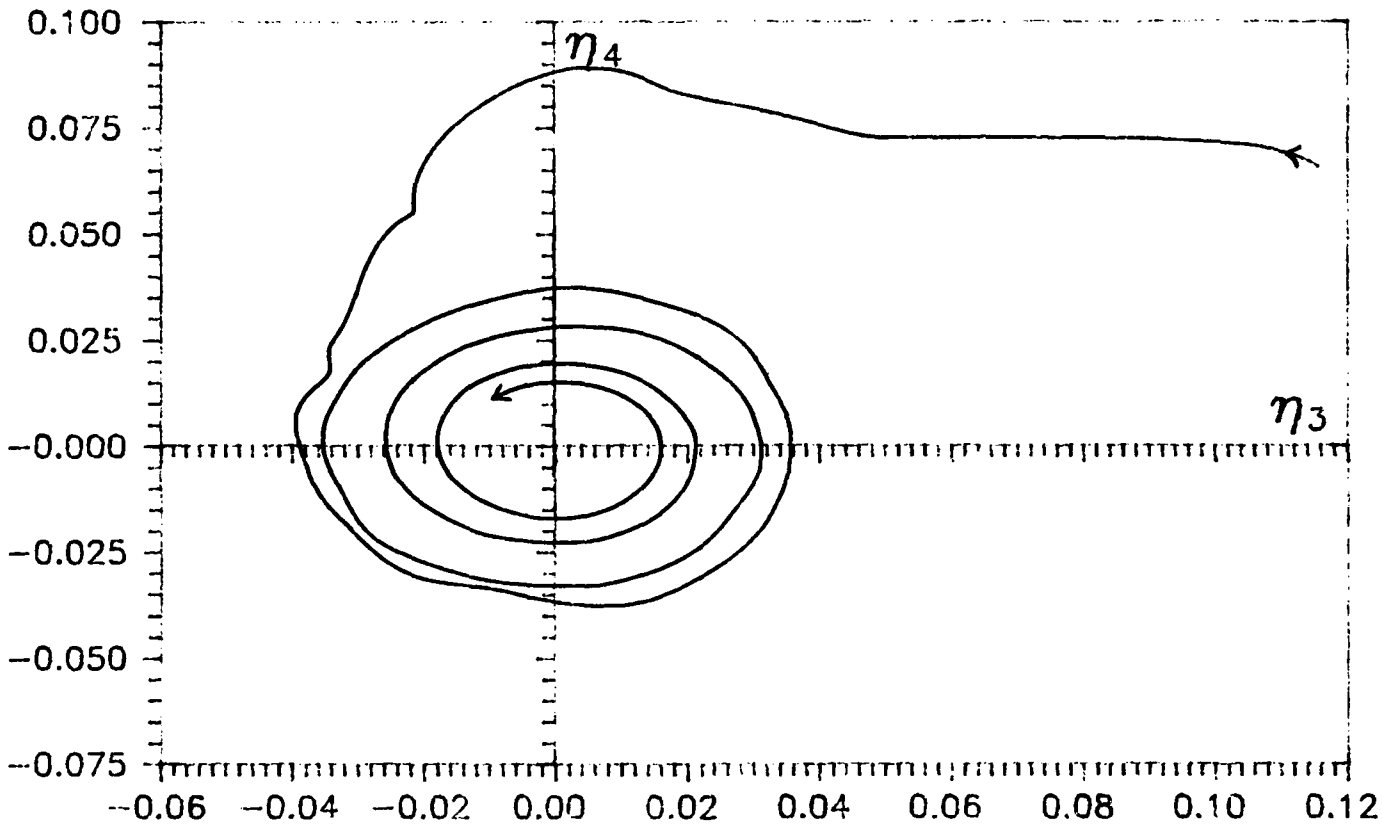

Figure 3.14 – Phase Portrait for Second Pair of Controlled Linearized Modes

3.4 Non-Linearized System

With 'small' disturbances the uncontrolled non-linear system behaves, as predicted by theory, like the linear system. Comparing Figures (3.15) through (3.21) to the linearized system figures, shows how close the uncontrolled response follows the linearized system. The irregular motion toward the end of the trace on figure (3.21) is due to the coupling of the η_1, η_2 pair since they are increasing in magnitude as time gets large. The controlled non-linearized system duplicates the controlled linearized response since the coupled effect of the η_1, η_2 pair does not appear since the controlled pair is now stable. This is illustrated in Figures (3.22) through (3.24).

The phase portraits of the controlled non-linear system show the effect of control on the system. For this study, initial disturbances were selected for the modal variables η_1 and η_2 but the initial values of η_3 and η_4 were selected to be zero. The linearized system has uncoupled modal responses, however as nonlinear effects become apparent the two separate phase planes η_1, η_2 and η_3, η_4 become coupled. This is the reason why, as the disturbances get large, initial points seemingly close together display very different responses.

With the magnitude of the disturbances for η_1 and η_2 kept below 0.25, the response is very similar to a linearized system. This is shown in Figures (3.25) through (3.28). As the disturbances grow, there is an increasing tendency to oscillate around the zero disturbance instead of returning to complete

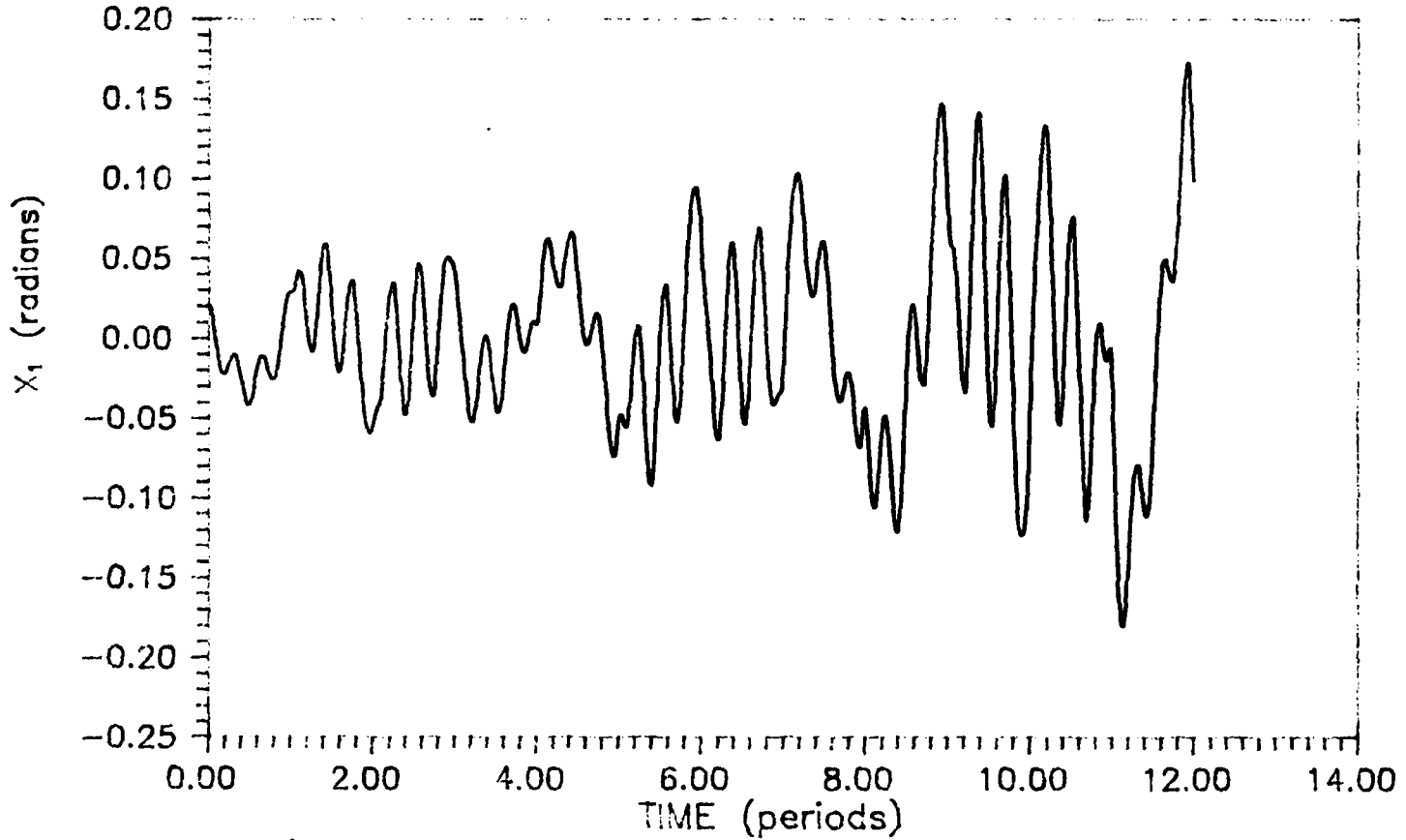

Figure 3.15 – Uncontrolled Non–Linearized X_1 response

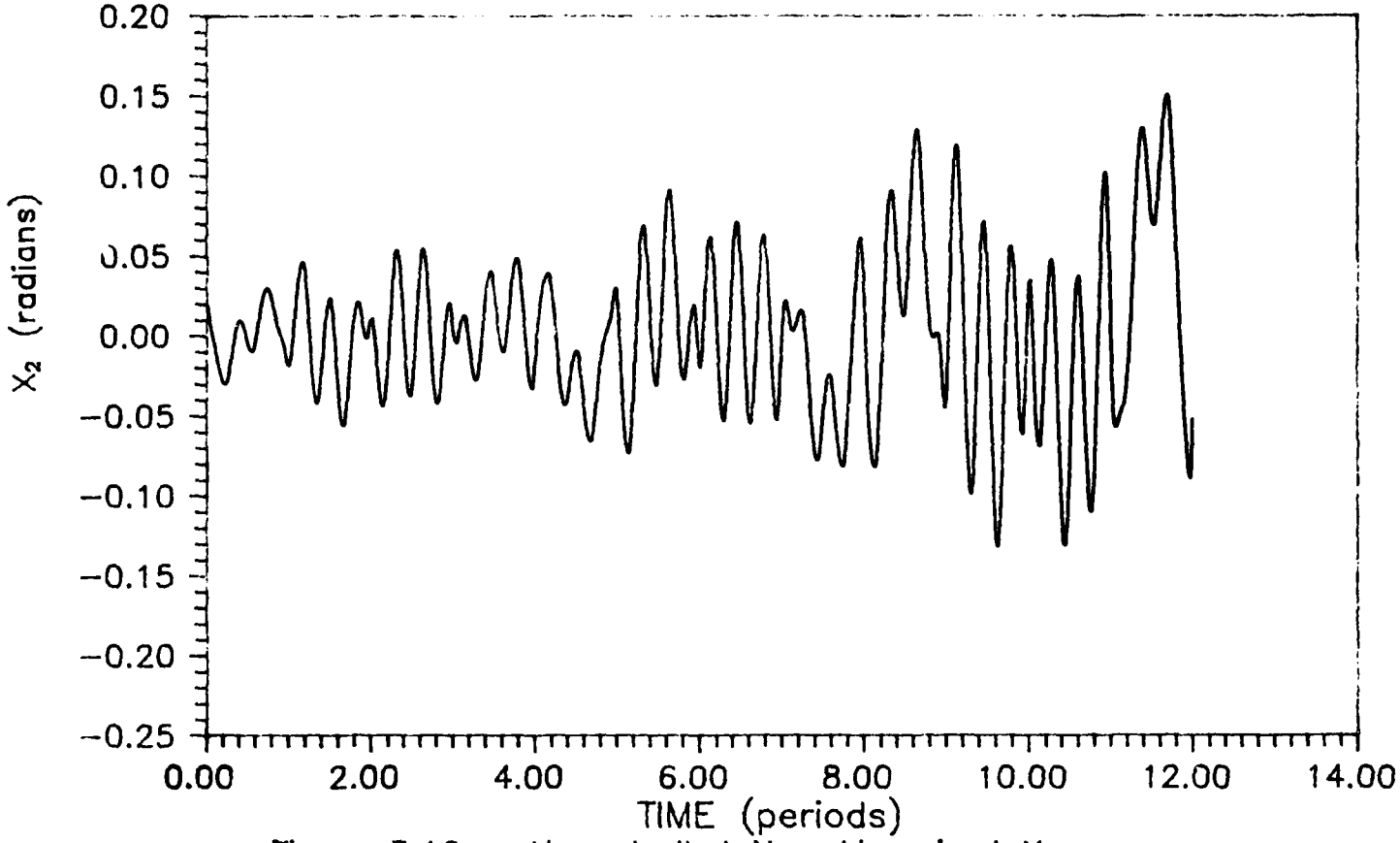

Figure 3.16 -- Uncontrolled Non-Linearized X_2 response

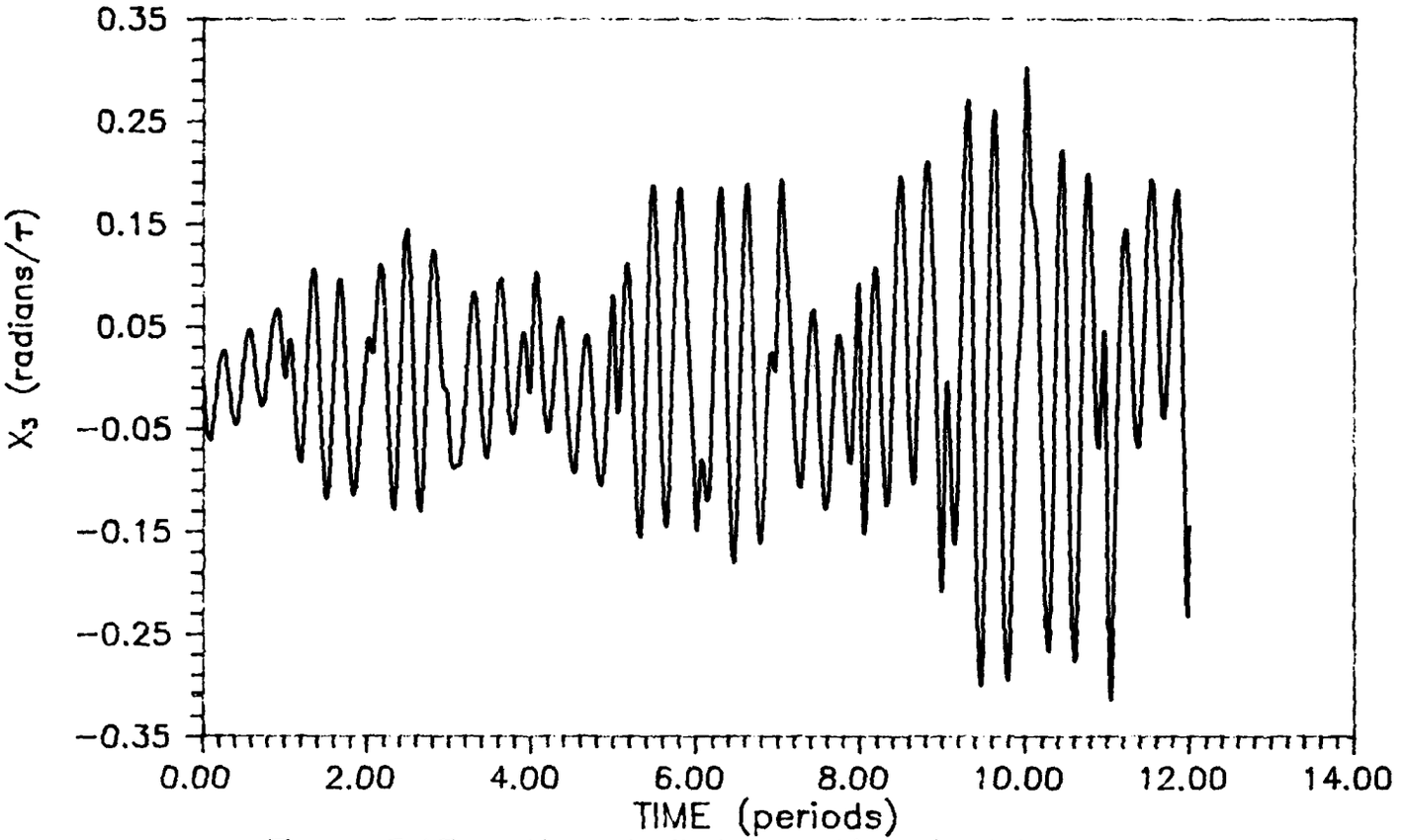

Figure 3.17 – Uncontrolled Non–Linearized X_3 response

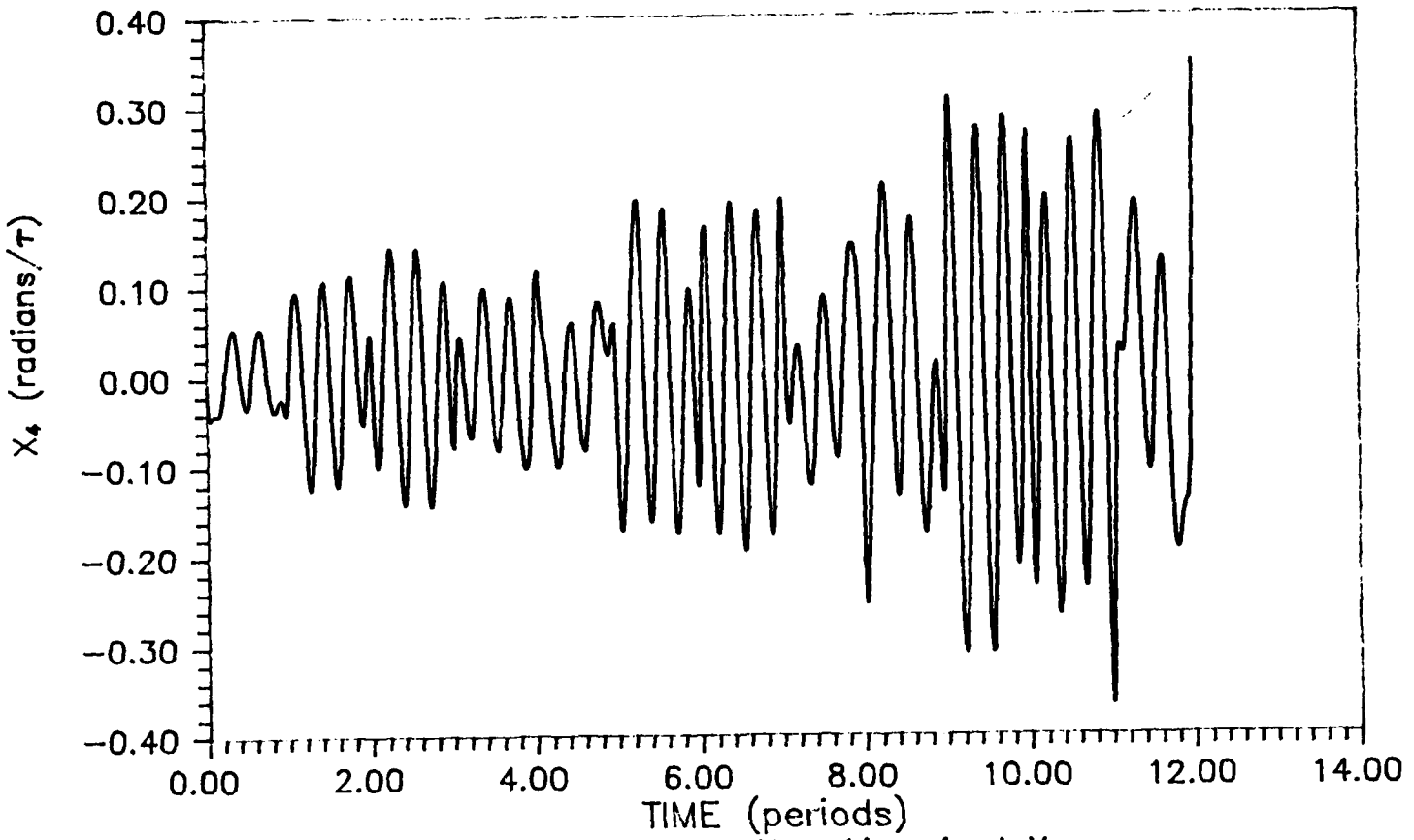

Figure 3.18 – Uncontrolled Non–Linearized X_4 response

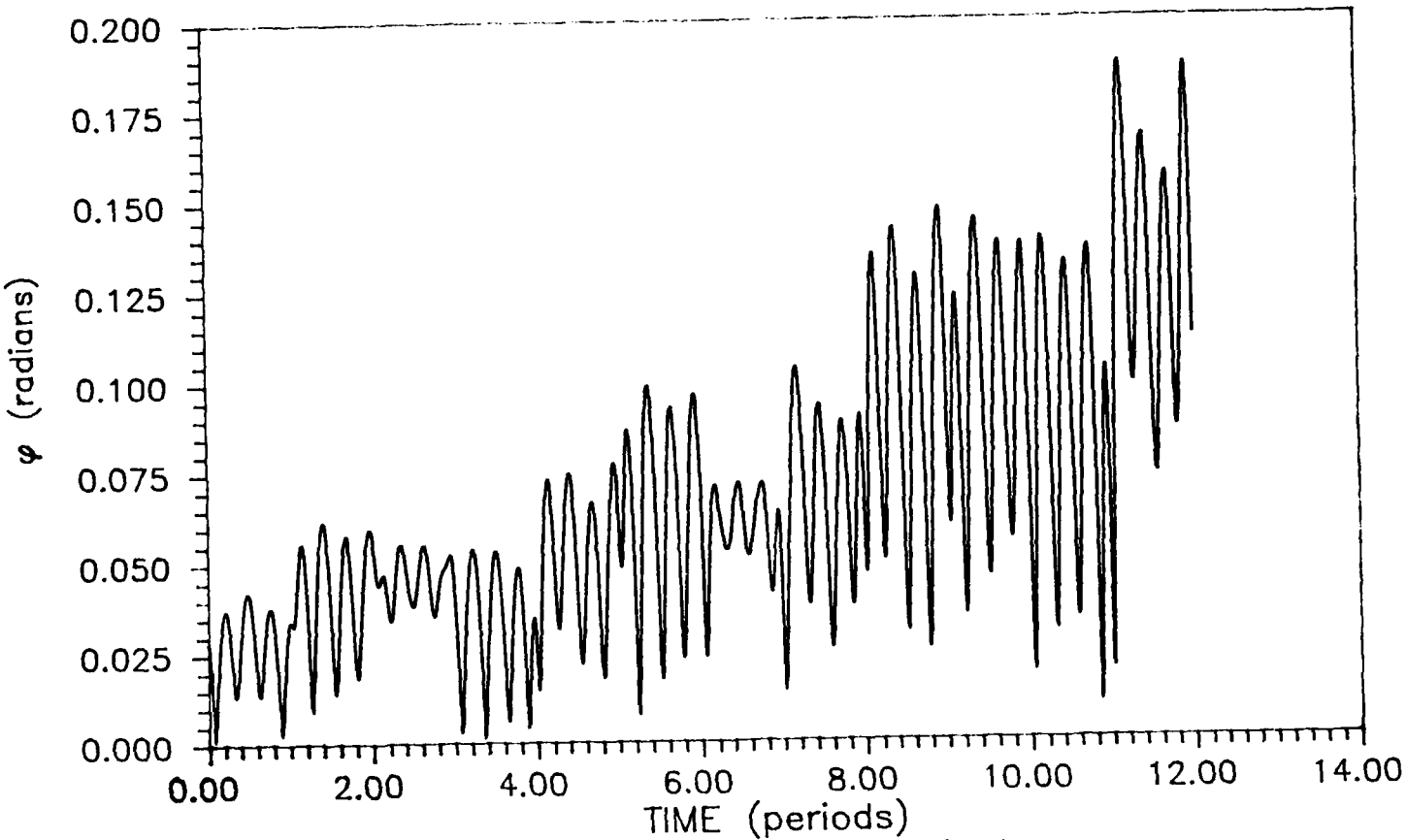

Figure 3.19 – Uncontrolled Non–Linearized φ response

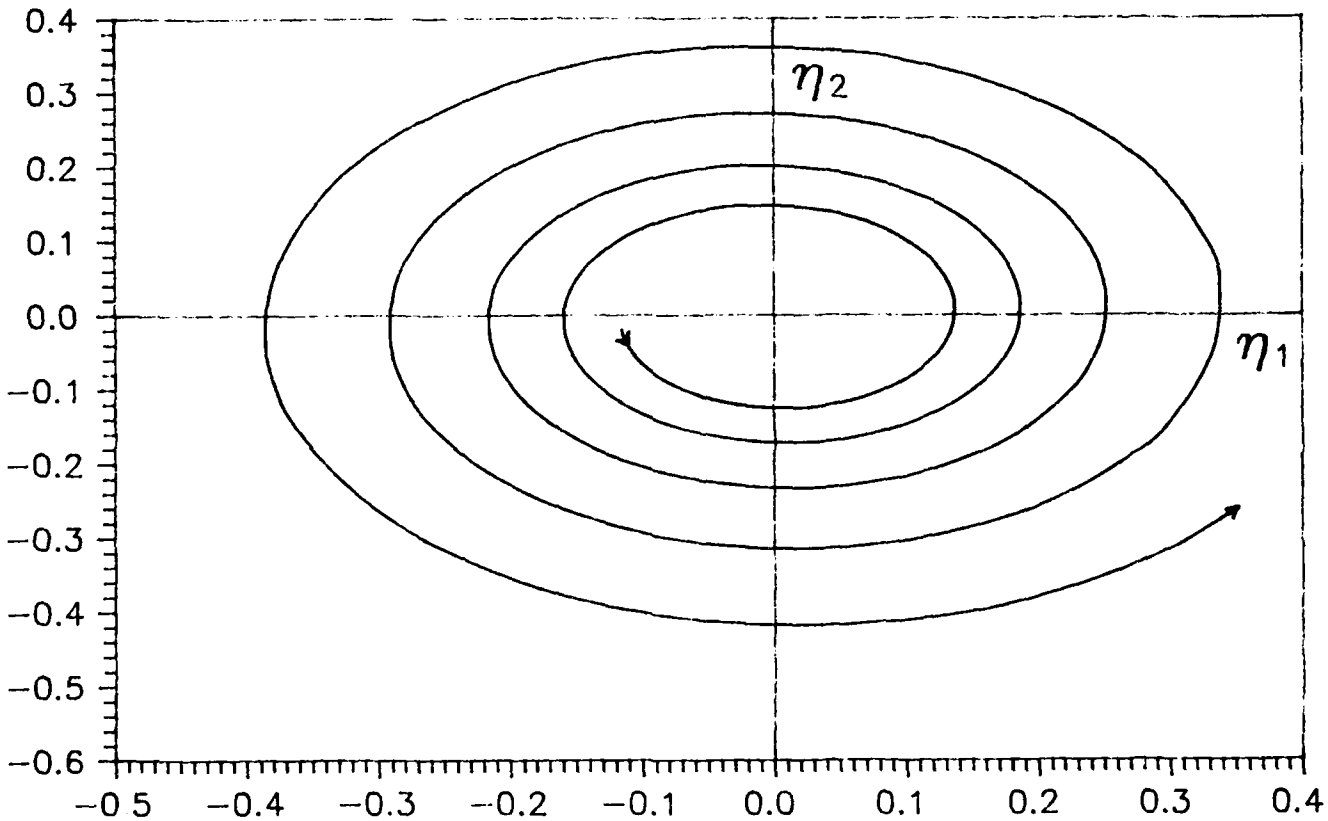

Figure 3.20 – Phase Portrait for Uncontrolled Non–Linearized Modal Variables

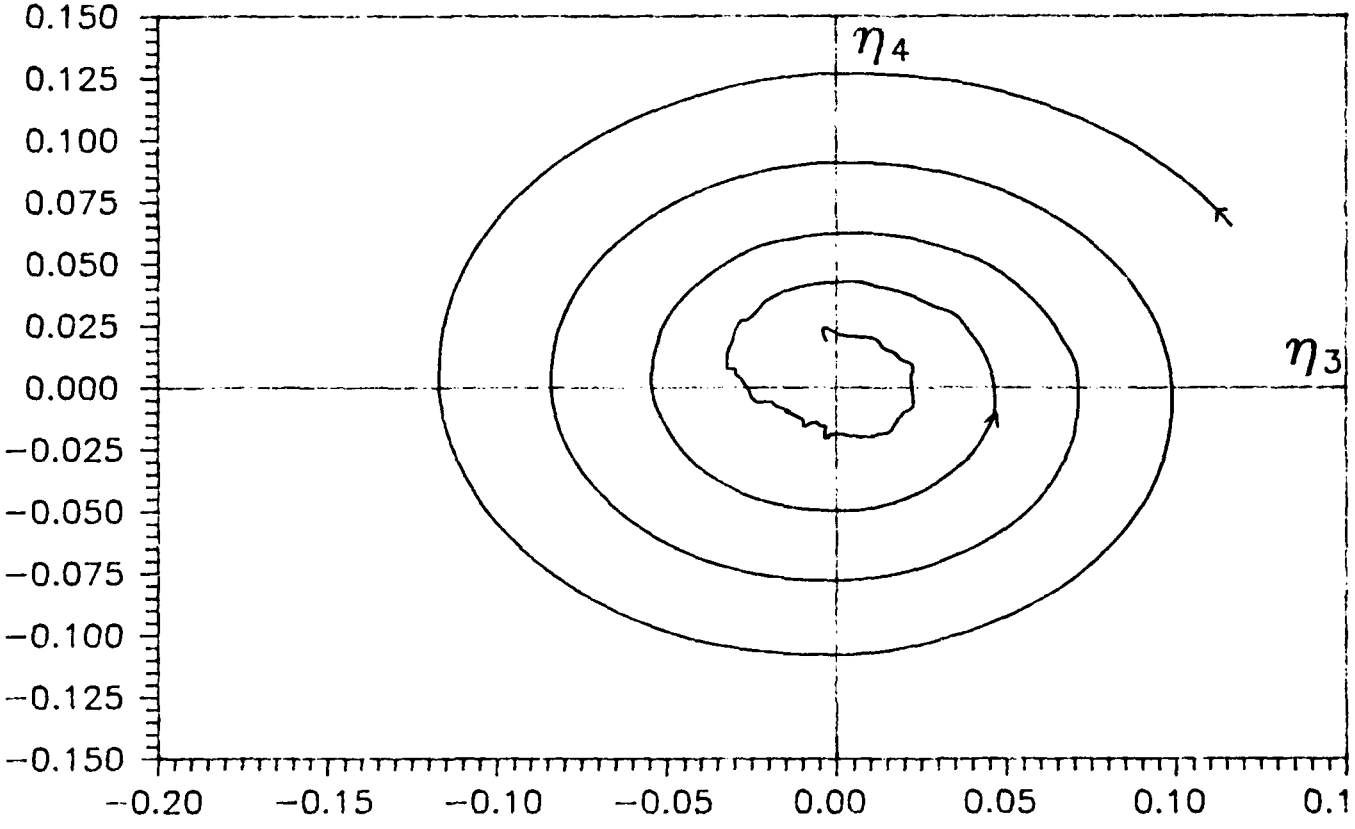

Figure 3.21 – Phase Portrait for Uncontrolled Non–Linearized Modal Variables η_3 and η_4

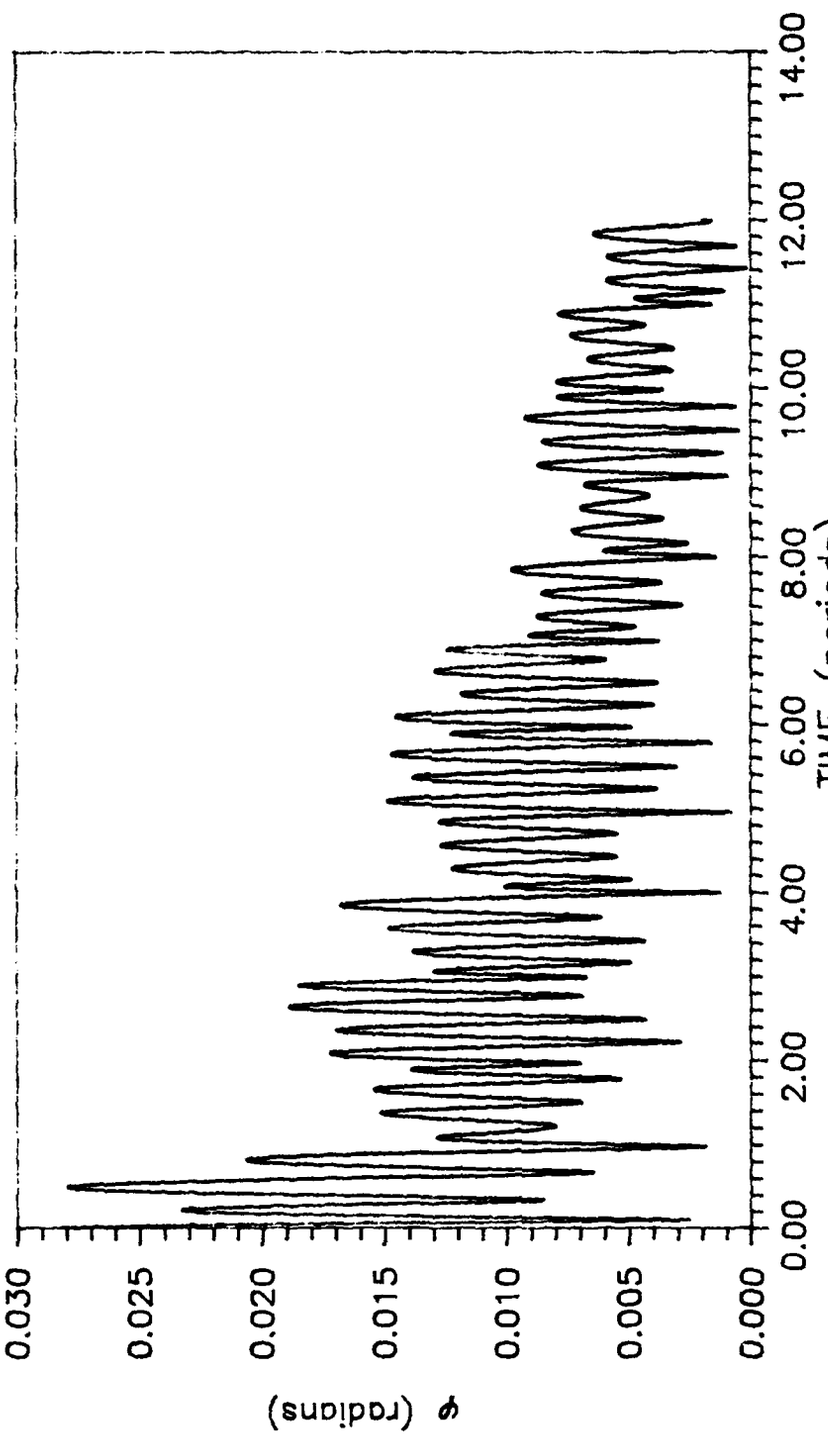

Figure 3.22 – Controlled Non–Linearized φ response

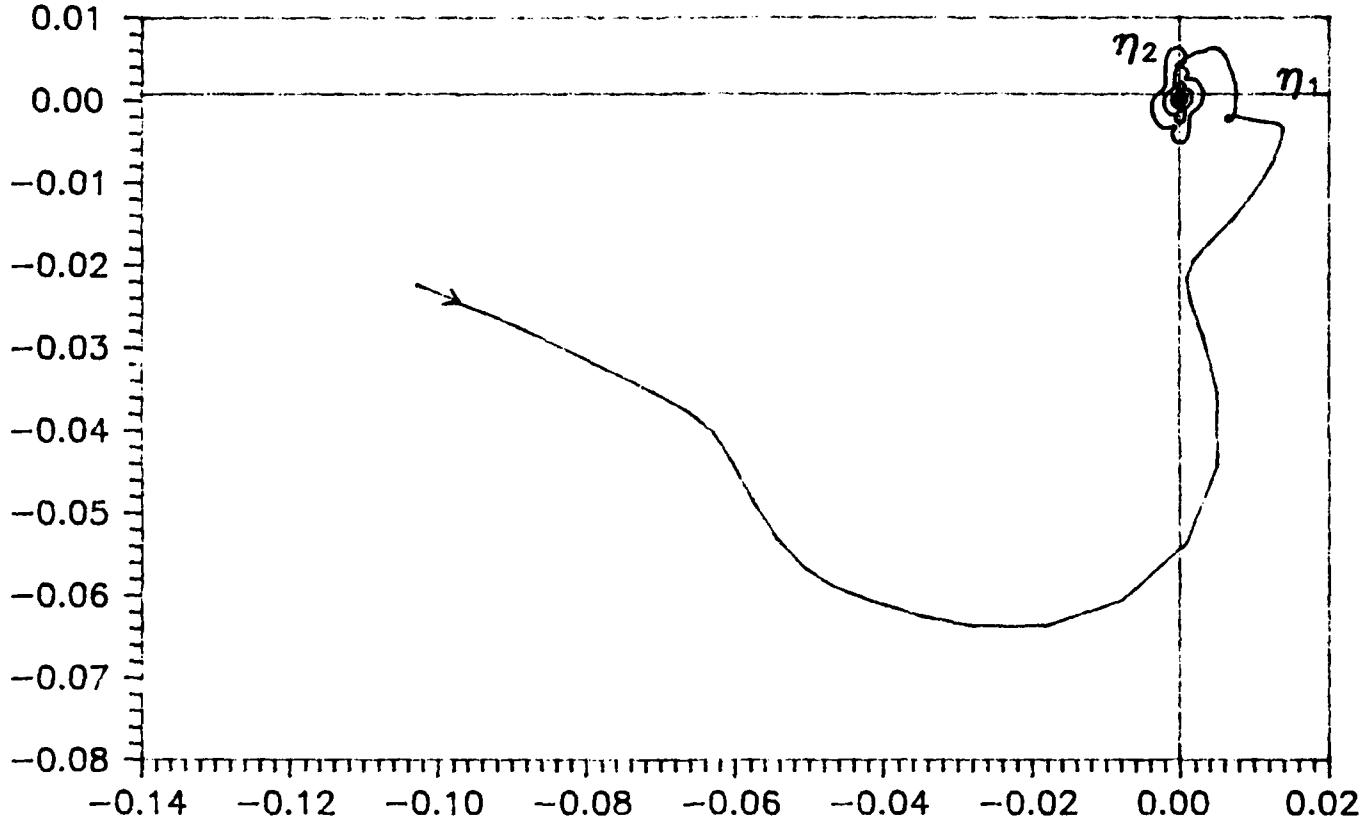

Figure 3.23 – Phase Portrait of Controlled Non–Linearized η_1 vs. η_2

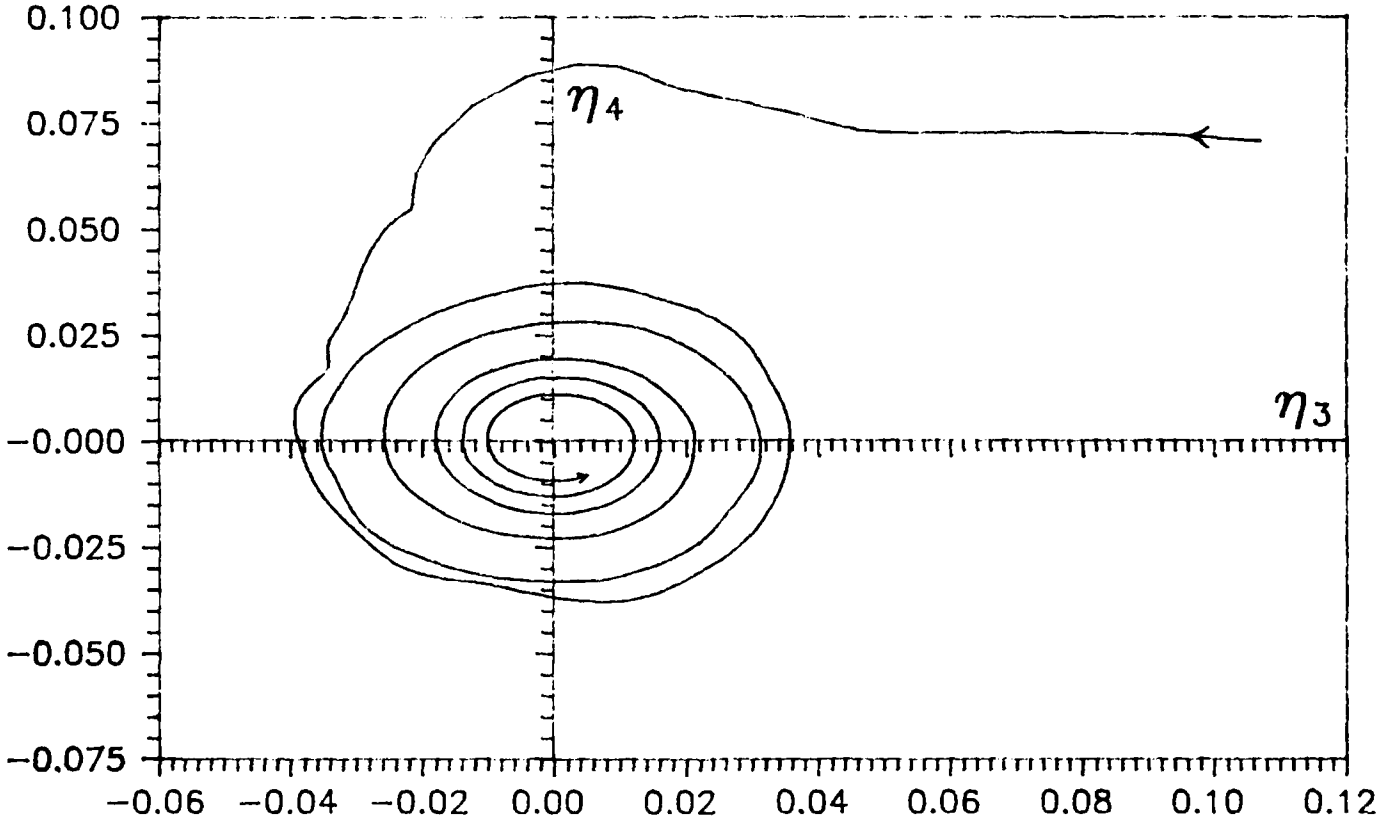

Figure 3.24 – Phase Portrait for Second Pair of Controlled Non–Linearized Modes

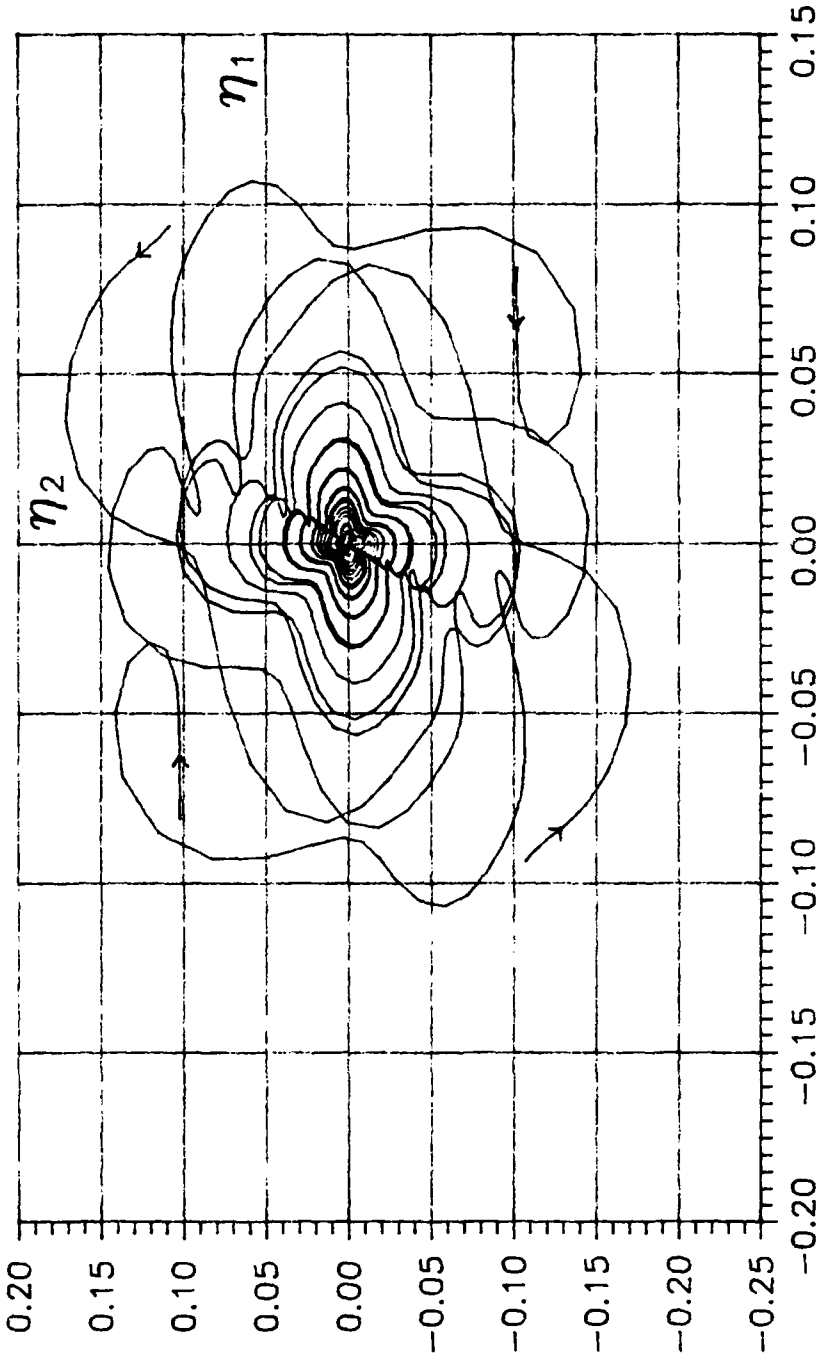

Figure 3.25 – Phase Portrait for η_1 & η_2 magnitude of 0.1

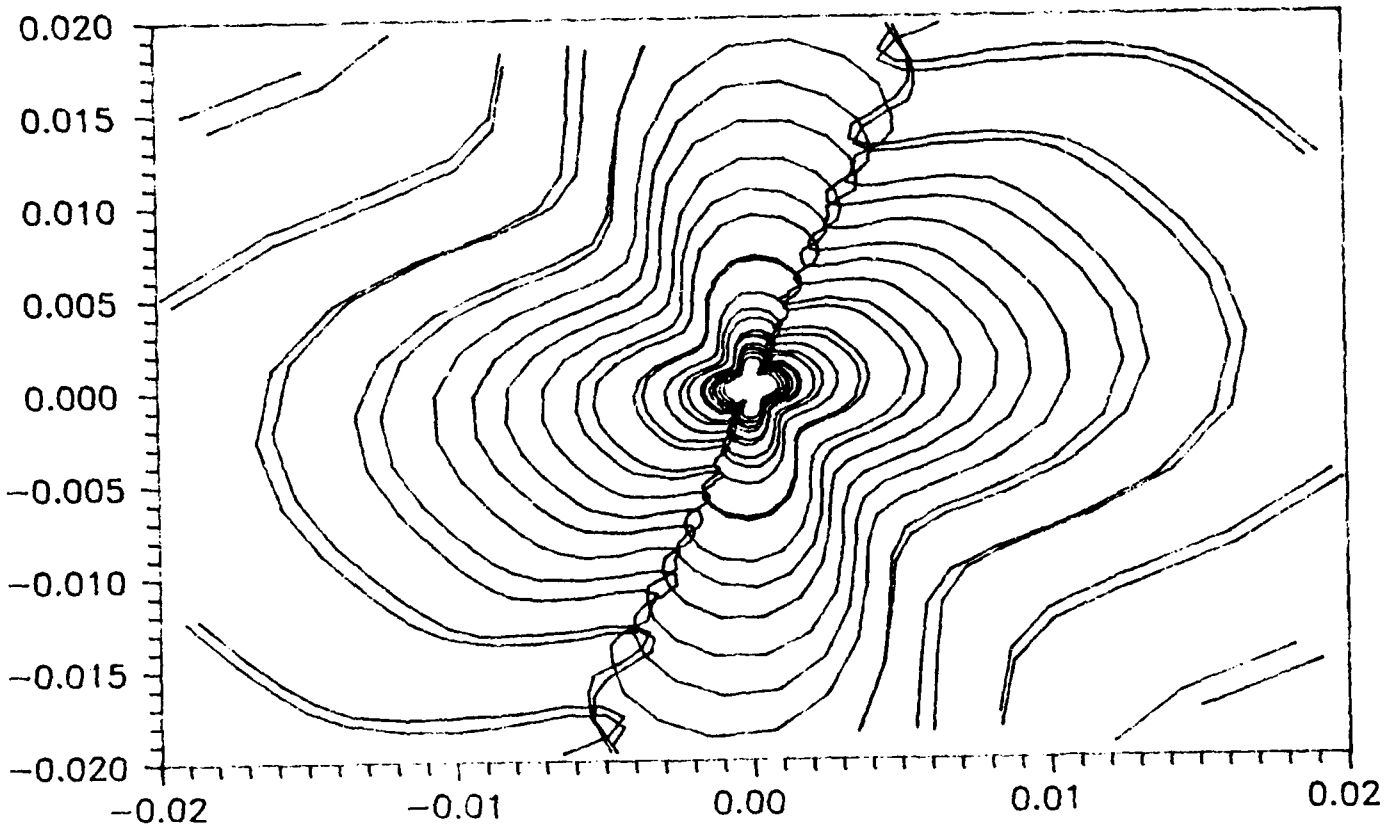

Figure 3.25e – Figure 3.25 Expanded

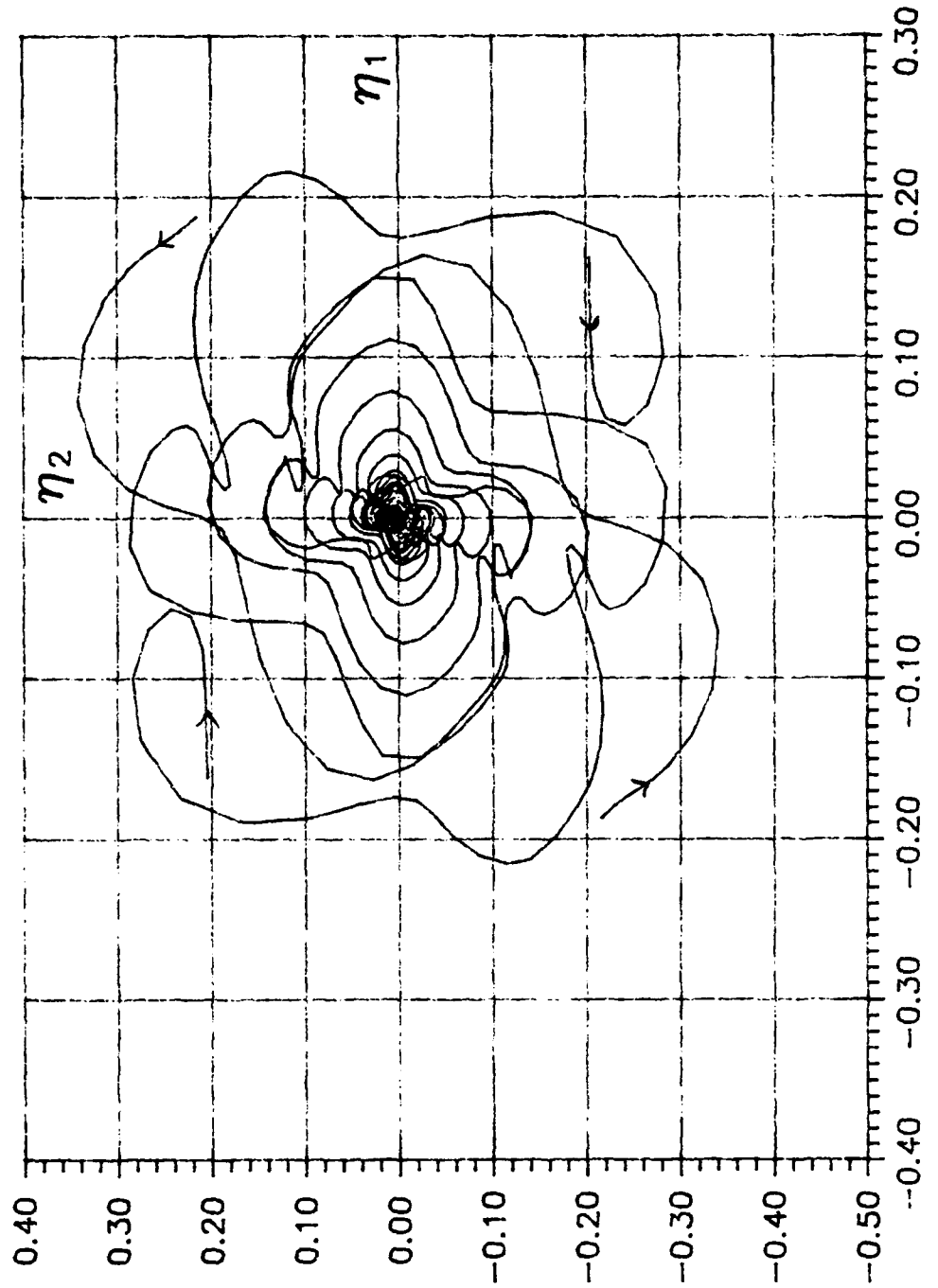

Figure 3.26 – Phase Portrait for η_1 & η_2 magnitude of 0.2

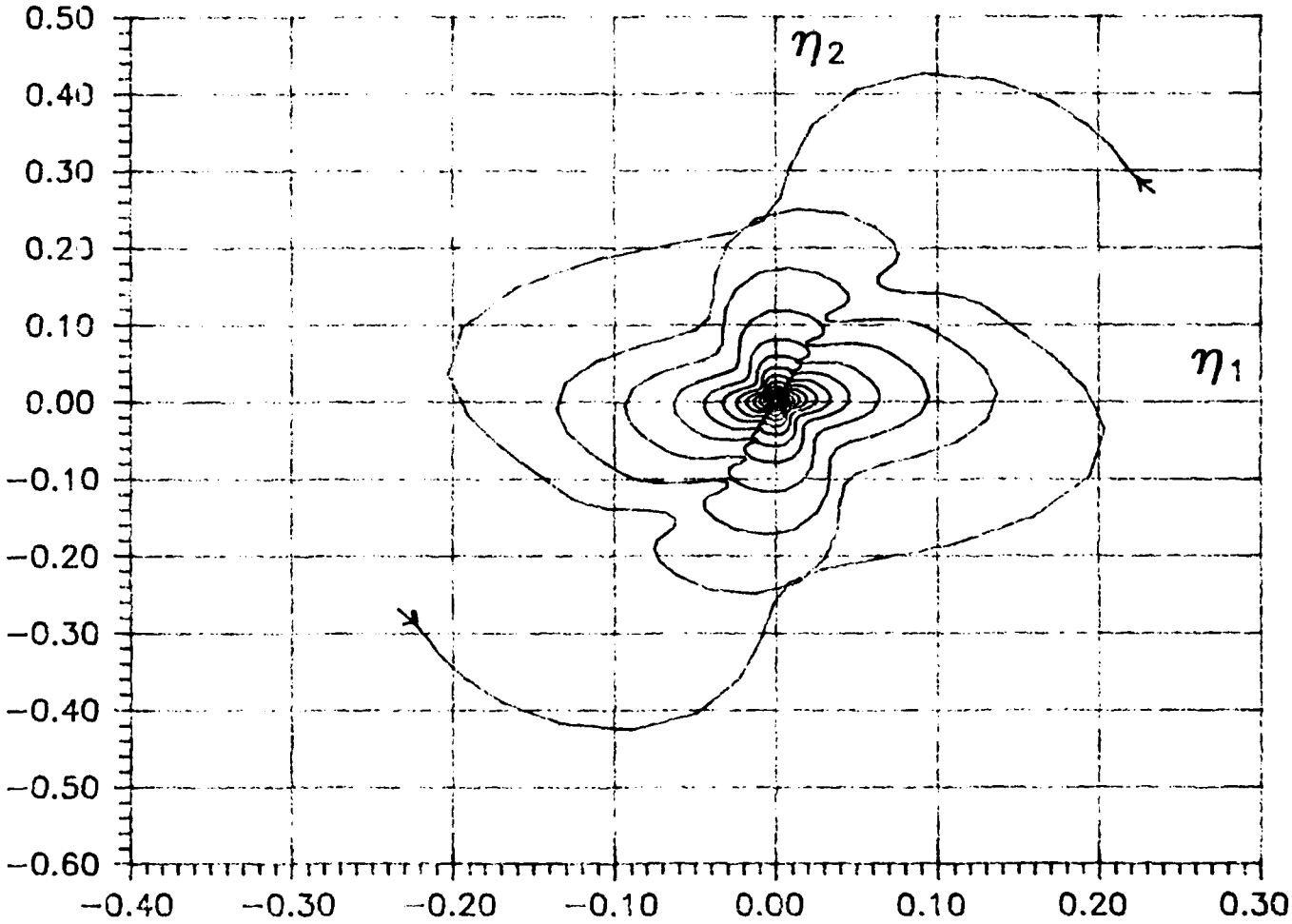

Figure 3.27 – Phase Portrait for η_1 & η_2 magnitude of 0.25 and same sign

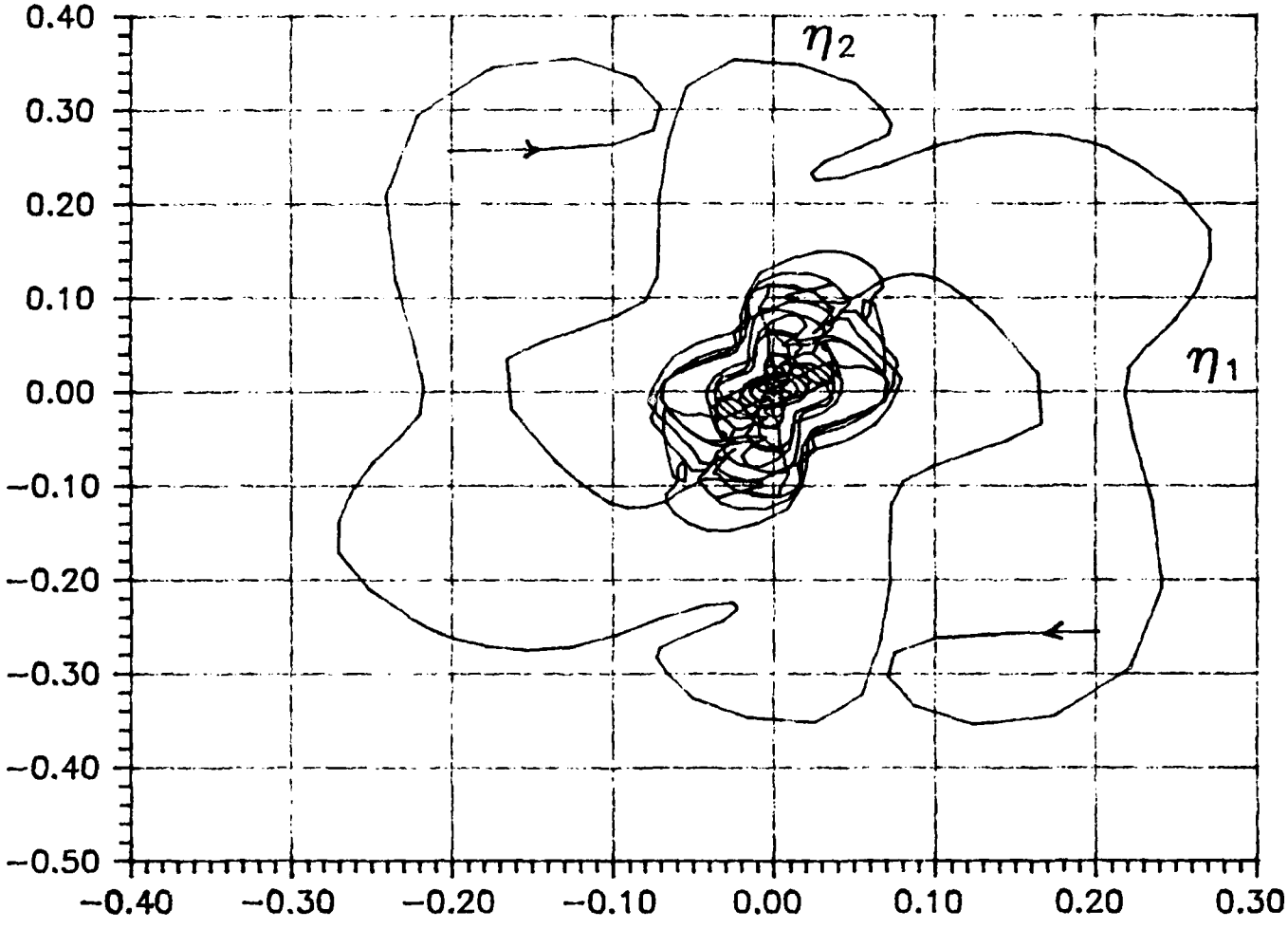

Figure 3.28 – Phase Portrait for η_1 & η_2 magnitude of 0.25 and opposite sign

stability. This indicates a region of chaos. This tendency appears to increase sooner in the second and fourth quadrants. Figures (3.29) through (3.31) illustrate this tendency. It can be seen in all the Phase Portraits that the plots are symmetrical about the origin even in the non-linear system. With even larger initial displacements the stable areas become narrower even in the first and third quadrant. The points shown in Figure (3.32) without curves are initial values which do not converge on the origin but oscillate. The traces of the curves that do converge in these figures appear to enter the stable area along the vertical axis.

If the new modal variables were found for the controlled system these plots should become smoother with the lines not crossing in the linear region since these new modal variables would again decouple the the two mode pairs. Using the uncontrolled modal variables still allows conclusions to be made with respect to the size of 'small' disturbances. It is evident from the phase portraits that a modal displacement magnitude less than 0.25 radians and radians/τ will result in a stable system with reducing magnitudes. Larger displacements will result in a reducing magnitude or chaos. Further investigation is warranted in this area to further define the value for 'small'. The use of controlled modal variables will produce more information.

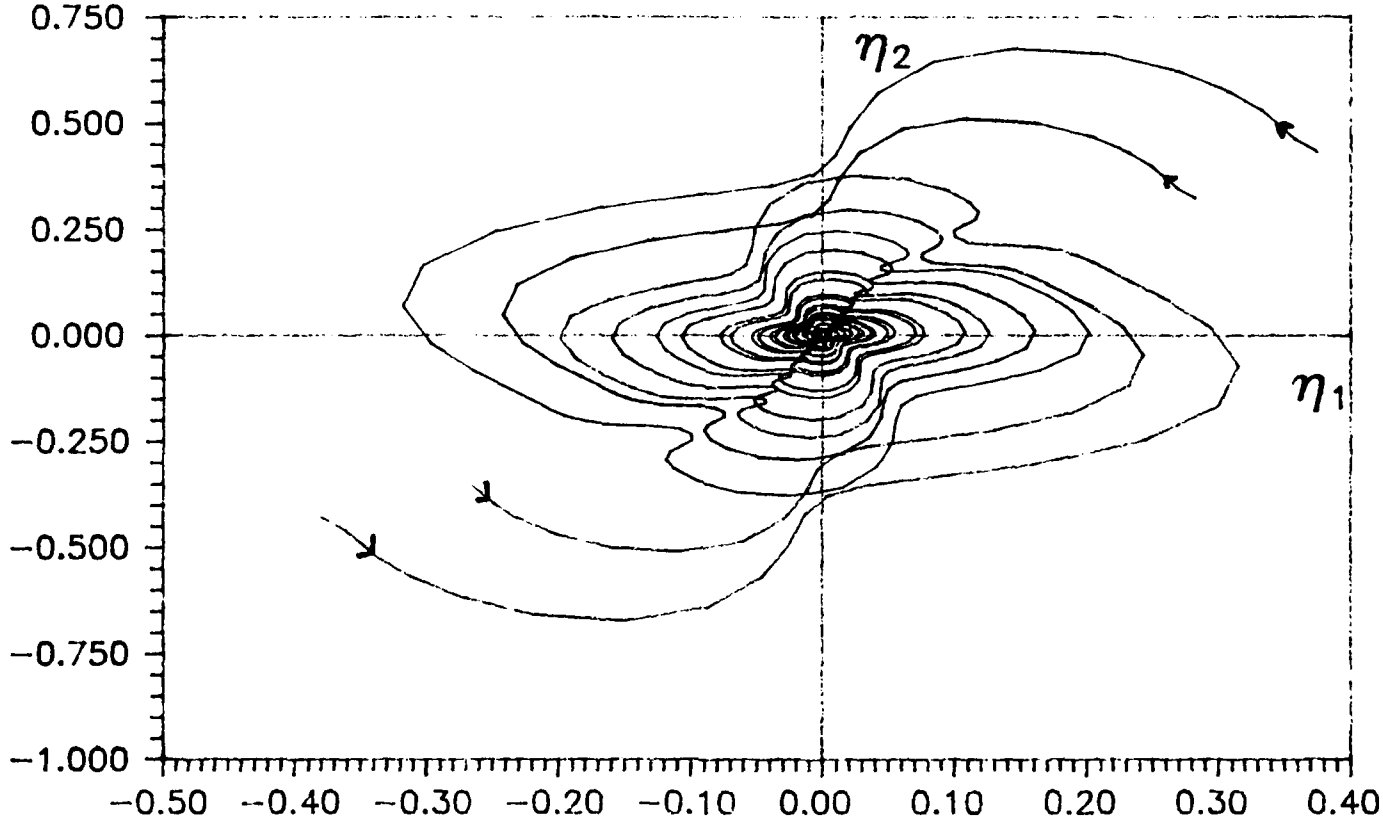

Figure 3.29 – Phase Portrait for Initial Magnitudes of 0.3 and 0.4 in 1st and 3rd Quadrants

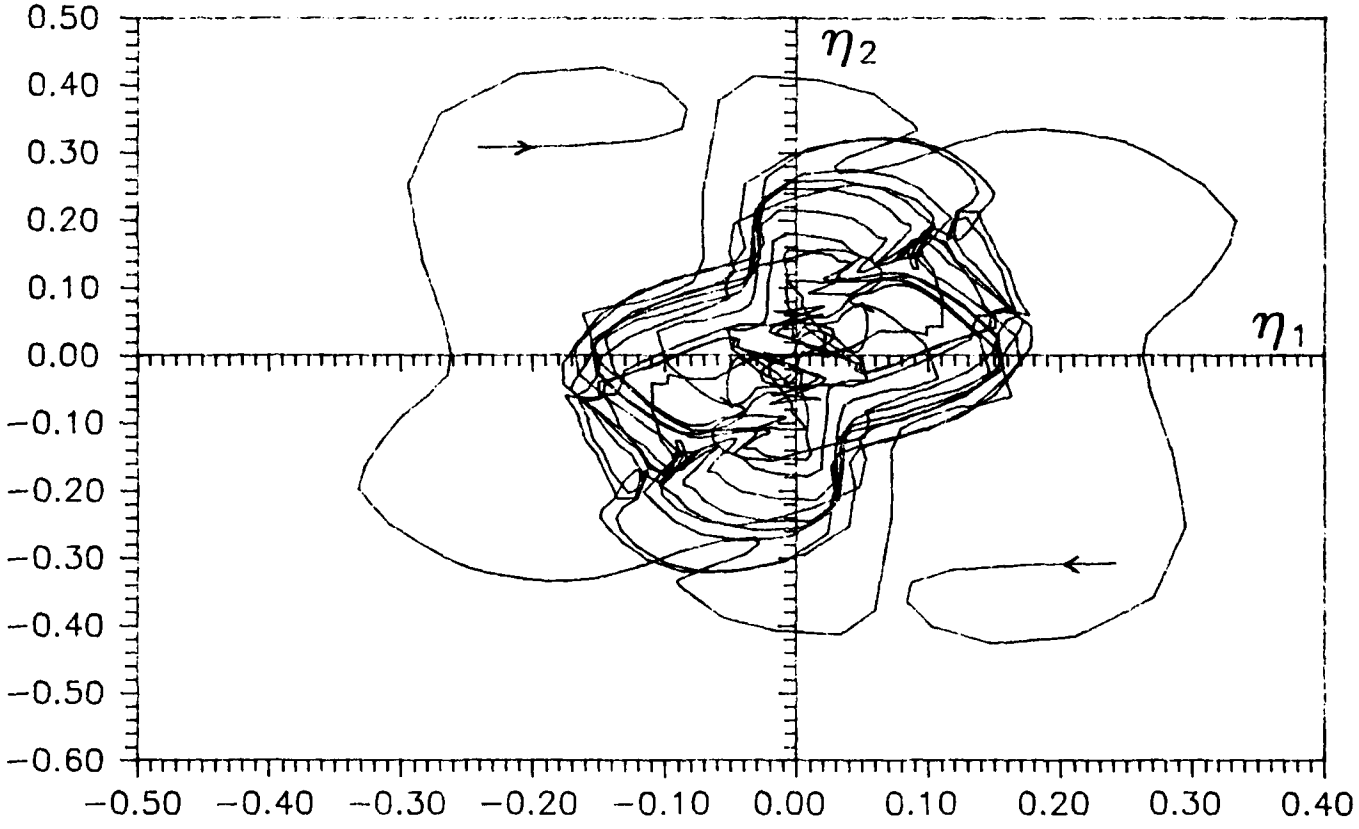

Figure 3.30 – Phase Portrait for Initial Magnitudes of 0.3 in 3rd and 4th Quadrants

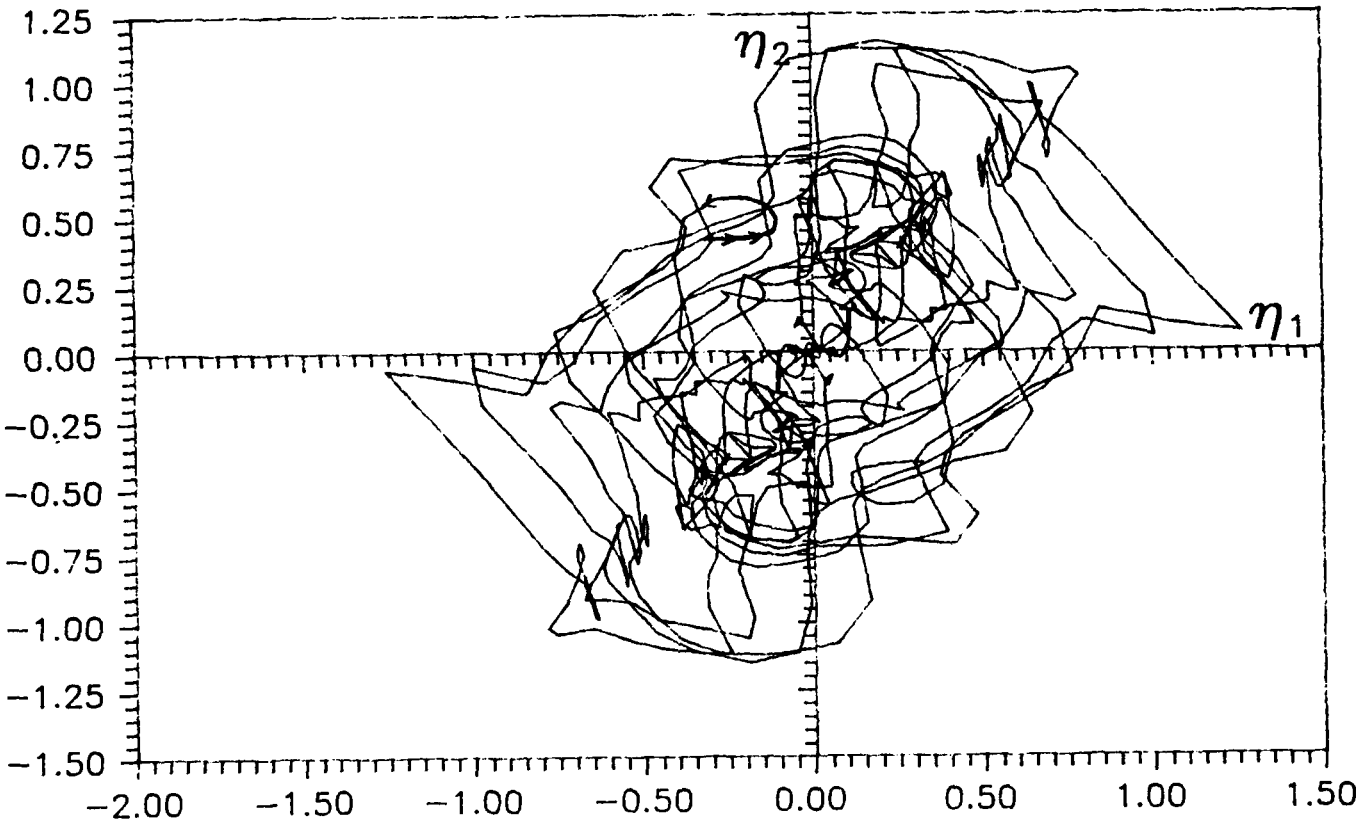

Figure 3.31 – Phase Portrgit for Initial Magnitudes of 0.4 in 3rd and 4th Quadrants

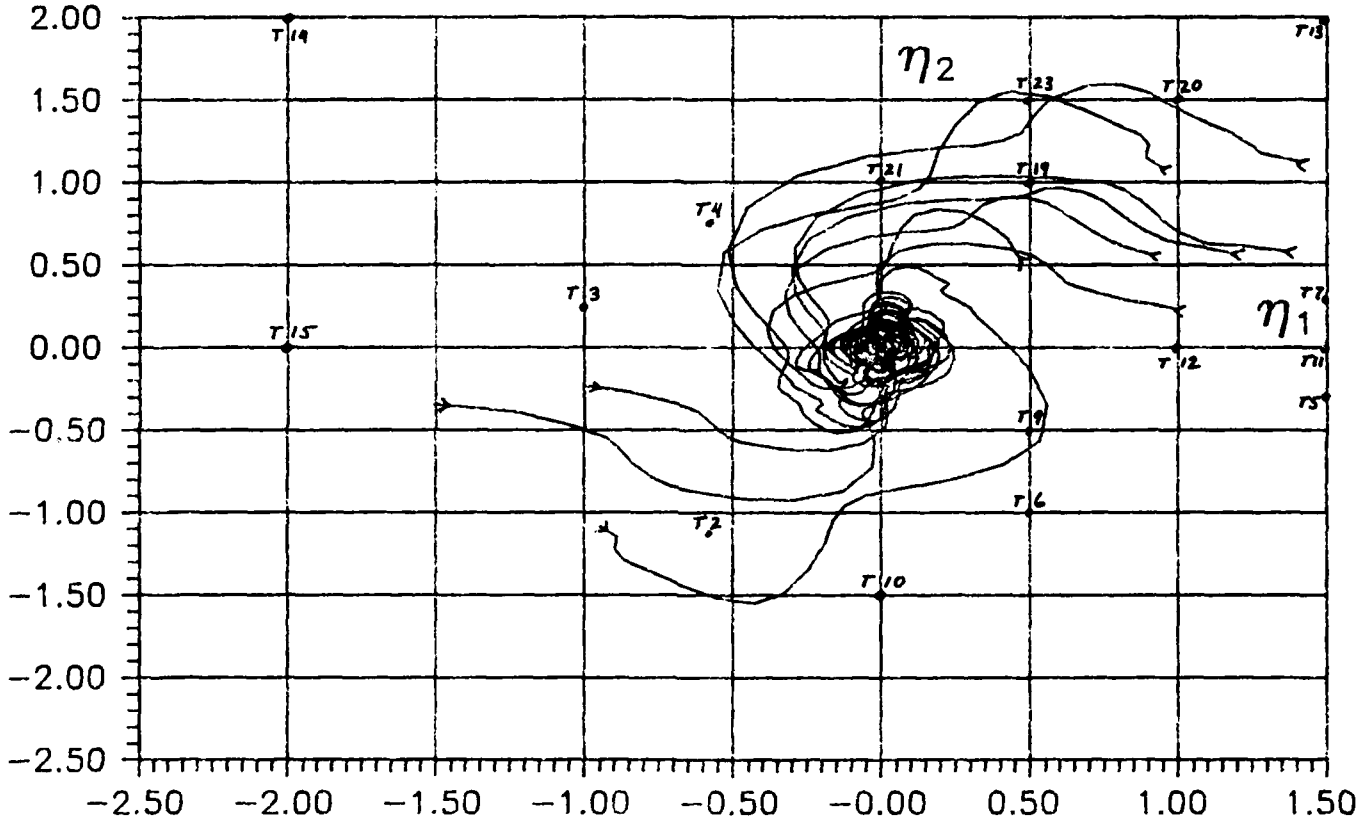

Figure 3.32 – Phase Portrait for Large Initial Magnitudes
(notice symmetry about origin)

Chapter 4

Conclusions and Recommendations

The results of the previous chapter leads to some important conclusions on the concept of small disturbances of a satellite system and the resulting motion of that satellite. It was shown scalar control works reasonability well on the system with two stable and two unstable modes. Left to be determined is a method in selecting the optimum gain of the feedback other than 'hit and miss'. Large gains do not necessarily produce the most stable system. While large gains may produce one root which is more stable, it is likely to push another root in the opposite direction toward instability. The modal variables used in this thesis is for the uncontrolled system and therefore do not decouple the controlled modes. However, the uncontrolled modal variables can provide information on the stability movement of the controlled modes, but further integration to obtain the new controlled modal variables would provide better information.

From the uncontrolled modal variables it is apparent that there are several regions of different stability. Under a value of 0.25 the non-linear equations behave linear. Outside this region, there exists an area where different initial conditions may or may not return the system to its original equilibrium point. Starting points, seemingly close together on a two dimensional plot, result in very different reactions. Some return to the center while others seem to oscillate in undamped but bounded movement about the center. This can be attributed to the

two dimensional representation of a four dimensional problem and to the use of uncontrolled modal variables in the controlled system.

Further study is warranted in four areas. First, the new modal variables should be found to further this investigation. Then this outer area of confusion can be studied. Also a method needs to be found for systematically determining the optimum gain for the feedback. Finally, study of control other than scalar should be investigated using the non-linear equations. Work on vector control with the controlled modal variables seems to be the next logical step.

Appendix A: Fourier Coefficients

Adjoint Solution Matrixx (first 10 terms)

L_{11}

n	a_n	b_n
0	.9242311168594710E+00	
1	-.6854529509025176E+00	.6926555705680942+00
2	-.4348864379633308E+00	-.16365727079734970+00
3	-.1243505852520843E-01	.19572202161513340+00
4	.1113693638003665E-02	-.12686939773981930+00
5	.2714625341132396E-01	-.50323452202868530-01
6	.3536628920488216E-01	-.16043095786327100-01
7	.3398411136041821E-01	-.45955632144451260-03
8	.2877108026556694E-01	.56528321933890080-02
9	.2272793285909652E-01	.72184457766034220-02
10	.1719119294606154E-01	.68012339356615030-02

L_{12}

n	a_n	b_n
0	.1225952800437708E+01	
1	-.2212420918689654E+01	.5820206413480934E+00
2	-.7401668126789335E+00	.4269529560564278E+00
3	-.5228195797654754E+00	.6112875661240712E-01
4	-.6759642857946536E-02	.1662875661240712E-03
5	.2080223891165860E-01	-.2817629049667971E-01
6	.3186080763242387E-01	-.3603346602853508E-01
7	.3169692364656334E-01	-.3422604878598152E-01
8	.2713412076597691E-01	-.2876258140367391E-01
9	.2152152407587097E-01	-.2260715215954215E-01
10	.1630200312669608E-01	-.1703811298128566E-01

Mode Controlability Element, g_i (first 30 terms)

n	a_n	b_n
0	.1967460398576639E+00	
1	.5173699814306124E+00	.1611886143123140E+00
2	.7676230805236048E-02	.6897673595227186E+00
3	.9436071392305762E+00	.6599075565223430E+00
4	-.2651106267160906E+00	-.1288616102659364E+00
5	-.2170659379275563E-01	.5798067376471739E-01
6	-.2406769170357917E-02	.4576824322517970E-01
7	.1101699016076314E-02	.3051217699305379E-01
8	.1505842531590358E-02	.1953038243976544E-01
9	.1237808414617844E-02	.1231450431329914E-01
10	.8913929114430876E-03	.7714018512527845E-02
11	.6068758572467093E-03	.4817728805472591E-02
12	.4013494912402667E-03	.3004941590834503E-02
13	.2610136202602805E-03	.1873444969883763E-02
14	.1679924698986054E-03	.1168053395432101E-02
15	.1073945888386856E-03	.7284763322974062E-03
16	.6834469780277933E-04	.4545299879918495E-03
17	.4335866054233590E-04	.2837514607110684E-03
18	.2744787174179565E-04	.1772389307880157E-03
19	.1734952804595234E-04	.1107726452879897E-03
20	.1095500361219531E-04	.6927229730155386E-04
21	.6912323480100846E-05	.4334497409023176E-04
22	.4359319069900982E-05	.2713735810857480E-04
23	.2748242086847370E-05	.1699981558207768E-04
24	.1732024486001318E-05	.1065537202337215E-04
25	.1091170288716139E-05	.6682569071913408E-05
26	.6870500555549305E-06	.4193482545194881E-05
27	.4321902615741710E-06	.2633131743897344E-05
28	.2714311273037677E-06	.1654434650785011E-05
29	.1700032999699712E-06	.1040206602273654E-05
30	.1059947298799529E-06	.6544726496219521E-06

Mode Controlability Element, g_2 (first 30 terms)

n	a_n	b_n
0	-.8485662975040417E+00	
1	.8940722429994378E+00	.7372634454690840E+00
2	.3048968178948835E+00	.4630341876507209E+00
3	-.4687404621391100E+00	.2696243410385000E+00
4	.4206761958670234E+00	-.3312935036039541E+00
5	.1283867701353021E+00	-.5444628884218237E-01
6	.7050456274260417E-01	-.2038005246048226E-01
7	.4155063057788683E-01	-.9211070496445791E-02
8	.2504585480937912E-01	-.4550326607660309E-02
9	.1525469710967192E-01	-.2369033936193885E-02
10	.9346806435631870E-02	-.1277057459080640E-02
11	.5749766993895167E-02	-.7056968883318756E-03
12	.3547389464991846E-02	-.3972796212121723E-03
13	.2193655289900357E-02	-.2269106961098245E-03
14	.1359102223893499E-02	-.1311146829333820E-03
15	.8434047857003097E-03	-.7648822753939278E-04
16	.5241167226920300E-03	-.4498160631354558E-04
17	.3261041899754050E-03	-.2663779232678486E-04
18	.2031250725458911E-03	-.1587260485321147E-04
19	.1266489989261756E-03	-.9511913970394263E-05
20	.7903700495813057E-04	-.5731335448143886E-05
21	.4936443336344516E-04	-.3472452098782203E-05
22	.3085464757136849E-04	-.2116339151937943E-05
23	.1929829938571555E-04	-.1298597983670829E-05
24	.1207752648957412E-04	-.8034108183284782E-06
25	.7562441233074551E-05	-.5022909152114280E-06
26	.4737255406691598E-05	-.3183890682409032E-06
27	.2968324990761331E-05	-.2055491278135706E-06
28	.1860854525971589E-05	-.1359438343434340E-06
29	.1165275981766767E-05	-.9273710683671869E-07
30	.7294485948520727E-06	-.6570885507472248E-07

Appendix B; Initial Values Data

Initial Values for Points not Traced on Figure 3.32

point	$\eta(0)$	$x(0)$	point	$\eta(0)$	$x(0)$
T1	$\begin{Bmatrix} -1.0 \\ -1.0 \\ 0.0 \\ 0.0 \end{Bmatrix}$	$\begin{Bmatrix} 0.1524 \\ -0.0661 \\ -1.0037 \\ -1.0000 \end{Bmatrix}$	T2	$\begin{Bmatrix} -0.6 \\ -1.2 \\ 0.0 \\ 0.0 \end{Bmatrix}$	$\begin{Bmatrix} 0.2366 \\ -0.1157 \\ -1.1053 \\ -0.6000 \end{Bmatrix}$
T3	$\begin{Bmatrix} -1.00 \\ 0.25 \\ 0.00 \\ 0.00 \end{Bmatrix}$	$\begin{Bmatrix} -0.1500 \\ 0.0924 \\ 0.0444 \\ -1.0000 \end{Bmatrix}$	T4	$\begin{Bmatrix} -0.6 \\ 0.8 \\ 0.0 \\ 0.0 \end{Bmatrix}$	$\begin{Bmatrix} -0.2473 \\ 0.1378 \\ 0.5717 \\ -0.6000 \end{Bmatrix}$
T5	$\begin{Bmatrix} 1.5 \\ -0.3 \\ 0.0 \\ 0.0 \end{Bmatrix}$	$\begin{Bmatrix} 0.2069 \\ -0.1290 \\ -0.0038 \\ 1.5000 \end{Bmatrix}$	T6	$\begin{Bmatrix} 0.5 \\ -1.0 \\ 0.0 \\ 0.0 \end{Bmatrix}$	$\begin{Bmatrix} 0.2867 \\ -0.1571 \\ -0.7559 \\ 0.5000 \end{Bmatrix}$
T7	$\begin{Bmatrix} 1.5 \\ 0.3 \\ 0.0 \\ 0.0 \end{Bmatrix}$	$\begin{Bmatrix} 0.0617 \\ -0.0530 \\ 0.4993 \\ 1.5000 \end{Bmatrix}$	T9	$\begin{Bmatrix} 0.5 \\ -0.5 \\ 0.0 \\ 0.0 \end{Bmatrix}$	$\begin{Bmatrix} 0.1657 \\ -0.0937 \\ -0.3367 \\ 0.5000 \end{Bmatrix}$
T10	$\begin{Bmatrix} 0.0 \\ -1.5 \\ 0.0 \\ 0.0 \end{Bmatrix}$	$\begin{Bmatrix} 0.3629 \\ -0.1902 \\ -1.2577 \\ 0.0000 \end{Bmatrix}$	T11	$\begin{Bmatrix} 1.5 \\ 0.0 \\ 0.0 \\ 0.0 \end{Bmatrix}$	$\begin{Bmatrix} 0.1343 \\ -0.0910 \\ 0.2478 \\ 1.5000 \end{Bmatrix}$
T12	$\begin{Bmatrix} 1.0 \\ 0.0 \\ 0.0 \\ 0.0 \end{Bmatrix}$	$\begin{Bmatrix} 0.0895 \\ -0.0607 \\ 0.1657 \\ 1.0000 \end{Bmatrix}$	T13	$\begin{Bmatrix} 1.5 \\ 2.0 \\ 0.0 \\ 0.0 \end{Bmatrix}$	$\begin{Bmatrix} -0.3495 \\ 0.1625 \\ 1.9248 \\ 1.5000 \end{Bmatrix}$
T14	$\begin{Bmatrix} -2.0 \\ 2.0 \\ 0.0 \\ 0.0 \end{Bmatrix}$	$\begin{Bmatrix} -0.6629 \\ 0.3749 \\ 1.3466 \\ -2.0000 \end{Bmatrix}$	T15	$\begin{Bmatrix} -2.0 \\ 0.0 \\ 0.0 \\ 0.0 \end{Bmatrix}$	$\begin{Bmatrix} -0.1791 \\ 0.1213 \\ -0.3304 \\ -2.0000 \end{Bmatrix}$
T19	$\begin{Bmatrix} 0.5 \\ 1.0 \\ 0.0 \\ 0.0 \end{Bmatrix}$	$\begin{Bmatrix} -0.1971 \\ 0.0964 \\ 0.9211 \\ 0.5000 \end{Bmatrix}$	T20	$\begin{Bmatrix} 1.0 \\ 1.5 \\ 0.0 \\ 0.0 \end{Bmatrix}$	$\begin{Bmatrix} -0.2733 \\ 0.1295 \\ 1.4229 \\ 1.0000 \end{Bmatrix}$
T21	$\begin{Bmatrix} 0.0 \\ 1.0 \\ 0.0 \\ 0.0 \end{Bmatrix}$	$\begin{Bmatrix} -0.2419 \\ 0.1268 \\ 0.8385 \\ 0.0000 \end{Bmatrix}$	T23	$\begin{Bmatrix} 0.5 \\ 1.5 \\ 0.0 \\ 0.0 \end{Bmatrix}$	$\begin{Bmatrix} -0.3181 \\ 0.1598 \\ 1.3403 \\ 0.5000 \end{Bmatrix}$

Bibliography

1) Calico, R.A., Wiesel, W.E., "Control of Time-Periodic Systems", Journal of Guidance, Control, and Dynamics, p. 671, volume 7, number 6, November-December 1984. reprinted, Soviet Journal Aeronautics/Space Technology, December 1986.

2) Calico, R.A., Yeakel, G.S., "Active Attitude Control of a Spinning Symmetric Satellite in an Elliptical Orbit", Air Force Institute of Technology, 1982.

3) Churchill, Ruel V., Woodbrown, James, Fourier Series and Boundary Value Problems, McGraw Hill, 1987.

4) Kane, T.R., and Barba, P.M., "Attitude Stability of a Spinning Satellite in an Elliptic Orbit", Journal of Applied Mechanics, pp.402-405, June 1966.

5) Kane,T.R., and Shippy, D.J., "Attitude Stability of a Spinning Unsymmetrical Satellite in a Circular Orbit", The Journal of the Astronautical Sciences, Vol.X, No.4, pp.114-119, Winter 1963.

6) Meirovitch,Leonard, Methods of Analytical Dynamics, McGraw Hill, New york, 1970.

7) Myers,G.E.,Active Control of Linear Periodic System With Two Unstable Modes, M.S. Thesis, Wright-Patterson AFB, Ohio Air Force Institute of Technology, Dec. 1982.

8) Reid,J.Gary, Linear System Fundamentals, McGraw Hill, New York, 1983.

VITA

Dale E. Shell, son of [redacted] Shell Sr. and [redacted] Shell, was born [redacted] He was raised in [redacted] Florida and graduated from [redacted] High School in [redacted] He attended Pensacola Junior College part-time and received an Associates of Science degree in Electrical Engineering Technology in 1972. He entered the Air Force in May 1976. In September, 1980, he entered Auburn University under the Air Force's Airman Education and Commissioning Program. March, 1983, he received a Bachelor of Science in Aerospace Engineering from Auburn University. He attended Officers Training School and was commissioned a second lieutenant in the United States Air Force in July 1983. In June 1987, he started his Master of Science degree in Astronautical Engineering at the Air Force Institute of Technology. Upon graduation in December 1988 he will be assigned to the 6595th Test and Evaluation Group, Vandenberg AFB California.

He married [redacted] and [redacted] They have two sons, [redacted]

UNCLASSIFIED

SECURITY CLASSIFICATION OF THIS PAGE

REPORT DOCUMENTATION PAGE

Form Approved
OMB No. 0704-0188

1a. REPORT SECURITY CLASSIFICATION unclassified	1b. RESTRICTIVE MARKINGS
2a. SECURITY CLASSIFICATION AUTHORITY	3. DISTRIBUTION/AVAILABILITY OF REPORT Approved for public release; Distribution unlimited
2b. DECLASSIFICATION/DOWNGRADING SCHEDULE	
4. PERFORMING ORGANIZATION REPORT NUMBER(S) AFIT/GA/AA/88D-09	5. MONITORING ORGANIZATION REPORT NUMBER(S)
6a. NAME OF PERFORMING ORGANIZATION School of Engineering 6b. OFFICE SYMBOL (If applicable) AFIT/ENY	7a. NAME OF MONITORING ORGANIZATION
6c. ADDRESS (City, State, and ZIP Code) Air Force Institute of Technology Wright-Patterson A.F.B. Ohio 45433	7b. ADDRESS (City, State, and ZIP Code)
8a. NAME OF FUNDING/SPONSORING ORGANIZATION 8b. OFFICE SYMBOL (If applicable)	9. PROCUREMENT INSTRUMENT IDENTIFICATION NUMBER
8c. ADDRESS (City, State, and ZIP Code)	10. SOURCE OF FUNDING NUMBERS PROGRAM ELEMENT NO. / PROJECT NO. / TASK NO / WORK UNIT ACCESSION NO.

11. TITLE (Include Security Classification)
Stability Solution to Linearized Equations of Motion for a Symmetric Spinning Satellite in an Elliptical Orbit Applied to the Non-linear Equations (unclassified)

12. PERSONAL AUTHOR(S)
Dale E. Shell, Captain USAF

13a. TYPE OF REPORT	13b. TIME COVERED	14. DATE OF REPORT (Year, Month, Day)	15. PAGE COUNT
M.S. Thesis	FROM _____ TO _____	1988 December	90

16. SUPPLEMENTARY NOTATION

17. COSATI CODES		
FIELD	GROUP	SUB-GROUP
22	03	

18. SUBJECT TERMS (Continue on reverse if necessary and identify by block number)
Satellite Attitude; Equations of Motion; Floquet Theory; Modal Control Theory; Elliptical Orbit Trajectories; Spin Stabilization; Theses (AFIT)

19. ABSTRACT (Continue on reverse if necessary and identify by block number)

Thesis Advisor: Dr. R. A. Calico
Professor of Aerospace Engineering
Department of Aeronautics and Astronautics

12 Jan 1989

20. DISTRIBUTION/AVAILABILITY OF ABSTRACT	21. ABSTRACT SECURITY CLASSIFICATION
☒ UNCLASSIFIED/UNLIMITED ☐ SAME AS RPT. ☐ DTIC USERS	unclassified

22a. NAME OF RESPONSIBLE INDIVIDUAL	22b. TELEPHONE (Include Area Code)	22c. OFFICE SYMBOL
Dr. Robert A. Calico	(513) 255-3517	AFIT/ENY

DD Form 1473, JUN 86 *Previous editions are obsolete.*

SECURITY CLASSIFICATION OF THIS PAGE
UNCLASSIFIED

The attitude of a spinning symmetrical satellite in an elliptical orbit is analyzed. The perturbed motion of the satellite is described by linear equations with periodic coefficients. Stability is determined by Floquet theory. Active control is added to the system and results lead to a linear periodic control law. Scalar control from the linearized system is implemented to evaluate the performance of the control law on the non-linear equations of motion. For small disturbances, it is illustrated the controlled non-linear response duplicates the linear case. For larger disturbances, phase portraits show the resulting behavior of the coupled modes. As the perturbed motion increases in magnitude stability regions appear. Initial motion results either a return to the initial equilibrium, an oscillation around the equilibrium point or divergence from the initial equilibrium. Keywords: [illegible]